

Geological Survey of Finland

Bulletin 388

**Geochemical alteration of gold occurrences in the late
Archean Hattu schist belt, Ilomantsi, eastern Finland**

by Kalevi Rasilainen



Geological Survey of Finland
Espoo 1996

Geological Survey of Finland, Bulletin 388

**GEOCHEMICAL ALTERATION OF GOLD OCCURRENCES IN THE
LATE ARCHEAN HATTU SCHIST BELT, ILOMANTSI, EASTERN
FINLAND**

by

KALEVI RASILAINEN

with 51 figures, 13 tables and 5 appendices

**GEOLOGICAL SURVEY OF FINLAND
ESPOO 1996**

Rasilainen, Kalevi. 1996. Geochemical alteration of gold occurrences in the late Archean Hattu schist belt, Ilomantsi, eastern Finland. Geological Survey of Finland, Bulletin 388, 80 pages, 51 figures, 13 tables and 5 appendices.

Numerous lode gold occurrences have been found adjacent to shear zones tens of kilometers in length within the late Archean Hattu schist belt in easternmost Finland. Major and trace element alteration patterns, based on analysis of 1038 rock samples, are reported here for mineralized host rocks in the Kelokorpi, Kuittila, Korvilansuo, Kivisuo, Elinsuo, Muurinsuo, and Rämepuro gold occurrences.

Weak Na depletion and Fe enrichment are common to all host rock types. Tonalites show median enrichments in Mn and Mg, and depletion in Na, while K and LOI have also commonly increased. Porphyry dikes display average depletions in Ca and Mn, and increases in LOI. Also Na and Mg depletion is ubiquitous. Magnesium is on average enriched in intermediate but depleted in mafic volcanic rocks, whereas both these rock types show median Mn enrichment. Slight Fe enrichment is the most frequent characteristic of sedimentary host rocks. The trace elements display generally similar alteration patterns irrespective of host rock. The strongest average enrichments (more than 100%) are shown by Au, Te, B, Bi, Ag, CO₂, W, As, and S. Tonalites record the most significant average CO₂ enrichment, the weakest average As enrichment, and no average B enrichment.

Excluding the tonalites, the Hattu occurrences are associated with atypically weak potassium metasomatism, hydration, and carbonatization. Compared with Archean lode gold deposits in Australia and Canada, they generally display somewhat weaker relative enrichments in Ag, As, Au, S, Te, and W. Conversely, B may be more enriched in mineralized volcanic rocks and porphyries in the Hattu schist belt than in many comparable regions.

The K-Rb-Ba systematics of the Hattu occurrences is consistent with a uniform source and origin for the ore fluids, as has been documented from Archean lode gold deposits world-wide. In the case of the mafic volcanic rocks, wallrock sulfidation may have caused gold precipitation. For the remaining host rocks, other fluid-wallrock reactions were probably critical.

Key words (Georef Thesaurus, AGI): gold ores, greenstone belts, geochemistry, hydrothermal alteration, mass transfer, Archean, Hattuvaara, Ilomantsi, Finland

Kalevi Rasilainen, Geological Survey of Finland, FIN-02150 ESPOO, FINLAND

ISBN 951-690-637-0
ISSN 0367-522X

Vammalan Kirjapaino Oy 1996

CONTENTS

Introduction	5
Geology of the Hattu schist belt	6
The Kuittila zone	7
The Hattuvaara zone	9
Materials and methods	10
Rock samples	10
Analytical techniques	10
Mass transfer calculations	12
Rock types and primary chemical compositions	12
Rock type classification	12
Least altered samples and background compositions	16
Primary geochemical variations	18
Geochemical alteration at the gold occurrences	20
Kelokorpi	20
Geochemical alteration	22
Kuittila	25
Geochemical alteration	27
Korvilansuo	30
Geochemical alteration	32
Kivisuo	35
Geochemical alteration	36
Muurinsuo	39
Geochemical alteration	41
Elinsuo	45
Geochemical alteration	46
Rämepuro	48
Geochemical alteration	51
Summary of geochemical alteration	54
Tonalites	54
Porphyry dikes	55
Volcanic rocks	56
Sedimentary rocks	58
Comparisons between the main rock types	59
Mineralogical interpretations	60
Tonalites	60
Porphyry dikes	61
Volcanic rocks	62
Sedimentary rocks	63
Large ion lithophile element geochemistry	64

Discussion	68
Comparison with previous work	68
Comparisons with Archean lode gold deposits in Australia and Canada	68
Tonalites and porphyry dikes	69
Volcanic rocks	71
Sedimentary rocks	72
Summary of comparisons with Archean lode gold deposits in Australia and Canada	73
Implications for wallrock alteration and gold deposition	74
Conclusions	76
Acknowledgments	77
References	77
Appendix 1. Background chemical compositions for volcanic rocks.	
Appendix 2. Background chemical compositions for sedimentary rocks.	
Appendix 3. Background chemical compositions for plutonic rocks.	
Appendix 4. Background chemical compositions for porphyry dikes.	
Appendix 5. References for the Australian and Canadian lode gold deposit data.	

INTRODUCTION

Structurally hosted lode gold deposits in metamorphic rocks form a distinct class of epigenetic precious-metal deposits, formed over a range of crustal depths from granulite to sub-greenschist facies conditions (Groves, 1993). Although polarized views exist on their timing and mode of formation, there is a general consensus that lode gold deposits were formed by large volumes of hydrothermal solutions flowing along structurally controlled pathways, and that gold precipitation was caused by changes in physicochemical conditions. The deposits are typically surrounded by alteration haloes caused by reactions between the hydrothermal fluid and the wall rocks. These alteration haloes can provide valuable information concerning the conditions of precipitation of gold and associated metals, as well as act as exploration guides.

Gold exploration within the late Archean Ilomantsi region in eastern Finland has been active since the middle of the 1980s and ongoing exploration has revealed many gold occurrences and extensive anomalies throughout more than 40 km of the Hattu schist belt. In 1986, the Ilomantsi Gold Project was initiated by the Geological Survey of Finland (Nurmi and Sorjonen-Ward, 1993) and since then, the area has been subject to active research, including rock geochemical studies of mineralization and alteration. Bornhorst et al. (1993) classified the main rock types within the schist belt into chemical subtypes and defined background contents of elements. Bornhorst and Rasilainen (1993) used factor analysis of mass transfer values to study geochemical affinities between elements and to identify persistent geochemical associations

related to mineralization. Rasilainen et al. (1993) studied the applicability of mobile gold-related elements as geochemical pathfinders in exploration on both regional and detailed scales.

All previous rock geochemical studies of alteration and mineralization were based on the statistical treatment of a large amount of heterogeneous rock geochemical data, or dealt with only a small set of gold-related trace elements. Consequently, a more detailed study of hydrothermal alteration within individual gold occurrences and host rock types was considered necessary. This study investigates the relation between hydrothermal alteration and gold concentration within the host rocks of the Kelokorpi, Kuittila, Korvilansuo, Kivisuo, Elinsuo, Muurinsuo, and Rämepuro gold occurrences within the Hattu schist belt. Emphasis is placed on major and trace element mass transfer within mineralized zones, and various host rock types are treated separately. Large ion lithophile element systematics of the gold occurrences is also dealt with briefly.

Earlier work (Bornhorst and Rasilainen, 1993; Bornhorst et al., 1993; Rasilainen et al., 1993) suggested that more careful analysis was needed to reveal the existence of major element mass transfer associated with gold-related hydrothermal alteration. To meet this requirement, previous classifications of the host rocks have been slightly refined, the methods of chemical subgrouping of the main rock types have been unified, and the number of rock subtypes has been increased in this study. The sample set has also been unified by discarding samples with incomplete or missing major element analytical data. Due to the

gradually changing nature of the epiclastic rocks from north to south along the schist belt (Sorjonen-Ward, 1993), the background sam-

ples have been re-selected from a more restricted and appropriate area within the southern part of the study area.

GEOLOGY OF THE HATTU SCHIST BELT

The Hattu schist belt forms the easternmost part of the late Archean Ilimantsi Greenstone Belt, located at the southern end of a discon-

tinuous zone of Archean supracrustal sequences extending approximately 200 km north to Russia (Fig. 1). The Hattu schist belt

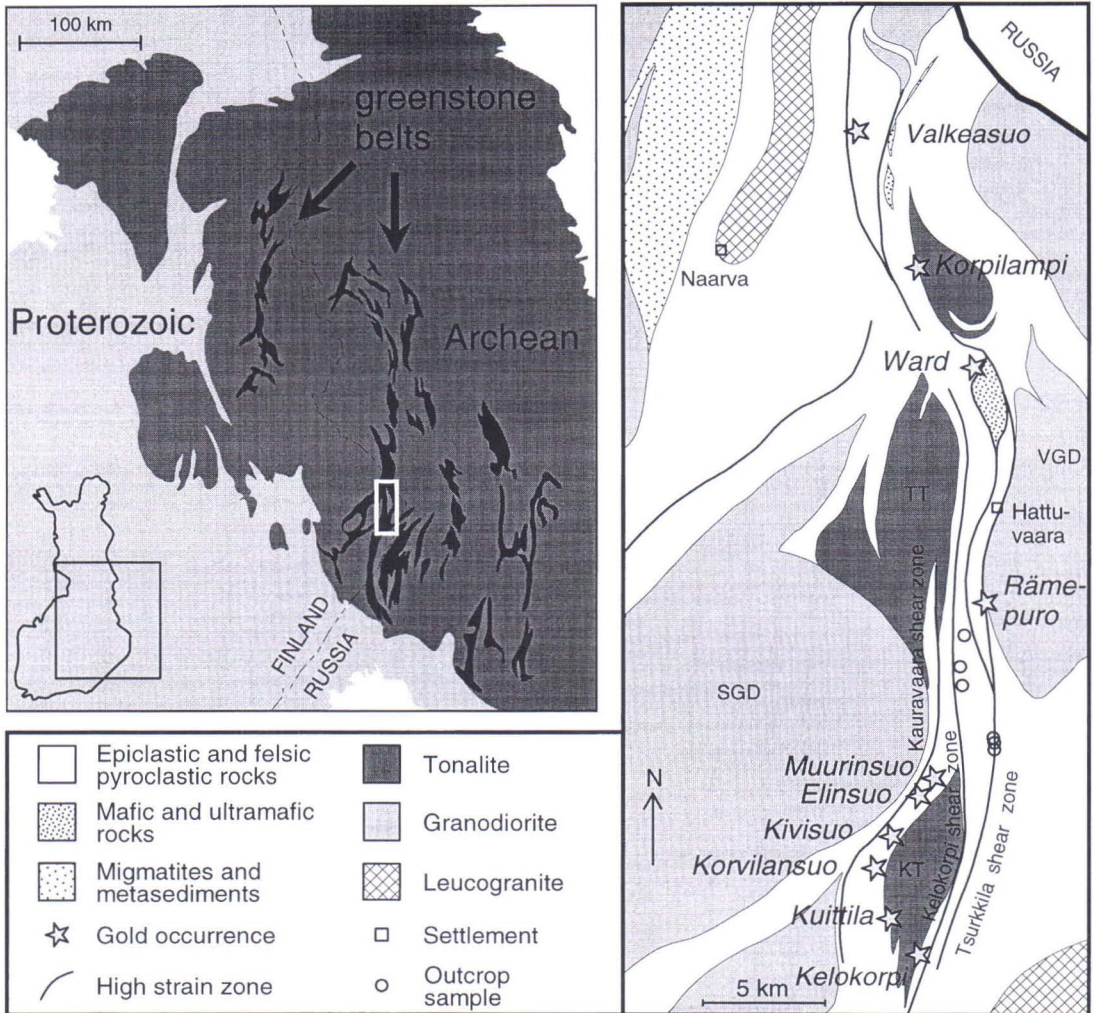


Fig. 1. Location and simplified geology of the Hattu schist belt. Locations of sampled outcrops north of the Muurinsuo gold occurrence are also shown. The regional map has been redrawn after Nurmi et al., 1993. KT: Kuittila Tonalite, TT: Tasaavaara Tonalite, SGD: Silvevaara Granodiorite, VGD: Viluvaara Granodiorite

consists of narrow, bifurcating, approximately north trending zones of supracrustal rocks anastomosing between and around syntectonic granitoid plutons. The belt is more than 50 km long but usually less than 5 km wide and at its narrowest part it is less than 2 km wide. The northern part of the belt is characterized by coarse-grained felsic volcanoclastic rocks with minor intercalated andesitic, basaltic and ultramafic lava flows, while the southern part, south of the village of Hattuvaara, is dominated by mica schists and graywackes of volcanoclastic origin (Nurmi et al., 1993; Sorjonen-Ward, 1993). The age of the earliest exposed volcanic rocks in the belt is about 2755 Ma (Vaasjoki et al., 1993). A series of ca. 2745 Ma old tonalite stocks and associated porphyry dikes intrude the supracrustal rocks. The metamorphic conditions during prograde metamorphism reached upper greenschist-lower amphibolite facies, as deduced from mineral assemblages and garnet-biotite geothermometry (O'Brien et al., 1993; Sorjonen-Ward, 1993).

Large-scale hydrothermal alteration is indicated both by extensive till geochemical anomalies of Au, As, and B overlapping the whole Hattu schist belt, and by more localized till and rock geochemical anomalies for many elements (e.g., As, Ag, Au, B, Bi, Mo, Te, W, loss on ignition (LOI), Na) overlying and surrounding zones of mineralized bedrock (Hartikainen and Nurmi, 1993; Rasilainen et al., 1993). More than 10 gold occurrences have been found adjacent to and within a number of high strain zones tens of kilometers

in length (Nurmi et al., 1993; Sorjonen-Ward, 1993). Gold is mostly hosted by clastic sedimentary rocks or tonalitic intrusions. Mineralized zones often transect lithologic boundaries, but contact zones with competent bodies such as tonalitic intrusions and felsic dikes are often mineralized. Gold is typically disseminated throughout sheared and hydrothermally altered schists. Gold-bearing quartz±tourmaline±carbonate veins are of minor importance and occur primarily in felsic intrusive rocks. Fine-grained native gold occurs mostly intergrown with tellurides and native bismuth as a discrete intergranular phase between silicates, sulfides and carbonates (Kojonen et al., 1993). The age of gold deposition has been constrained to between 2.74–2.70 Ga, which postdates early regional deformation and metamorphism and is less than 50 Ma younger than the main phase of granitoid intrusion (Nurmi, 1993). However, metamorphic textures indicate recrystallization of altered assemblages such that the regional metamorphic peak broadly coincided with or postdated gold deposition (Sorjonen-Ward, 1993).

The Hattu schist belt can be divided into four gold potential zones, based mainly on till geochemical anomalies and structural features of the bedrock. They are, from south to north, the Kuittila, Hattuvaara, Pampalo, and Hosko anomaly zones (Nurmi et al., 1993). Only gold occurrences from the Kuittila and Hattuvaara zones are included in this study, because of the lack of chemical analyses of samples from the other zones.

The Kuittila zone

The Kuittila zone includes both the Kuittila Tonalite and the adjoining schists on both sides of the tonalite stock (Figs. 1 and 2), and is best defined by till geochemical anomalies, in particular positive Au, Te, and LOI, and negative Na anomalies (Hartikainen and Nurmi, 1993). The zone trends southward from

near the northern tip of the Kuittila Tonalite and is bounded on the northwest by the Kau-ravaara shear zone, and on the southeast by the Kelokorpi and Tsurkkila shear zones. The Kuittila zone continues some kilometers to the south from the southern end of the Kuittila Tonalite, but delineating its boundaries there

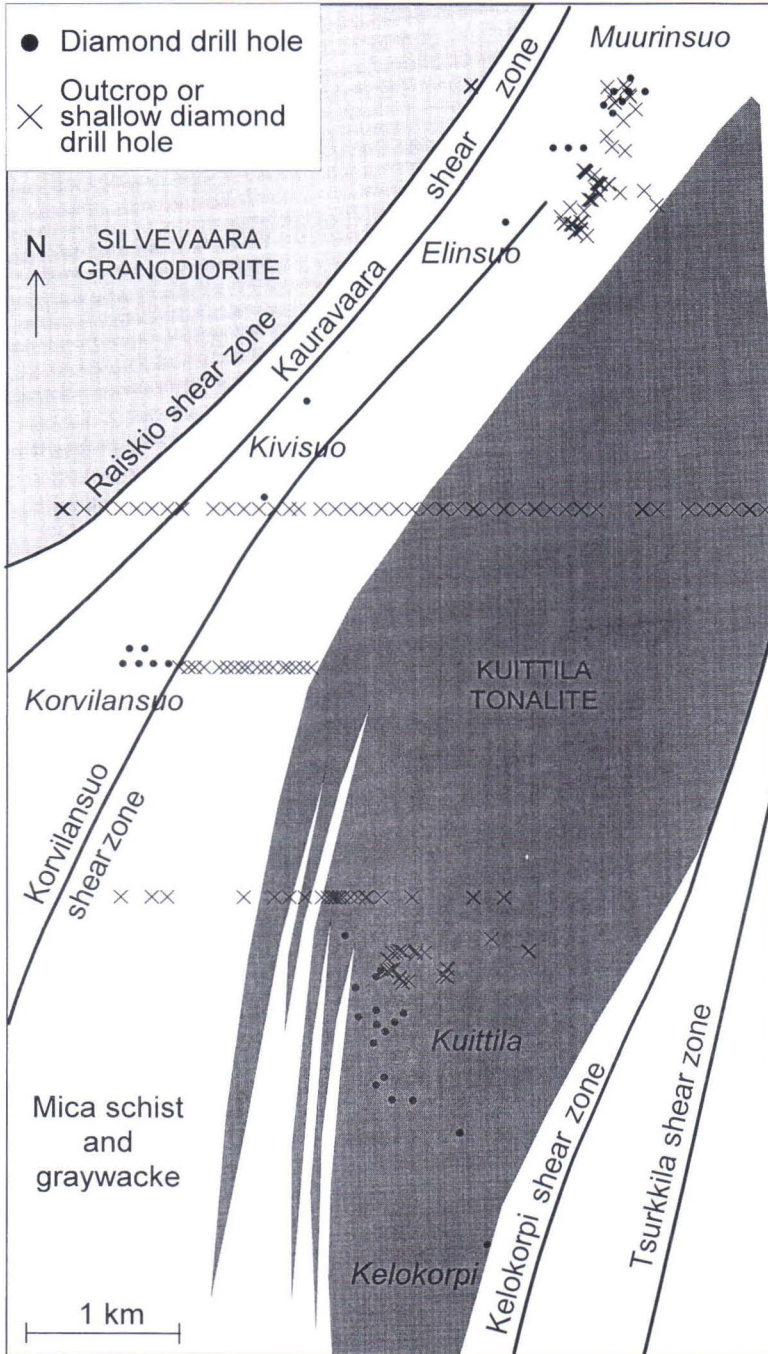


Fig. 2. Simplified geology of the Kuittila zone, including locations of sampled diamond drill holes and outcrops.

accurately has not been possible, due to inadequate exposure and lack of drilling.

The Kuittila Tonalite is a lenticular, sheet-like body which dips about 60° to the west, beneath the schist belt. The tonalite is typically medium-grained, equigranular and foliated, with quartz, plagioclase, biotite, and muscovite as the main minerals. Hornblende is absent and potassium feldspar is rare (Nurmi et al., 1993; Kojonen et al., 1993). Within mineralized zones, the tonalite has been affected by hydrothermal alteration. Where strongest, this alteration has caused partial or total breakdown of primary plagioclase and biotite, and their replacement by a quartz-sericite-calcite mineral assemblage (Sorjonen-Ward, 1993).

Porphyry dikes, varying in thickness from a few centimeters to several tens of meters, with phenocrysts of quartz and plagioclase are common in the Kuittila zone, especially at the western margin of the pluton. They are geochemically similar to the Kuittila Tonalite, and their abundance increases near the tonalite, suggesting a close relationship. However, the intrusive relationship between the dikes and the tonalite has not been established.

The supracrustal rocks belong to the Korvilansuo Formation and are probably among the oldest exposed units in the Hattu schist belt (Sorjonen-Ward, 1993). The thickness of strata separating these rocks from their original depositional basement, and the nature of the original basement, is unknown. The supracrustal rocks are mostly turbiditic feld-

spathic graywackes that alternate with more pelitic horizons (Nurmi et al., 1993). Thickness of individual beds varies from tens of centimeters to several meters (Sorjonen-Ward, 1993). The schists show widespread hydrothermal alteration, as indicated by the abundance of chlorite-sericite-biotite dominated mineral assemblages. Disseminated sulfides are sparse and quartz veining is insignificant. Primary lithologic layering has been preserved in many outcrops and depositional grading and current bedding are sporadically present (Sorjonen-Ward, 1993). Mafic intercalations up to several meters in thickness are relatively common. On the basis of chemical composition, the supracrustal rocks closely resemble rocks that have been interpreted as volcanoclastic elsewhere in the belt. Thus, they probably represent reworking and distal deposition of relatively locally derived material (O'Brien et al., 1993).

The Kuittila zone can further be subdivided into two parts, the Korvilansuo-Muurinsuo subzone in the north, and the Kelokorpi-Kuittila subzone in the south (Fig. 2). In the Korvilansuo-Muurinsuo subzone, which includes the Korvilansuo, Kivisuo, Elinsuo, and Muurinsuo gold occurrences, mineralized zones occur consistently within the sedimentary rocks along the northwestern boundary of the Kuittila Tonalite. In the less continuous Kelokorpi-Kuittila subzone, which includes the Kelokorpi and Kuittila gold occurrences, mineralized rocks are mostly tonalites.

The Hattuvaara zone

The Hattuvaara zone (Fig. 1) is manifested by locally intense deformation and alteration of the schists, together with anomalous concentrations of As, Bi, and Te in till near the margin of the Viluvaara granodiorite (Nurmi

et al., 1993). However, the extent of this zone has not yet been precisely defined. The only known gold occurrence within the zone is situated at Rämepuro.

MATERIALS AND METHODS

Rock samples

Rock sampling in the Hattu schist belt was carried out by the Ilomantsi Gold Project during 1986–1990. This study is based on a total of 1038 samples taken from outcrops (82 samples), shallow diamond drill cores (87 samples) and exploration diamond drill cores (869 samples from 38 drill holes). The locations of the sampled drill holes and outcrops are given in Figs. 1 and 2, and in more detail in connection with the descriptions of the individual gold occurrences (Figs. 15, 19, 23, 30, and 37).

The main purpose of outcrop and shallow diamond drill core sampling was to obtain geochemically representative samples of the various rock types of the schist belt and the granitoids. A large proportion of these samples were taken outside the mineralized areas. Outcrop samples were also taken in proximity to gold occurrences at Kuittila (14 samples) and Muurinsuo (51 samples). Diamond drill core material from mineralized zones was

sampled in order to study the geochemistry of gold mineralization.

Samples were selected from diamond drill cores according to their gold contents to obtain a representative set from barren hanging-wall rock through to barren footwall rock or the cores were analyzed completely. The drill cores were halved in 0.5 to 1 m intervals taking into consideration lithologic contacts, veins, and major petrographic changes.

The shallow diamond drill cores are mostly 2 to 10 m long, and 1 m of homogeneous rock was selected for multi element analysis. Each outcrop sample consists of three subsamples representing the same rock type and taken by portable diamond drilling equipment from a small area. For all outcrops and shallow diamond drill cores, care was taken to collect only visually fresh samples without signs of alteration, mineralization, foreign inclusions, or veins.

Analytical techniques

Outcrop samples and halved 0.5–1 m drill core samples were crushed with a jaw crusher to less than 3 mm grain size. Crushed samples were split and about 100 g of each was milled with a swing mill using a carbon steel pan. Drill core samples of desired length (usually 1–5 m) were combined from the 0.5–1 m subsamples by weighing an amount proportional to the length of each subsample and mixed thoroughly. Chemical analyses were done using many analytical techniques during 1986–1990 at the laboratories of the Geological Survey of Finland (GSF) in Rovaniemi and Kuopio, and at X-Ray Assay Laboratories Ltd. (XRAL) in Toronto, Canada. The analytical techniques and detection limits are summarized in Table

1. Although most elements were analyzed by at least two different methods, no apparent biases were detected in studying the results.

Gold was analyzed at the GSF by graphite furnace atomic absorption spectrometry (GFAAS) using 5 to 20 g of sample material. The technique, involving aqua regia digestion and reductive coprecipitation of Au using Hg as a collector and stannous chloride as a reductant (Niskavaara and Kontas, 1990), allows reliable determination of Au down to 1 ppb level. Higher detection limits were used for mineralized drill core samples. Silver and Te were analyzed by GFAAS, at the GSF using the same technique as for Au and at XRAL after acid extraction.

Table 1. Analytical techniques, detection limits, and number of samples analyzed by each technique. AAS: atomic absorption spectrometry; DCP: direct current plasma atomic emission spectrometry; FAAS: flame atomic absorption spectrometry; FADCP: fire assay direct current plasma atomic emission spectrometry; GFAAS: graphite furnace atomic absorption spectrometry; ICP-MS: inductively coupled plasma mass spectrometry; LECO: sulphur analyzer; NA: instrumental neutron activation; WET: wet chemistry; XRF: X-ray fluorescence spectrometry. XRAL: X-Ray Assay Laboratories Ltd.; GSF: Geological Survey of Finland.

Element	Method	Laboratory	Detection limit (ppm)	Number of samples	Element	Method	Laboratory	Detection limit (ppm)	Number of samples
SiO ₂	XRF	XRAL	100	1038	Cr	NA	XRAL	0.5	92
TiO ₂	XRF	XRAL	100	1038		NA	XRAL	2	83
Al ₂ O ₃	XRF	XRAL	100	1038		DCP	XRAL	2	3
Fe ₂ O ₃	XRF	XRAL	100	1038		XRF	XRAL	10	860
MnO	XRF	XRAL	100	1038	Cu	DCP	XRAL	0.5	181
MgO	XRF	XRAL	100	1038		FAAS	GSF	1	857
CaO	XRF	XRAL	100	1038	Li	AAS	XRAL	1	597
Na ₂ O	XRF	XRAL	100	1038		AAS	XRAL	10	83
K ₂ O	XRF	XRAL	100	1038	Mo	FAAS	GSF	1	358
P ₂ O ₅	XRF	XRAL	100	1038		DCP	XRAL	1	499
LOI	XRF	XRAL	100	1038		ICP-MS	XRAL	1	6
						NA	XRAL	2	92
Ag	GFAAS	GSF	0.01	361		NA	XRAL	5	83
	GFAAS	XRAL	0.02	470	Ni	FAAS	GSF	1	857
	DCP	XRAL	0.5	207		DCP	XRAL	1	181
As	FAAS	XRAL	0.1	860	Pb	FAAS	GSF	1	857
	NA	XRAL	1	95		DCP	XRAL	2	181
	NA	XRAL	2	83	Rb	ICP-MS	XRAL	1	6
Au	GFAAS	GSF	0.001	178		XRF	XRAL	10	1032
	FADCP	XRAL	0.004	3	S	XRF	XRAL	50	6
	GFAAS	GSF	0.01	727		LECO	GSF	100	1032
	GFAAS	GSF	0.02	91	Sr	ICP-MS	XRAL	1	3
	GFAAS	GSF	0.05	39		XRF	XRAL	10	1035
B	NA	XRAL	0.5	15	Te	GFAAS	GSF	0.001	178
	DCP	XRAL	10	1023		GFAAS	GSF	0.01	358
Ba	XRF	XRAL	10	1038		GFAAS	XRAL	0.02	470
Bi	DCP	XRAL	0.1	92	W	FAAS	GSF	1	115
	FAAS	XRAL	0.1	857		NA	XRAL	1	582
	ICP-MS	XRAL	0.1	6		ICP-MS	XRAL	1	38
	DCP	XRAL	0.5	83		NA	XRAL	3	83
Co	NA	XRAL	0.1	92		FAAS	GSF	10	91
	NA	XRAL	1	83	Zn	DCP	XRAL	0.5	181
	ICP-MS	XRAL	1	6		FAAS	GSF	1	857
	FAAS	GSF	1	857	Zr	ICP-MS	XRAL	1	6
CO ₂	WET	XRAL	100	1038		XRF	XRAL	10	1032

Mass transfer calculations

The mass transfer calculations are based on an equivalent mass assumption (Grant, 1986) and were performed using the equation

$$\Delta M_i = (IR \times c_i^a - c_i^o) \times M^o$$

where M_i is the change of mass of component i relative to the original mass, and c_i^a and c_i^o are the concentrations of component i in the altered rock (a) and the original precursor rock (o) in units defined by M^o , the equivalent mass before alteration. IR, the inverse of an isocon as defined by Grant (1986), is called the immobile element ratio, and is a correction factor based on the contents of one or more elements assumed to have remained immobile during alteration:

$$IR = c_j^o / c_j^a$$

where c_j^o is the concentration of an immobile component j in the precursor rock and c_j^a is its concentration in the altered rock. For derivation of the mass transfer equation and IR, see Bornhorst and Rasilainen (1993).

The validity of mass transfer calculations according to the above equation is dependent on the estimation of IR and correct choice of parent rock. Consequently, the selection of the elements used to estimate IR is critical.

Because no element can be regarded as invariably immobile, using a number of relatively immobile elements to estimate IR is preferable. In lode gold deposits, Ti, Al, and Zr usually appear to be immobile, at least during the less intense phases of gold-related wall-rock alteration (Perring et al., 1990; Groves and Foster, 1991). These elements have also been found to be immobile within the gold occurrences of the Hattu schist belt (Bornhorst and Rasilainen, 1993). For every sample, three values of IR were calculated using each of these elements in turn, and the median of these values was used as an estimate of the sample IR. Usually the IR values calculated using the individual elements are very close to each other. The median, being less sensitive than the mean to mobility of one of the elements is considered to represent the sample IR best.

The concentrations of certain components, especially Bi, CO₂, Mo, and W are often below the analytical detection limit. In such cases, a value equal to the detection limit divided by two was assigned to the element in question and this causes some uncertainty to the calculated mass transfer values. For any sample, mass transfer could not be calculated for elements with both pre-alteration and present concentrations below the detection limit.

ROCK TYPES AND PRIMARY CHEMICAL COMPOSITIONS

Rock type classification

The rocks of the Hattu schist belt have experienced metamorphic conditions that reached upper greenschist–lower amphibolite facies, although the prefix 'meta' is not used here in rock names. Where possible, names corresponding to the unaltered precursor ma-

terial are used (e.g., graywacke instead of quartz-feldspar schist) but where the nature of the precursor is uncertain, a descriptive name (e.g., sericite-chlorite schist) is used. Nevertheless, all the rocks have experienced the same degree of metamorphism, even though

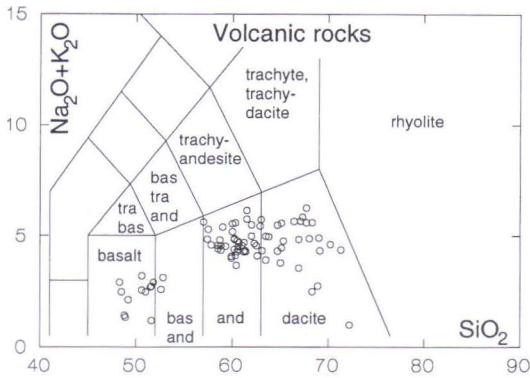


Fig. 3. SiO_2 - $\text{Na}_2\text{O}+\text{K}_2\text{O}$ diagram for the Hattu schist belt volcanic rocks. bas and: basaltic andesite, and: andesite, tra bas: trachybasalt, bas tra and: basaltic trachyandesite.

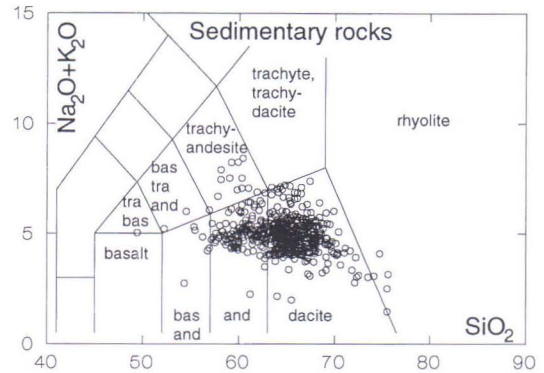


Fig. 4. SiO_2 - $\text{Na}_2\text{O}+\text{K}_2\text{O}$ diagram for the Hattu schist belt sedimentary rocks to facilitate comparisons with the igneous rocks. bas and: basaltic andesite, and: andesite, tra bas: trachybasalt, bas tra and: basaltic trachyandesite.

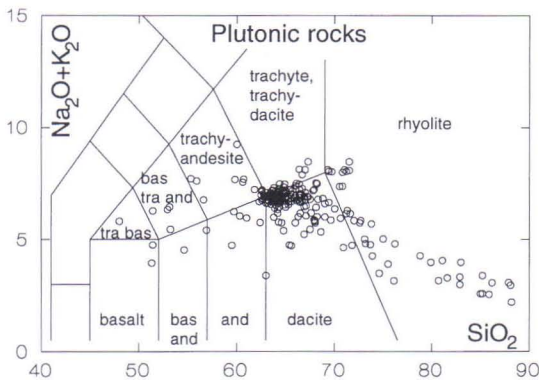


Fig. 5. SiO_2 - $\text{Na}_2\text{O}+\text{K}_2\text{O}$ diagram for the Hattu schist belt plutonic rocks. bas and: basaltic andesite, and: andesite, tra bas: trachybasalt, bas tra and: basaltic trachyandesite.

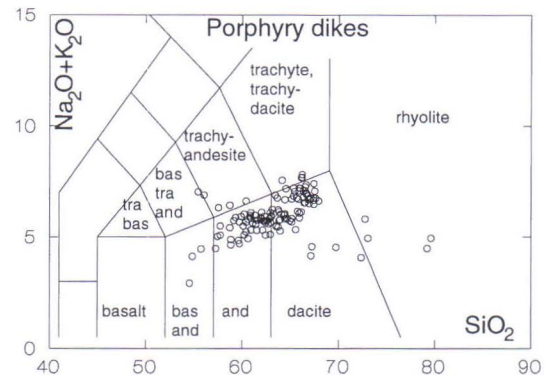


Fig. 6. SiO_2 - $\text{Na}_2\text{O}+\text{K}_2\text{O}$ diagram for the Hattu schist belt porphyry dikes. bas and: basaltic andesite, and: andesite, tra bas: trachybasalt, bas tra and: basaltic trachyandesite.

the degree of deformation is variable.

The rocks of the Hattu schist belt can be grouped into four main groups. Clastic sedimentary rocks are the most abundant, especially in the southern part of the belt, where this study is concentrated. Plutonic rocks include the Kuittila Tonalite and some small mafic (gabbroic) sills at Korvilansuo. Felsic porphyry dikes and volcanic rocks are the least abundant main rock types.

When calculating mass transfer, the compo-

sition of an altered rock is compared with the composition of its precursor, which must be either known or estimated. The more uncertain the precursor composition, the more inaccurate is the resulting calculation. All the main rock types in the Hattu schist belt show large variations in chemical composition, which can lead to inaccuracies in mass transfer calculations (Figs. 3–6). To reduce this problem, Bornhorst et al. (1993) divided the rock types into chemical subtypes using ratios

Table 2. Total length (m) of analyzed drill core for the rock types and subtypes from individual gold occurrences. The number of available drill holes, as well as their locations with respect to the mineralized zones, are different for each gold occurrence. Consequently, the sample lengths do not represent actual proportions of the rock types in the study area.

Rock type/ subtype	Non- prospect	Räme- puro	Muurin- suo	Elin- suo	Kivi- suo	Korvilan- suo	Kuittila	Kelo- korpi
Volcanic rocks								
Mafic	-	15.70	24.65	-	0.55	1.00	-	-
Intermediate 1	1.00	109.00	-	-	-	-	-	78.20
Intermediate 2	-	50.50	88.00	-	-	7.75	-	-
Sedimentary rocks								
subtype 1	8.85	12.50	7.95	-	26.80	6.00	-	-
subtype 2	9.60	67.55	212.10	8.00	68.90	39.50	13.00	-
subtype 3	2.50	12.00	498.00	47.55	54.80	152.90	-	5.65
subtype 4	6.80	34.50	127.40	12.65	6.70	176.60	11.00	-
Plutonic rocks								
subtype 1	-	-	-	-	-	37.65	-	-
subtype 2	42.15	4.45	4.80	-	-	13.30	892.00	44.75
subtype 3	10.50	34.70	-	-	-	72.20	10.00	-
subtype 4	10.90	-	-	-	-	-	-	-
Porphyry dikes								
subtype 1	-	7.20	135.55	0.60	1.60	-	-	-
subtype 2	1.00	-	50.45	3.65	2.60	-	-	-
subtype 3	19.65	-	-	-	-	119.30	-	8.85

of immobile elements. To decrease the compositional variation within the subtypes further, the number of subtypes was expanded in this study. To unify the classification process, the ratios Zr/Ti and Al/Fe were used for all the rock types. These elements are usually immobile in gold-related hydrothermal alteration (e.g., Perring et al., 1990). Both Zr/Ti and Al/Fe tend to increase with increasing SiO₂ and decreasing MgO contents in igneous rocks, reflecting magmatic differentiation processes. In sedimentary rocks, these ratios effectively reflect the proportions of mafic and felsic minerals. The results of this classification were checked against plots of other usually immobile elements (e.g., Ni, Cr, Sc, Th, REE) and their ratios. Where most intense, alteration has also affected the immobile element ratios, and in cases where the effect of alteration could be confirmed visually (e.g., quartz-tourmaline brecciation, bititization in shear zones), samples were clas-

sified according to their nearest unaltered neighbors. In general, measures were taken to minimize the variation of subtypes within a continuous magmatic rock unit. The sedimentary rocks have heterogenous compositions because rhythmic depositional units are often thin-bedded, and accordingly the alternation of subtypes within sedimentary units could not be reduced.

The volcanic rocks were classified into three subtypes: mafic, intermediate 1 and intermediate 2 (Fig. 7); there are no ultramafic volcanic rocks among the samples. The mafic samples form a separate cluster on the Zr/TiO₂ - Al₂O₃/Fe₂O₃ diagram, but the intermediate samples form a single continuous cluster. The subdivision of the intermediate samples into two subtypes is arbitrary and aimed at reducing chemical variation within the subtypes. Some samples of the intermediate subtype 2 are relatively felsic. The geographic distribution of the samples belonging

to these subtypes is uneven: the mafic and intermediate subtype 2 samples are mainly from Rämepuro and Muurinsuo, while the samples of the intermediate subtype 1 are

from Rämepuro and Kelokorpi (Table 2).

The sedimentary rocks were divided into four subtypes (Fig. 8). Due to the continuous spread in chemical composition of the sedi-

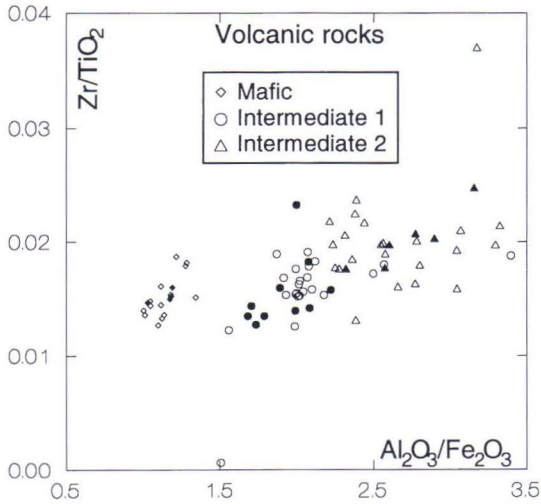


Fig. 7. Division of volcanic rocks into chemical subtypes. The least altered samples are shown as filled symbols. For selection criteria for the least altered samples, see text.

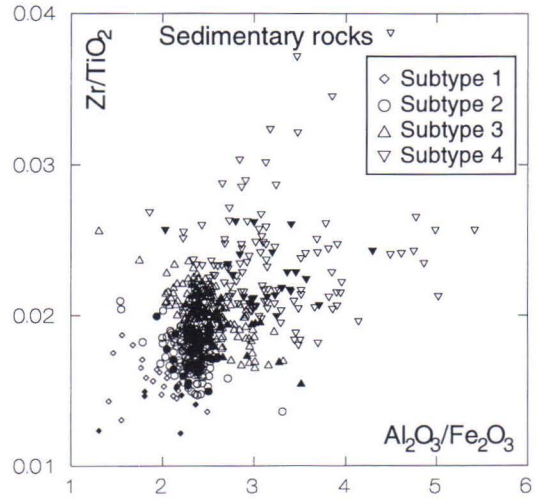


Fig. 8. Division of sedimentary rocks into chemical subtypes. The least altered samples are shown as filled symbols. For selection criteria for the least altered samples, see text.

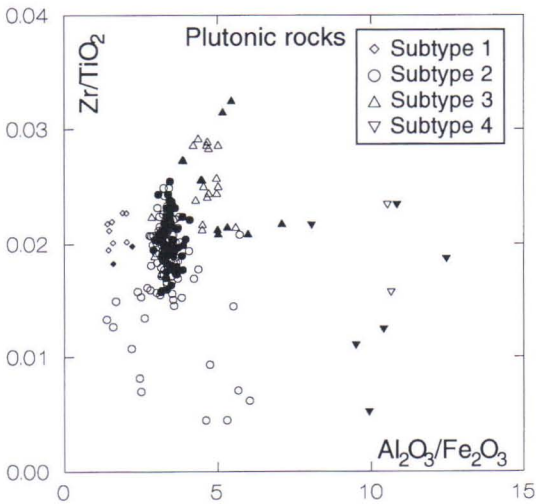


Fig. 9. Division of plutonic rocks into chemical subtypes. The least altered samples are shown as filled symbols. For selection criteria for the least altered samples, see text.

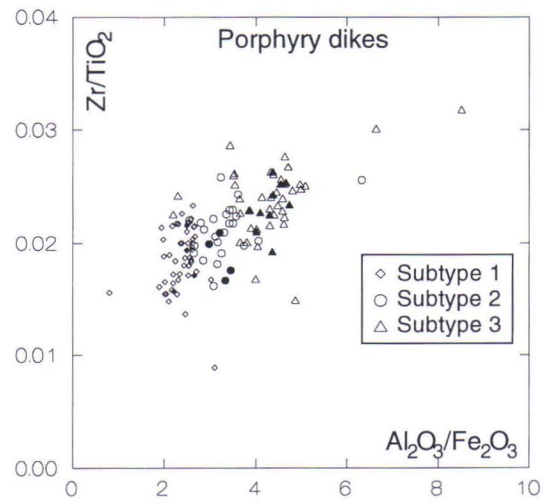


Fig. 10. Division of porphyry dikes into chemical subtypes. The least altered samples are shown as filled symbols. For selection criteria for the least altered samples, see text.

mentary rocks, the classification is entirely arbitrary and is only aimed at reducing the variation of the element concentrations. The sedimentary subtypes are distributed more or less evenly among the gold occurrences containing sedimentary rocks.

The plutonic rocks were divided into four subtypes (Fig. 9). The mafic gabbroic samples of subtype 1 form a separate cluster on the $Zr/TiO_2 - Al_2O_3/Fe_2O_3$ diagram. Subtype 2 represents typical Kuittila Tonalite, and most of the samples, including those that are least altered cluster within a restricted area. The scatter in a small part of the subtype 2 samples on the $Zr/TiO_2 - Al_2O_3/Fe_2O_3$ diagram is very probably due to hydrothermal alteration. Subtype 3 forms a loose cluster above and to the right of the subtype 2 samples, and subtype 4, which represents the central phase of

the Kuittila Tonalite, is separated from the other subtypes by a higher Al_2O_3/Fe_2O_3 ratio. The geographic distribution of the plutonic subtypes is irregular. Rocks of subtype 1 occur only at Korvilansuo, and subtype 2 is practically restricted to Kuittila and Kelokorpi (Table 2). Subtype 3 occurs mainly at Korvilansuo and Rämepuro, and subtype 4 is also restricted to a limited area outside mineralized zones.

Porphyry dike samples form a coherent and continuous cluster on the $Zr/TiO_2 - Al_2O_3/Fe_2O_3$ diagram (Fig. 10). Consequently, the subdivision is arbitrary, and was only done to reduce variation in chemical abundances. The porphyry dikes were divided into three subtypes. Subtypes 1 and 2 are concentrated around Muurinsuo, while subtype 3 occurs mostly at Korvilansuo (Table 2).

Least altered samples and background compositions

Most of the samples analyzed from the southern part of the Hattu schist belt represent core material from diamond drill holes penetrating mineralized rocks. Accordingly, samples that definitely lie outside the mineralized zones are few. The restricted distribution of some rock subtypes also places limitations on the selection of unaltered samples. As a first approximation, the least mineralized samples ($Au \leq 5$ ppb) without obvious visual signs of mineralization were taken to represent the least altered rocks of the Hattu schist belt. For the igneous rocks, $100 \times K_2O / (K_2O + Na_2O) - K_2O + Na_2O$ diagrams (after Hughes, 1973) were used to discriminate hydrothermally altered samples further (Figs. 11–13). The sedimentary rocks were plotted on a similar diagram (Fig. 14) for comparison. The volcanic, plutonic, and sedimentary rocks define similar trends which exceed the limits of the spectrum of igneous compositions. This indicates hydrothermal alteration of a significant proportion of the igneous samples. Although the

limits of the igneous spectrum are not directly applicable to sedimentary rocks, the similarities in the trends of the igneous and sedimentary rocks suggest that most of the sedimentary samples are also somewhat altered. Nearly all of the volcanic mafic and intermediate subtype 1 samples plot outside the igneous spectrum. Consequently, even the least altered compositions of these rock types, represented by the least mineralized samples, are altered, at least with respect to the alkali metals. For the plutonic rocks, the porphyry dikes, and the volcanic intermediate subtype 2, the least mineralized samples plot mainly within the igneous spectrum. For these rock types, the selection of the least altered samples was refined by discarding those samples that plot outside the igneous spectrum. No trimming of the least altered sedimentary rock samples was done based on the $100 \times K_2O / (K_2O + Na_2O) - K_2O + Na_2O$ diagram.

The least altered samples were used to estimate the primary chemical compositions of

the main rock types. The estimated background compositions of all the rock subtypes are given in Appendices 1–4. The present estimates agree generally with the previous estimates made by Bornhorst et al. (1993) using fewer rock subtypes.

Due to the widespread alteration within the Hattu schist belt, the least altered abundances of certain elements associated with mineralization (Ag, As, Au, B, Bi, CO₂, Mo, S, Te, W) are unrealistically high for many rock sub-

types. Values from other subtypes of the same rock type or from the literature were therefore used to estimate the background abundances in these cases. The abundance of gold in primary igneous rocks is usually well below 5 ppb, and only rarely exceeds 10 ppb (Tilling et al., 1973). Most researchers have reported average values equal or smaller than 2 ppb for gold in igneous and sedimentary rocks of Archean to recent age (e.g., Anhaeusser et al, 1975; Kwong and Crocket, 1978; Saager and

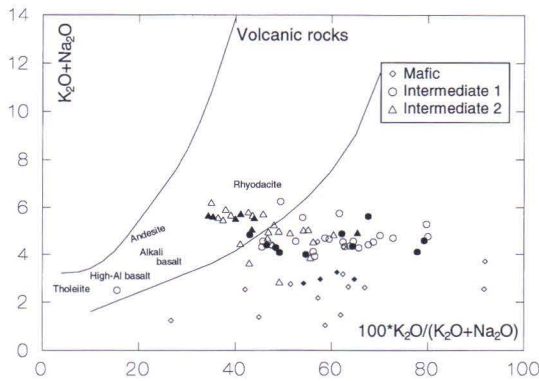


Fig. 11. Hughes diagram showing volcanic rock compositions. Samples with Au ≤ 5 ppb and without obvious signs of mineralization are shown as filled symbols.

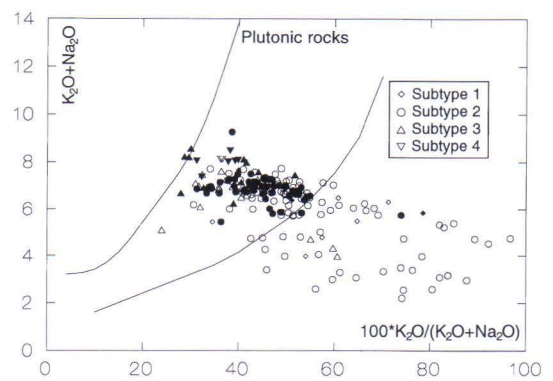


Fig. 12. Hughes diagram showing plutonic rock compositions. Samples with Au ≤ 5 ppb and without obvious signs of mineralization are shown as filled symbols.

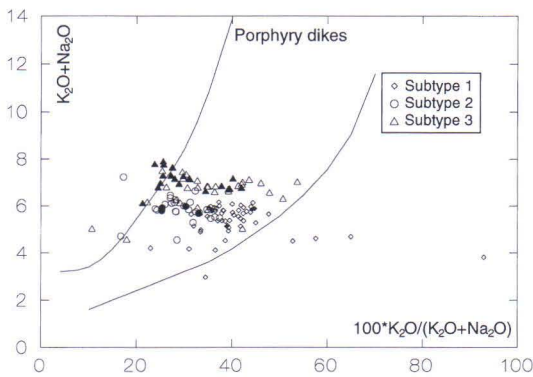


Fig. 13. Hughes diagram showing porphyry dike compositions. Samples with Au ≤ 5 ppb and without obvious signs of mineralization are shown as filled symbols.

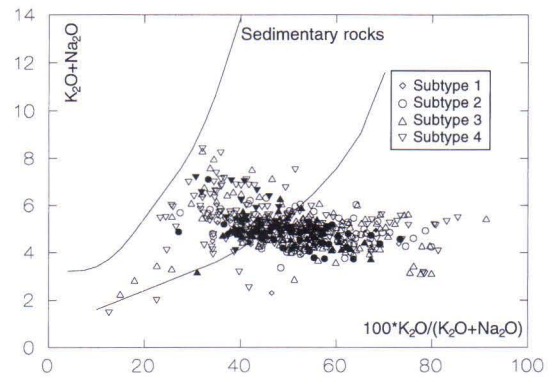


Fig. 14. Hughes diagram showing sedimentary rock compositions. Samples with Au ≤ 5 ppb and without obvious signs of mineralization are shown as filled symbols.

Meyer, 1984; Kontas et al., 1986, 1990; Nurmi et al., 1991). Crocket (1991) reports somewhat higher group averages for Precambrian volcanic rocks (4.2–12.4 ppb), but only 1.5 ppb for Precambrian granitic plutons. The value of 2 ppb, which was selected to represent the background abundance of gold for most of the rock subtypes within the Hattus schist belt agrees well with published data and with the low values for some subtypes (see

Appendices 1–4). The estimated background values of Ag (0.06–0.1 ppm), As (2–3 ppm), B (15–20 ppm), Bi (0.05 ppm), Mo (2 ppm), Te (10–73 ppb), and W (1–2 ppm) for some of the subtypes are based on either values from the other subtypes of the same rock type or published data (Govett, 1983, and references therein). The values of CO₂ (0.02–0.15%) and S (0.01–0.31%) are based on values from other subtypes of the same rock type.

Primary geochemical variations

Primary compositional variations (i.e., variations not caused by alteration) within the rocks cause ostensible mobility in mass transfer calculations. The amount of this primary variation was estimated by calculating the mass transfer of every element for each of the main rock types using the previously selected least altered samples. The mass transfer values of the elements were plotted on probability plots separately for each rock type. The distribution of the mass transfer values approaches normal or log-normal distribution for most of the elements, with a small number of obvious outliers. The outliers were discarded and statistics were calculated for the mass transfer of the elements for every rock type. Two standard deviations from the median, defined using this trimmed set of least altered samples, were selected as the limits beyond which the gain or loss of an element within a mineralized zone can reasonably be attributed to hydrothermal alteration. The estimated limits of background compositional variation for the main rock types are given in Table 3. The ranges of major element primary abundances for the igneous rocks are usually no more than half of the ranges defined by Bornhorst and Rasilainen (1993), and vary from equal to half for the sedimentary rocks. The ranges of primary abundances of most of the trace elements vary from equal to half of those of

Bornhorst and Rasilainen (1993), but the ranges of As, B, CO₂, Mo, S, and Te are larger for some rock types. The lower estimated primary geochemical variation for most elements is due to the larger number of rock subtypes used in this study, and to the fact that the primary variation limits were defined separately for each rock type, while Bornhorst and Rasilainen (1993) pooled all the unaltered samples.

For most of the rock subtypes, the abundances of Ag, As, Au, B, Bi, CO₂, Mo, S, Te, and W for the least altered samples are unrealistically high, and the background estimates are based on either published data or values from another subtype. Consequently, these elements appear enriched within the set of the least altered samples, and their distributions deviate most from normality or log-normality. A notable number of samples at the lower end of the compositional range, for which mass transfer could not be calculated because both the sample contents and the background contents are below detection limits, tend to increase this bias, especially for Ag, Au, Bi, and CO₂. Consequently, the defined limits of background compositional variation for Ag, As, Au, B, Bi, CO₂, Mo, S, Te, and W are large and are likely to include a hydrothermal component.

Table 3. Alteration within the least altered rocks: averages and estimated limits of variability caused by primary variations in background composition. N: trimmed number of samples (total number of samples for the rock group is shown in parentheses); s: standard deviation for the trimmed set of samples. Alteration is expressed as mass change of an element divided by its background abundance.

Element	Volcanic rocks			Sedimentary rocks			Plutonic rocks			Porphyry dikes						
	N (20)	Median -2s	Median +2s	N (115)	Median -2s	Median +2s	N (76)	Median -2s	Median +2s	N (19)	Median -2s	Median +2s				
Si	15	-0.09	0.01	0.10	109	-0.22	0.00	0.21	70	-0.13	0.00	0.13	15	-0.09	0.00	0.08
Ti	18	-0.03	0.01	0.05	112	-0.04	0.00	0.04	71	-0.04	0.00	0.04	18	-0.10	0.00	0.10
Al	15	-0.07	0.00	0.07	108	-0.11	0.00	0.11	71	-0.09	0.00	0.09	17	-0.07	0.00	0.07
Fe	17	-0.15	0.02	0.18	104	-0.09	0.00	0.10	70	-0.09	0.01	0.12	14	-0.09	-0.02	0.05
Mn	16	-0.19	-0.03	0.13	105	-0.34	0.03	0.40	68	-0.23	0.05	0.32	17	-0.27	-0.01	0.25
Mg	18	-0.12	0.02	0.17	111	-0.14	0.00	0.15	64	-0.10	0.02	0.14	15	-0.20	0.01	0.22
Ca	18	-0.56	-0.05	0.46	109	-0.64	-0.02	0.61	66	-0.23	0.03	0.28	15	-0.15	0.01	0.17
Na	17	-0.36	-0.02	0.32	110	-0.45	0.03	0.51	63	-0.18	0.00	0.18	16	-0.16	-0.02	0.13
K	15	-0.21	0.03	0.26	108	-0.32	-0.02	0.27	71	-0.28	0.02	0.32	14	-0.28	-0.02	0.24
P	15	-0.12	-0.04	0.04	106	-0.29	0.01	0.30	68	-0.09	0.00	0.09	17	-0.13	0.01	0.14
LOI	16	-0.25	-0.02	0.20	106	-0.29	0.01	0.31	63	-0.66	-0.09	0.48	15	-0.29	0.00	0.29
Ag	9	-0.33	1.64	3.60	89	-0.54	0.71	1.95	24	-0.99	-0.09	0.81	12	-0.34	0.25	0.84
As	17	-1.00	3.48	23.74	86	-1.00	-0.23	1.24	72	-1.00	-0.01	1.60	17	-1.00	1.38	3.79
Au	7	-1.00	-0.49	0.19	46	-1.00	-0.05	1.43	64	-1.00	0.00	1.53	6	-1.00	-0.25	1.15
B	15	-1.00	2.57	7.49	112	-1.00	2.01	11.93	70	-1.00	-0.09	2.00	13	-1.00	0.42	1.96
Ba	19	-0.43	0.01	0.45	107	-0.42	-0.03	0.36	65	-0.19	0.02	0.23	16	-0.33	0.06	0.44
Bi	11	1.90	4.93	7.95	108	-0.94	0.00	0.94	7	0.66	3.00	5.34	9	-0.64	1.17	2.98
Co	16	-0.24	0.00	0.24	106	-0.41	-0.03	0.35	69	-0.25	0.00	0.25	17	-0.45	-0.02	0.41
CO ₂	6	-1.00	0.54	2.10	44	-1.00	1.66	5.67	68	-1.00	3.72	11.29	14	-1.00	14.09	37.21
Cr	17	-0.19	0.04	0.27	99	-0.20	0.00	0.20	65	-0.22	0.03	0.29	18	-0.55	0.04	0.63
Cu	19	-0.48	0.02	0.51	106	-0.39	0.02	0.42	67	-1.00	0.00	1.28	16	-0.50	0.03	0.55
Li	10	-0.09	0.08	0.25	88	-0.47	0.00	0.48	68	-0.51	-0.06	0.39	11	-0.09	0.00	0.10
Mo	12	0.06	1.00	1.93	108	-1.00	0.89	3.82	52	-1.00	3.10	18.02	15	-0.93	0.45	1.84
Ni	16	-0.21	0.01	0.24	105	-0.47	-0.04	0.39	62	-0.17	0.02	0.21	14	-0.24	0.04	0.31
Pb	19	-0.66	-0.02	0.63	85	-0.56	0.14	0.84	64	-0.78	-0.03	0.72	15	-0.56	-0.01	0.54
Rb	18	-0.23	-0.01	0.22	112	-0.37	-0.01	0.36	70	-0.44	-0.01	0.41	17	-0.28	-0.05	0.18
S	16	-0.49	3.80	8.08	110	-0.68	0.57	1.81	54	-1.00	-0.46	9.58	14	-1.00	3.31	10.79
Sr	14	-0.45	0.02	0.49	110	-0.57	0.03	0.63	63	-0.29	-0.03	0.24	17	-0.28	-0.03	0.23
Te	13	1.25	4.93	8.60	96	-0.95	1.22	3.38	57	-1.00	0.02	1.33	15	-1.00	6.77	15.33
W	13	-0.73	2.05	4.84	61	-1.00	5.00	13.45	55	-1.00	2.35	12.80	15	-1.00	0.00	2.08
Zn	17	-0.24	0.02	0.28	109	-0.65	-0.13	0.40	72	-0.30	0.00	0.30	14	-0.17	-0.03	0.12
Zr	17	-0.08	0.00	0.08	111	-0.10	0.01	0.12	70	-0.20	0.00	0.20	16	-0.07	0.00	0.07

GEOCHEMICAL ALTERATION AT THE GOLD OCCURRENCES

Hydrothermal alteration is widespread throughout the Hattu schist belt and evident at the gold occurrences. Most of the sampled drill holes intersect or are situated within zones of alteration manifested by quartz-sericite-biotite-chlorite assemblages, disseminated iron sulfides, and elevated contents of Au (usually more than 10 ppb), Te (usually more than 100 ppb), and typically of one or

more of Ag, As, B, Bi, and S (Rasilainen et al., 1993). The width of these anomalous zones varies from several tens to hundreds of meters (Hartikainen and Nurmi, 1993). These wide alteration zones contain narrow, highly mineralized zones in which Au concentration equals or exceeds 1 ppm. Samples from the highly mineralized zones at each gold occurrence, together with contiguous samples that are less mineralized though still carrying at least 100 ppb Au, were used to study hydrothermal alteration associated with gold mineralization. A cutoff value of 100 ppb Au was selected to ensure that all the samples are clearly mineralized above the local background abundances. The zones of highest gold concentration are likely to coincide with the greatest fluid fluxes during mineralization, and to represent areas where interaction between the hydrothermal fluid and the host rocks was most intimately associated with gold mineralization. The results of the mass transfer calculations are given below for each gold occurrence. Terms used in the following text for the magnitude of mass change are given in Table 4. They are purely descriptive and do not constitute any rigorous classification of alteration intensity.

Table 4. Descriptive terms for alteration used in the text. Alteration of an element is expressed as mass change divided by background abundance.

Alteration	Description
Enrichment	Intense
	Strong
	Moderate
	Slight
Depletion	Moderate
	Strong

Kelokorpi

The Kelokorpi gold occurrence is located at the southeast margin of the Kuittila Tonalite, approximately 1.5 km southeast of the Kuittila gold occurrence (Fig. 2). Till geochemical anomalies define zones of elevated gold contents parallel to the tonalite contact (Nurmi et al., 1993), but only one of these anomalies has been drilled. No outcrops exist in the vicinity of the occurrence, and the following descriptions of the host rocks are based on drill core material from diamond drill hole 329 (Fig. 15). This drill hole intersects two mineralized

zones, one hosted by tonalite and the other by an intermediate schist of tuffaceous origin. Other rock types include graywacke and occasional, roughly concordant porphyry dikes (Nurmi et al., 1993). A $\text{SiO}_2 - \text{Na}_2\text{O} + \text{K}_2\text{O}$ diagram for the igneous rocks at Kelokorpi is given in Fig. 16 and average chemical compositions of least mineralized and strongly mineralized host rocks are given in Table 5.

The tonalite is weakly deformed and altered, and sheared in the mineralized zone. It contains thin quartz-carbonate veins with some

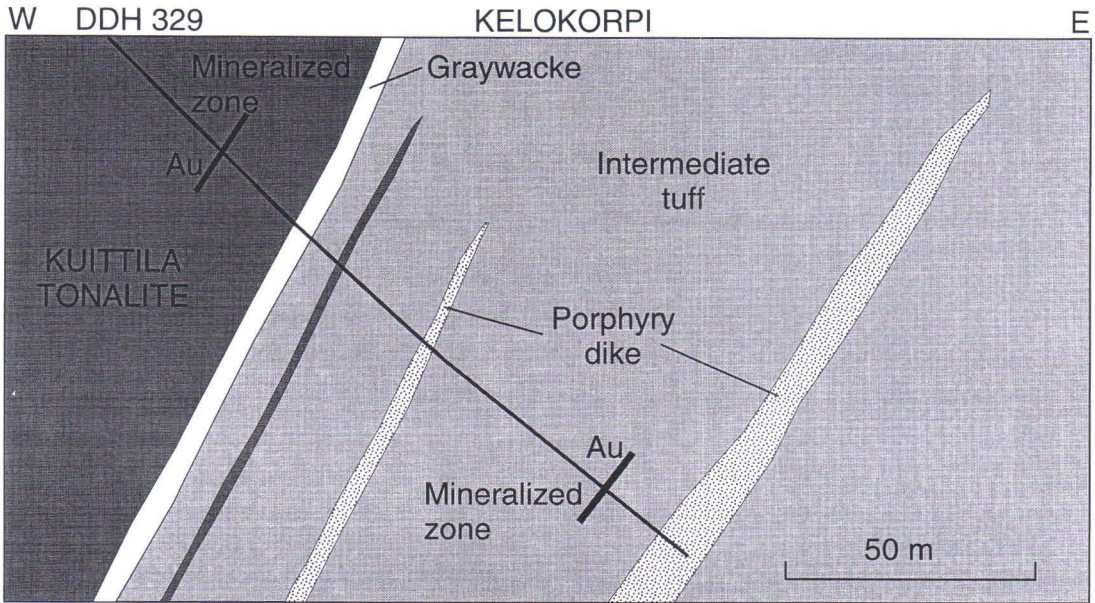


Fig. 15. Vertical cross-section through the Kelokorpi gold occurrence.

pyrite, pyrrhotite, chalcopyrite, sphalerite, galena, and sporadic molybdenite (Kojonen et al., 1993). Hydrothermal alteration has resulted in partial breakdown of plagioclase to sericite and calcite, and variable alteration of biotite to chlorite. The gold ore zone ($Au \geq 1$ ppm) is only 1 m wide, with a gold grade of 1.2 ppm.

Major minerals within the intermediate tuff are biotite, quartz, muscovite, potassium feldspar, and plagioclase. The rock contains sparse, but pervasive, disseminated pyrrhotite, sphalerite, and chalcopyrite, and occasional arsenopyrite, molybdenite, and tellurides (Kojonen et al., 1993). Zones rich in tourmaline are common. Primary depositional layering has been preserved in places, but strongly sheared and recrystallized mylonitic zones are also present (Nurmi et al., 1993). Hydrothermal alteration is more distinct than in the tonalite, and is manifested by sericite- and chlorite-dominated assemblages, as well as partial alteration of ilmenite to rutile. The gold ore zone is 2 m wide, grading 4.5 ppm. Native gold has been reported in quartz-tour-

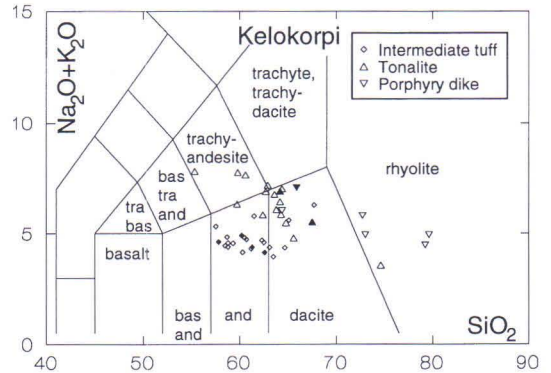


Fig. 16. SiO_2 - Na_2O+K_2O diagram for the Kelokorpi igneous rocks. The least altered samples are shown as filled symbols. bas and: basaltic andesite, and: andesite, tra bas: trachybasalt, bas tra and: basaltic trachyandesite.

maline veins in association with tourmaline, molybdenite, arsenopyrite, tellurides, and pyrrhotite (Kojonen et al., 1993).

All of the Kelokorpi samples are from diamond drill hole 329 (Fig. 15) since no other drill holes exist in the area. The length of the drill core samples varies from 1 to 6 m, with an average of 3 m.

Table 5. Median compositions of the least mineralized ($Au < 100$ ppb) and strongly mineralized ($Au \geq 1000$ ppb) host rocks at the Kelokorpi occurrence. Int volc: intermediate volcanic rocks; Ton: Kuittila Tonalite; Porp: porphyry dikes. Number of samples is shown in parentheses.

	Least mineralized			Strongly mineralized	
	Int volc (16)	Ton (11)	Porp (5)	Int volc (2)	Ton (1)
SiO ₂ %	60.25	62.90	72.70	63.50	64.30
TiO ₂ %	0.79	0.48	0.34	0.65	0.45
Al ₂ O ₃ %	17.50	15.50	13.00	15.05	14.50
Fe ₂ O ₃ %	8.45	5.03	3.24	7.79	4.82
MnO %	0.08	0.08	0.06	0.10	0.09
MgO %	4.14	2.84	1.63	4.48	2.66
CaO %	1.09	3.69	2.15	1.69	4.06
Na ₂ O %	1.58	3.92	4.26	2.14	2.49
K ₂ O %	3.03	3.02	1.77	2.39	3.32
P ₂ O ₅ %	0.11	0.17	0.12	0.09	0.15
LOI %	3.08	1.77	0.93	2.04	2.16
Ag ppm	0.16	0.24	0.08	0.46	6
As ppm	27	5.2	17	39	3.8
Au ppb	10	20	10	4515	1290
B ppm	96	72	36	205	20
Ba ppm	431	816	448	231	865
Bi ppm	0.3	1	0.1	0.7	56
Co ppm	33	19	10	32	22
CO ₂ %	0.02	1.60	0.24	0.03	1.79
Cr ppm	369	105	90	311	96
Cu ppm	67	48	22	48	70
Li ppm	44	45	49	62	35
Mo ppm	3.5	6	3	31	3
Ni ppm	159	36	26	135	42
Pb ppm	12	26	15	21	205
Rb ppm	106	108	76	105	112
S %	0.45	0.20	0.11	0.45	0.37
Sr ppm	112	625	291	132	454
Te ppb	40	300	20	720	4800
W ppm	2	4	1	1.5	6
Zn ppm	82	136	59	103	282
Zr ppm	129	100	72	112	71

Geochemical alteration

The sampled drill hole is within a zone of hydrothermal alteration characterized by consistent enrichment or depletion of various

elements along the whole length (150 m) of the drill hole. Both the tonalite and the tuff are enriched in Ag, As, Au, B, Bi, Mo, S, and Te (Fig. 17). The tonalite also shows enrichments in Co, CO₂, Cu, Pb, W, and Zn, while the tuff is depleted in Ca, Li, and Sr. However, only Au is consistently above the limit of background variation. Bismuth, Pb, S, and Te lie outside the background variation limits in the tonalite, as does Li in the tuff.

The drill hole intersects two narrow highly mineralized zones ($Au \geq 1$ ppm), one within tonalite and the other within intermediate tuff (Fig. 17). A summary of mass changes within these highly mineralized zones, and within adjacent less strongly mineralized zones ($0.1 \text{ ppm} \leq Au < 1 \text{ ppm}$) is given in Fig. 18.

Major element mobility is modest within the tonalite. The most important major element changes are depletion of Na and increases of LOI and K. The changes are strongest within the less intensely mineralized rocks immediately adjacent to the highly mineralized zone (Figs. 17 and 18). Manganese, Mg, Fe, and Ti show slight enrichments, especially within the highly mineralized zone. The average enrichment of Ca is within the limits of background variation. For the trace elements, intense enrichments within the highly mineralized zone are shown in decreasing degrees of enrichment by Bi, Au, Te, Ag, S, Pb, and CO₂. Strong enrichments are shown by Zn and Cu, and moderate to slight enrichments by Co and Ni. Strontium is slightly depleted. The enrichments of W, As, Mo, and Cr, and the depletions of Li and Zr are within the limits of background variation. Excluding As, Cr, and Ni, all these elements display at least a small local anomaly coinciding with the mineralized zone (Fig. 17). These anomalies are usually only slightly broader than the mineralized zone, and their peaks occur adjacent to the highest Au values. Only the Ag, Bi, and Te anomalies coincide precisely with the Au peak.

Major element mobility is also modest within the intermediate tuff (Figs. 17 and 18).

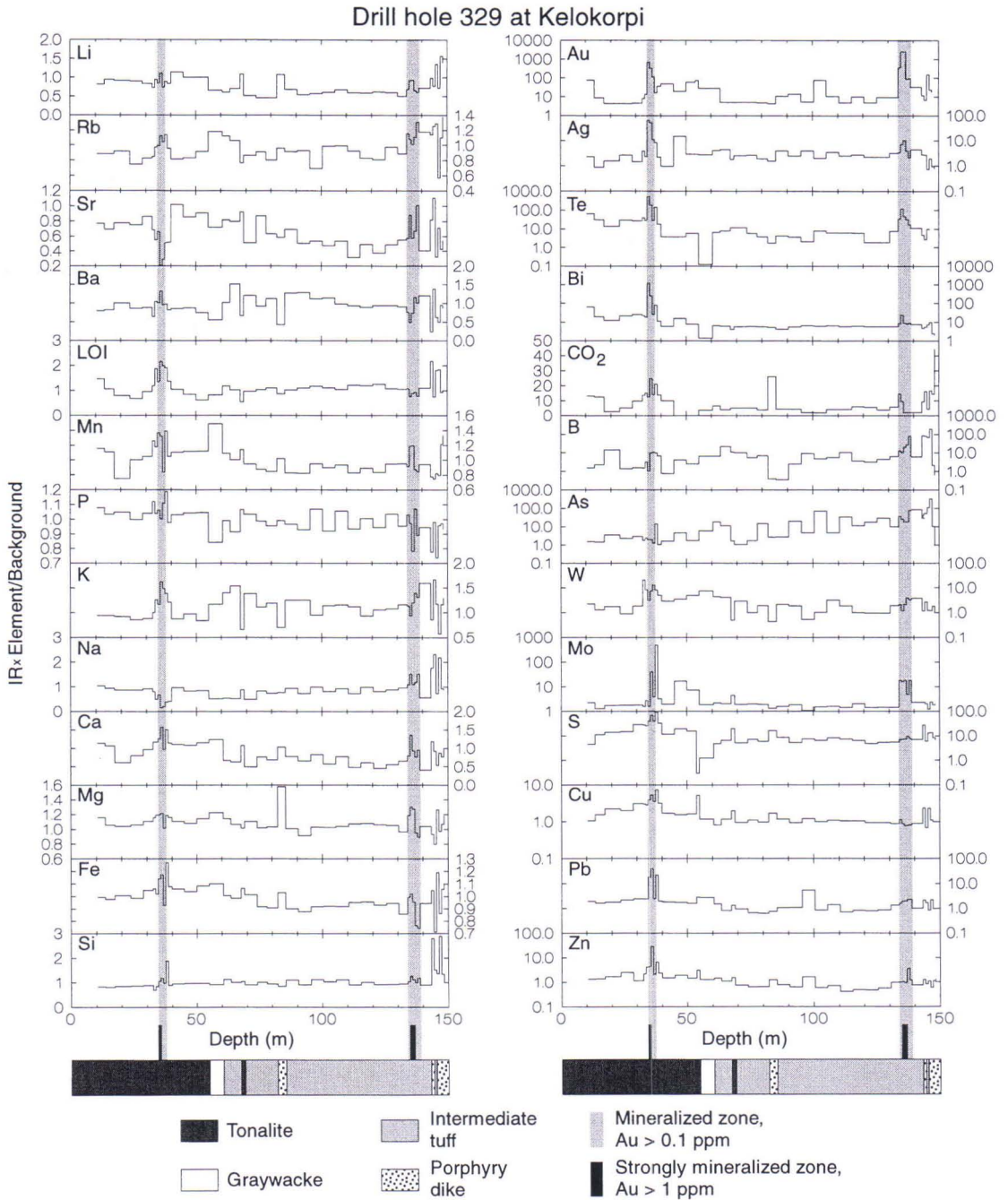


Fig. 17. Mobility versus depth for selected elements within diamond drill hole 329 at Kelokorpi. Mobility is expressed as $IR \times c^a/c^b$, where IR is the immobile element ratio and c^b and c^a are the concentrations of component c before and after alteration, respectively.

Magnesium, Mn, and Si show slight enrichments within the highly mineralized zone, but are within the limits of background variation in the contiguous less intensely mineralized rocks. The pattern of Ca mobility is similar, but the average Ca changes do not exceed the limits of background variation. In contrast to the tonalite, Na is enriched and LOI shows slight decrease, but both remain within the limits of background variation. Potassium is slightly enriched and Fe and Ti are slightly depleted, especially within the less intensely mineralized rocks. In the highly mineralized zone, intense enrichments are shown in decreasing degree by Au, Te, Mo, Bi, and B, strong enrichments by Ag, CO₂, and Pb, and slight enrichment by Zr. The enrichments of As, S, W, Cr, and Ni, and the depletions of Ba,

Sr, and Cu, fall within the limits of background variation. The abundance of CO₂ exceeds the detection limit of 0.01% in only one of the three samples from the less intensely mineralized zone. Because the contents of CO₂ in the least altered intermediate tuff are also below 0.01%, CO₂ mass change could not be calculated for most of the less mineralized samples, and is not shown in Fig. 18. Excluding Te, B, and Mo, the local anomalies of the enriched or depleted elements are either very modest or absent altogether. Enrichment of As increases approximately by two orders of magnitude over an interval of 65 m along the drill hole, and defines an increasing trend toward the contact zone between the tuff and the porphyry dike, adjacent to the mineralized zone. Two narrow zones within the porphyry

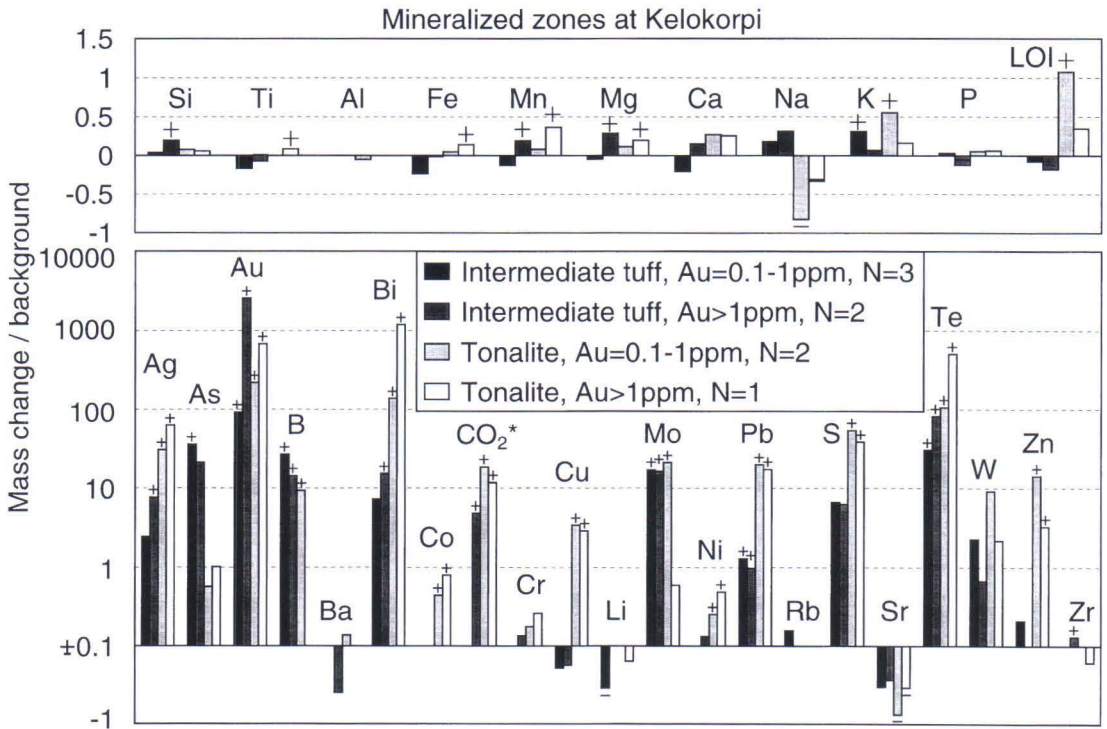


Fig. 18. Summary of relative mass changes within the mineralized zones intersected by diamond drill hole 329 at Kelokorpi. Relative changes less than or equal to $\pm 10\%$ have been omitted for the trace elements. To make comparisons of gains and losses easier, the scale for the depletions in the lower diagram is also logarithmic. A plus sign above the bar or a minus sign below the bar indicates that the value is outside the limit of background variation. CO₂*: Intermediate tuff, Au=0.1-1 ppm, N=1, not shown.

are clearly enriched in Si, Al, Na, LOI, and B, reflecting silicification and tourmalinization

of the porphyry. Nevertheless, neither zone shows anomalous gold values.

Kuittila

The Kuittila gold occurrence is located at the southwestern margin of the Kuittila Tonalite (Figs. 2 and 19). There are very few natural outcrops in the area, and the till cover is thick, up to 10 m in places. Bedrock samples have been obtained from 18 diamond drill holes and from exploration trenches.

Gold occurs along a north-south trending zone approximately 1 km long and several hundred meters wide at the contact between the Kuittila Tonalite and the supracrustal rocks. Two stages of mineralization have been identified: an older molybdenum-tungsten mineralization associated with two sets of northwest to west northwest-trending subvertical quartz veins, and a somewhat later gold mineralization associated with northwest trending sinistral shear zones with quartz-carbonate veining, silicification, and sericitization (Nurmi et al., 1993). Barren veins containing milky quartz trend between north and northeast and cut the older molybdenite-scheelite quartz veins, and another set of barren quartz-tourmaline veinlets cuts the milky quartz veins. The relation of these latter two sets of veins to the gold-bearing veins is unknown (Nurmi et al., 1993). All the mineralized zones included in this study are hosted by the Kuittila Tonalite. Average chemical compositions of least mineralized and strongly mineralized host rocks are given in Table 6.

The unaltered tonalite has plagioclase, quartz, biotite, and muscovite as major minerals, and is typically medium-grained and equigranular, with randomly oriented subhedral plagioclase grains and oriented aggregates of fine-grained biotite (Ojanen, 1993; Kojonen et al., 1993; Sorjonen-Ward, 1993). Gold occurs in the quartz-sericite shear zones and in veins within the tonalite. The mica

schist enclaves and screens are usually not mineralized or notably altered. Sheared and bleached zones, with typical mineral assemblages containing quartz, albite, sericite, calcite, potassium feldspar, biotite and epidote, extend for up to several meters from the quartz lodes (Nurmi et al., 1993). The most intensely altered zones are dominated by quartz, sericite, and carbonate (Kojonen et al., 1993). The alteration is also evident in the trend toward higher

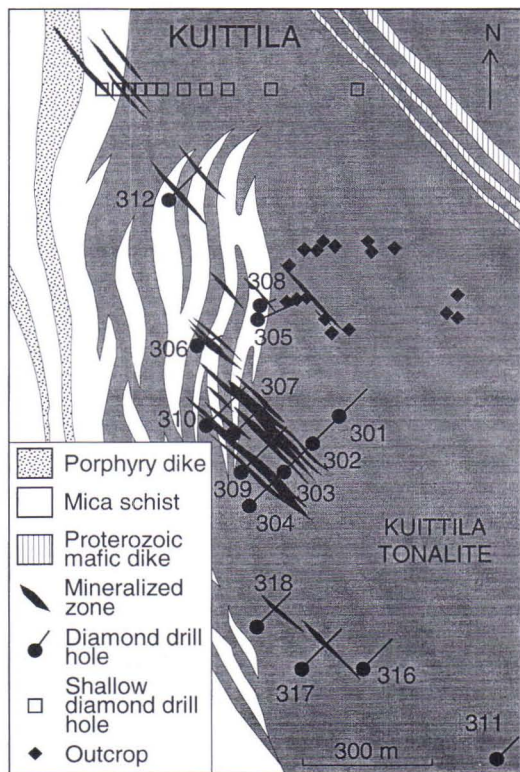


Fig. 19. Simplified geology and location of sampled diamond drill holes and outcrops at the Kuittila gold occurrence. The map has been redrawn after Nurmi et al., 1993.

Table 6. Median compositions of the least mineralized ($Au < 100$ ppb) and strongly mineralized ($Au \geq 1000$ ppb) tonalite at the Kuittila occurrence. Number of samples is shown in parentheses. For the least mineralized tonalites, Ag and Bi are based on 41 and 47 samples, respectively.

	Least mineralized (88)	Strongly mineralized (10)
SiO ₂ %	64.65	79.30
TiO ₂ %	0.43	0.20
Al ₂ O ₃ %	14.80	7.13
Fe ₂ O ₃ %	4.42	2.34
MnO %	0.07	0.05
MgO %	2.36	1.4
CaO %	3.55	1.54
Na ₂ O %	3.44	0.96
K ₂ O %	3.17	2.62
P ₂ O ₅ %	0.15	0.09
LOI %	2.27	1.31
Ag ppm	0.16	1.25
As ppm	2.2	1.4
Au ppb	8	2150
B ppm	21	5
Ba ppm	881	720
Bi ppm	0.05	0.15
Co ppm	13	12
CO ₂ %	1.51	0.68
Cr ppm	87	78
Cu ppm	23	14
Li ppm	47	41
Mo ppm	61	23
Ni ppm	32	24
Pb ppm	14	27
Rb ppm	134	107
S %	0.08	0.01
Sr ppm	595	234
Te ppb	17	140
W ppm	31	7
Zn ppm	60	47
Zr ppm	86	27

SiO₂ contents on the SiO₂ - Na₂O+K₂O diagram (Fig. 20). Total sulfide abundances are low and sulfides occur mainly as minor disseminations, aggregates, and veinlets of pyrite and pyrrothite, with some copper, zinc, and lead sulfides, molybdenite, scheelite, ilmenite, and rutile (Kojonen et al., 1993).

Gold grades of 2–5 ppm over several meters

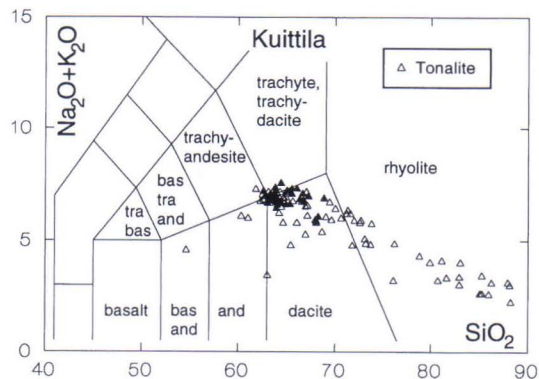


Fig. 20. SiO₂ - Na₂O+K₂O diagram for the Kuittila occurrence. The least altered samples are shown as filled symbols. bas and: basaltic andesite, and: andesite, tra bas: trachybasalt, bas tra and: basaltic trachyandesite.

occur in individual drill core intersections, and the maximum gold content recorded over a single 1 m interval is 19.4 ppm. In spite of this, no continuous ore-grade zones have been delineated. Native gold is fine grained (up to some tens of microns) and is erratically distributed within the quartz veins, mainly as inclusions or intergrowths with pyrite, in association with infrequent tellurides (Kojonen et al., 1993).

The molybdenite-scheelite-bearing quartz veins are most abundant in the northern part of the Kuittila area, to the northeast of the highest gold abundances (Nurmi et al., 1993). The veins are usually several centimeters thick. Molybdenite and scheelite occur both within the veins and in adjacent tonalite accompanied by iron sulfides and minor chalcopyrite. Maximum contents of molybdenum and tungsten are 0.2% over intervals of several meters (Nurmi et al., 1993).

The alteration of tonalite and its relation to gold mineralization was studied in more detail using core samples from diamond drill hole 309 (core lengths 1–5 m/sample, on average 2 m) as well as from the exploration trenches (Fig. 19). Mineralized zones ($Au \geq 1$ ppm) intersected by drill hole 309 are 2 to 6 m wide, and the anomalous values of other elements associated with gold are usually restricted to the same

interval. Consequently, samples from the other drill holes representing on average 15 m of drill core are not suitable for detailed studies. The least altered tonalite intersected by drill hole 309 is silicified, and commonly sheared, with sporadic quartz veins and a weak sulfide (mostly pyrite) dissemination (Ojanen, 1993). High gold values are associated with stronger silicification, quartz±calcite vein brecciation and strong sericitization or biotitization.

Geochemical alteration

Calculated mobilities of selected elements are shown in Fig. 21. For B, Bi, and S, more than 50% of the samples have values below the detection limits of 10 ppm, 0.1 ppm, and 0.01%, respectively. Since the primary concentration of Bi in tonalite is also below 0.1 ppm, mass transfer of Bi could not be calculated for samples with less than 0.1 ppm Bi. For B and S, the least altered contents are greater than or equal to the detection limits.

Within the studied interval (100–200 m), the drill hole coincides with a zone of hydrothermal alteration characterized by consistent enrichments above the background variation limits of Ag, Au, Te, Cr, Mg, Pb, and Si (Fig. 21). Although CO₂, Mo, W, Bi, K, Li, and Rb are also consistently enriched, and Sr is consistently depleted, some of their changes fall within the limits of background variation. The altered zone contains four narrower mineralized zones with more than 1 ppm Au, one hosted by a quartz-biotite breccia, one by silicified tonalite and two by sericitized quartz vein breccias (Fig. 21). A summary of mass changes within the highly mineralized (Au ≥ 1 ppm) and contiguous less mineralized (0.1 ppm Au ≤ 1 ppm) rocks is given in Fig. 22.

The highest Au value, 19.4 ppm, occurs within a zone of quartz-biotite breccia (at 127–128 m, Fig. 21) in silicified tonalite. The most notable major element changes are strong increases of LOI, Ca, Mn, and Mg, all of which are greatest within the intensely

mineralized zone (Fig. 22). Silicon, Fe, P, K, and Ti show moderate to slight enrichments, and Na shows slight depletion. Of the trace elements, Au, Te, CO₂, Mo, and Ag are intensely enriched, Bi, B, Pb, Co, Li, and Cr are strongly enriched, and Zn and Rb are moderately enriched within the highly mineralized zone. The enrichment of W, as well as the slight depletions of Cu, Sr, As, and S, do not exceed the limits of background variation. Excluding Cu and W, all these elements show at least a slight positive or negative anomaly peak coinciding with the highly mineralized zone (Fig. 21). For many elements, especially Si, Mg, Na, Li, B, As, Cu, and S, the strongest anomaly peak does not correspond to the highly mineralized zone, and the strongest Mo enrichment falls completely outside the zone affected by gold mineralization.

The second highly mineralized zone (at 155–161 m, Fig. 21) occurs within silicified tonalite. Major element mobility is modest, being recorded by slight enrichments of K, Si, Mg, Al, and P (Fig. 22). The slight increase of LOI is nevertheless within the limits of background variation. In the highly mineralized zone, Au, Te, Ag, Bi, and Mo are intensely enriched, Pb and As are strongly enriched, and Li, Rb, Ba, and Cr are moderately to slightly enriched. The enrichments of W, CO₂, S, Cu, Co, and Ni, and the depletions of B, Sr, Zn and Zr fall within the limits of background variation. Compared with local background values, no major elements show significant anomalies within the mineralized zone, and only Ag, As, B, Bi, Te, and W exhibit clear anomalies coinciding with the Au anomaly. It is noteworthy that although B is on average depleted within the highly mineralized zone, it shows a narrow positive anomaly adjacent to the highly mineralized zone (Fig. 21).

The remaining two highly mineralized zones (at 170–176 m and 191–195 m, Fig. 21) are hosted by quartz vein breccias within strongly silicified and sericitized tonalite. Major element mobility is characterized by strong in-

Drill hole 309 at Kuittila

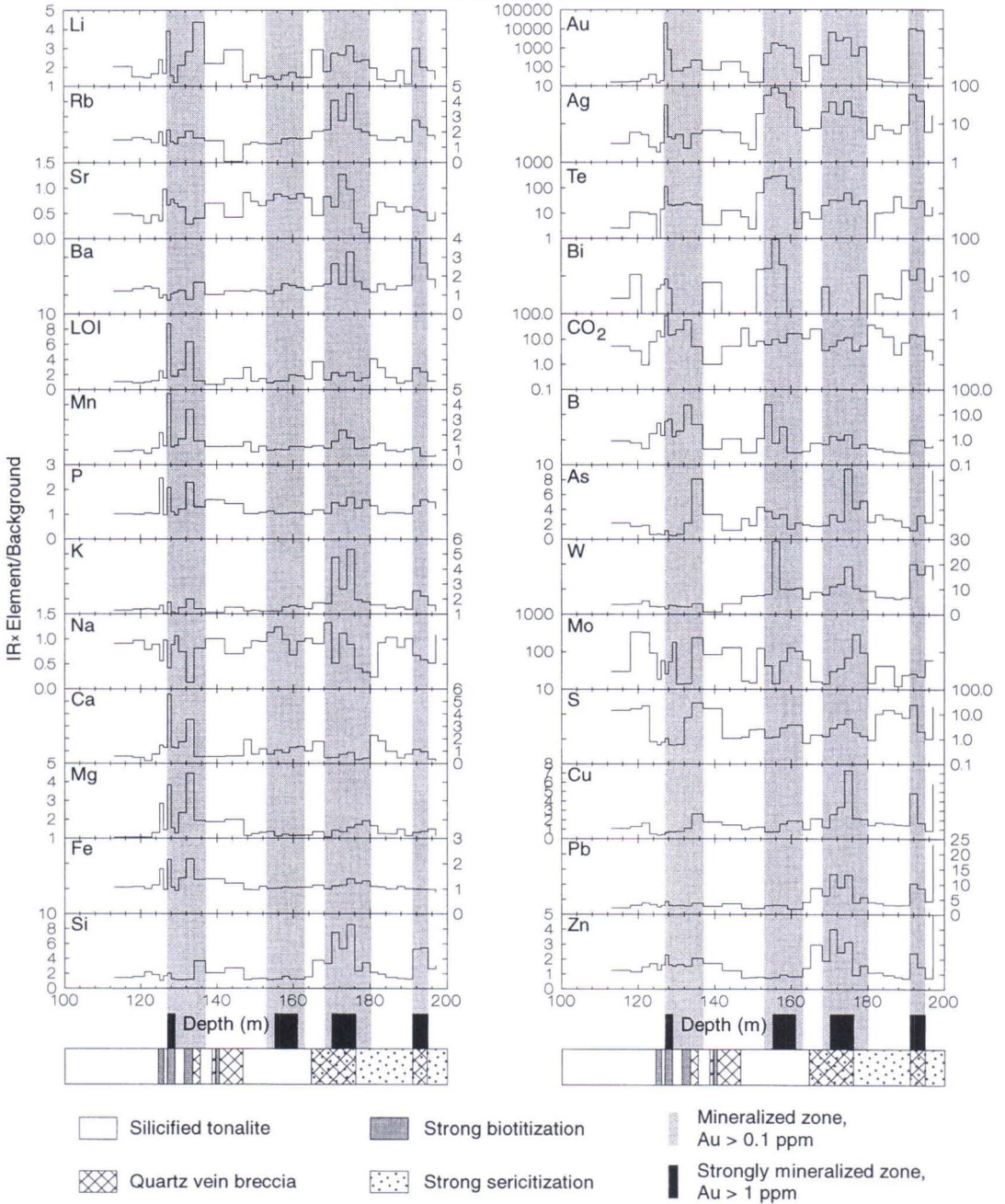


Fig. 21. Mobility versus depth for selected elements within diamond drill hole 309 at Kuittila. Mobility is expressed as $IR \times c^a/c^b$, where IR is the immobile element ratio and c^a and c^b are the concentrations of component c before and after alteration, respectively.

creases of Si, K and LOI (Fig. 22). Aluminium, Mn, P, and Mg are moderately to slightly enriched and Na shows slight depletion. Calcium is moderately depleted and Fe is weakly enriched within the adjoining less intensely mineralized rocks. Gold, Ag, Te, Mo, and W are intensely enriched, Pb, Cu, Cr, As, Rb, Li, Ba, Zn, and Ni are strongly enriched, and Co is moderately enriched within the highly mineralized zone. Zirconium and Sr show moderate and slight depletions, respectively. Enrichments of CO₂ and S do not exceed the limits of background variation. Mass change of Bi for these zones is not shown in Fig. 22 because it could be calculated for only 2 out of 5 samples. However, Bi is strongly to intensely enriched in both of these samples

(Fig. 21). Most of the altered elements exhibit at least slight anomaly peaks either above or below local background values, coinciding with the mineralized zones (Fig. 21). Again, B shows slight positive anomalies above the local, depleted background.

The similarity of the LOI and CO₂ anomalies, which is strongest where the mineralized zone is characterized by biotitization, suggests that a large part of the volatile phase consists of CO₂. This is verified by the raw data for LOI and CO₂, which show that CO₂ forms 70.9–85.5%, 56.1–76.5%, and 20.0–50.0% of the volatile phase within the highly mineralized zones of the quartz-biotite breccia, the silicified tonalite, and the quartz-sericite breccia types, respectively.

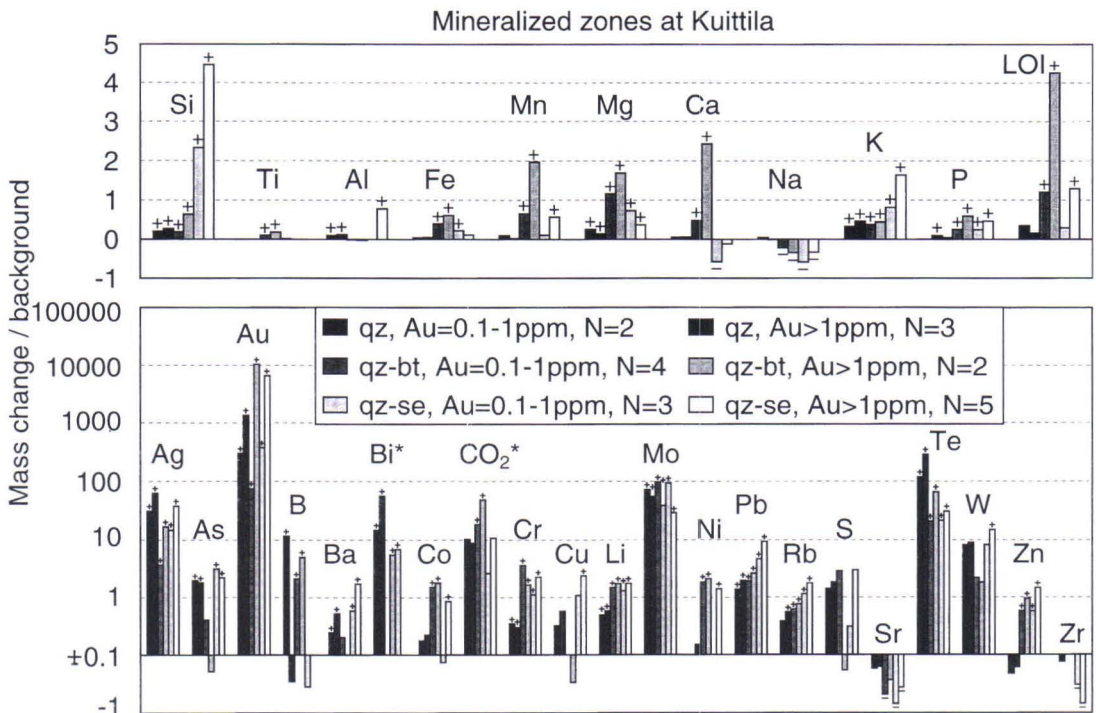


Fig. 22. Summary of relative mass changes within the mineralized zones intersected by diamond drill hole 309 at Kuittila. Relative changes less than or equal to $\pm 10\%$ have been omitted for the trace elements. To make comparisons of gains and losses easier, the scale for the depletions in the lower diagram is also logarithmic. A plus sign above the bar or a minus sign below the bar indicates that the value is outside the limit of background variation. qz: quartz alteration, qz-bt: quartz-biotite alteration, qz-se: quartz-sericite alteration. Bi*: qz, Au=0.1–1 ppm, N=1; qz, Au>1 ppm, N=2; qz-bt, Au=0.1–1 ppm, N=0; qz-se, Au=0.1–1 ppm, N=2; qz-se, Au>1 ppm, N=2, not shown.

Korvilansuo

The Korvilansuo-Kivisuo area includes several Au anomaly zones in bedrock, delineated by both till and bedrock geochemistry (Nurmi et al., 1993). The Korvilansuo gold occurrence is situated within the schists west of the contact with the Kuittila Tonalite, approximately 3 km northwest of the Kuittila occurrence (Figs. 2 and 23). A narrow mineralized zone occurs to the east of the Korvilansuo shear zone near the margin of the Kuittila Tonalite but the most strongly mineralized rocks occur to the west of the shear zone, near the northern end of a porphyritic tonalite dike almost 100 m thick. High gold concentrations occur principally in sericitized and chloritized mica schists and to a lesser degree in silicified and partly tourmalinized porphyry dikes. All the mineralized zones from Korvilansuo included in this study are located within sedimentary rocks. Average chemical compositions of least mineralized and strongly mineralized host rocks are given in Table 7.

The westward younging sedimentary sequence between the Korvilansuo and Kau-ravaara shear zones consist mostly of thin- to medium-bedded feldspathic graywackes, intruded by dikes of quartz-plagioclase porphyry and tonalite, together with several gabbroic dikes or sills interpreted as an integral part of the supracrustal sequence (Sorjonen-Ward, 1993). Proterozoic mafic dikes are also present, discordantly truncating Archean structures. The drill holes intersect some narrow mafic tuffaceous interlayers within the graywackes, and a mafic pyroclastic horizon about 20 m thick occurs to the northwest of the mineralized zones. The graywackes are overlain in the northwest by coarser and thicker units containing conglomeratic intercalations with pelitic clasts and well-rounded feldspar-rich fragments usually less than 5 cm in diameter (Sorjonen-Ward, 1993). Both the sedimentary rocks and the porphyry dikes

have suffered widespread and pervasive hydrothermal alteration and shearing, and in places they are effectively recrystallized ultramylonites (Nurmi et al., 1993).

The graywackes consist of biotite, muscovite, and chlorite in varying proportions, with quartz, potassium feldspar, and plagioclase (Kojonen et al., 1993). Chemical data for the sedimentary rocks have been plotted on a $\text{SiO}_2 - \text{Na}_2\text{O} + \text{K}_2\text{O}$ diagram to enable comparison with the igneous rocks (Fig. 24). Almost totally sericitized pseudomorphs after andalusite porphyroblasts occur in places, and tourmaline is locally abundant (Nurmi et al., 1993). Sulfide disseminations consist of pyrrhotite, chalcopyrite, and pyrite with minor sphalerite and ilmenite. Arsenopyrite and galena are occasionally encountered. Hydrothermal alteration has converted ilmenite to rutile. Gold occurs within the mica schists both as disseminations and as concentrations in quartz-tourmaline veins some tens of centimeters thick. Fine-grained native gold occurs as inclusions within sulfides, or at sulfide-sulfide and sulfide-silicate grain boundaries. Fine-grained Au-Ag-Bi-Pb tellurides and native bismuth occur commonly with gold, especially within the quartz-tourmaline veins (Kojonen et al., 1993). The highest gold grade recorded is 15.2 ppm over a 0.5 m interval, but gold grades of 2–4 ppm over several meters are more typical.

The Korvilansuo samples were taken from six diamond drill holes along two E-W profiles (Fig. 23). The southern profile (drill holes 325–328) intersects a narrow, rather weakly mineralized zone, while the northern profile intersects a more strongly mineralized zone further west. Attention was focused on drill holes 325, 355, and 356, since these holes intersect the most strongly mineralized rocks in the area. Samples from drill hole 325 represent 1.2 to 5 m of core (average 5 m) and

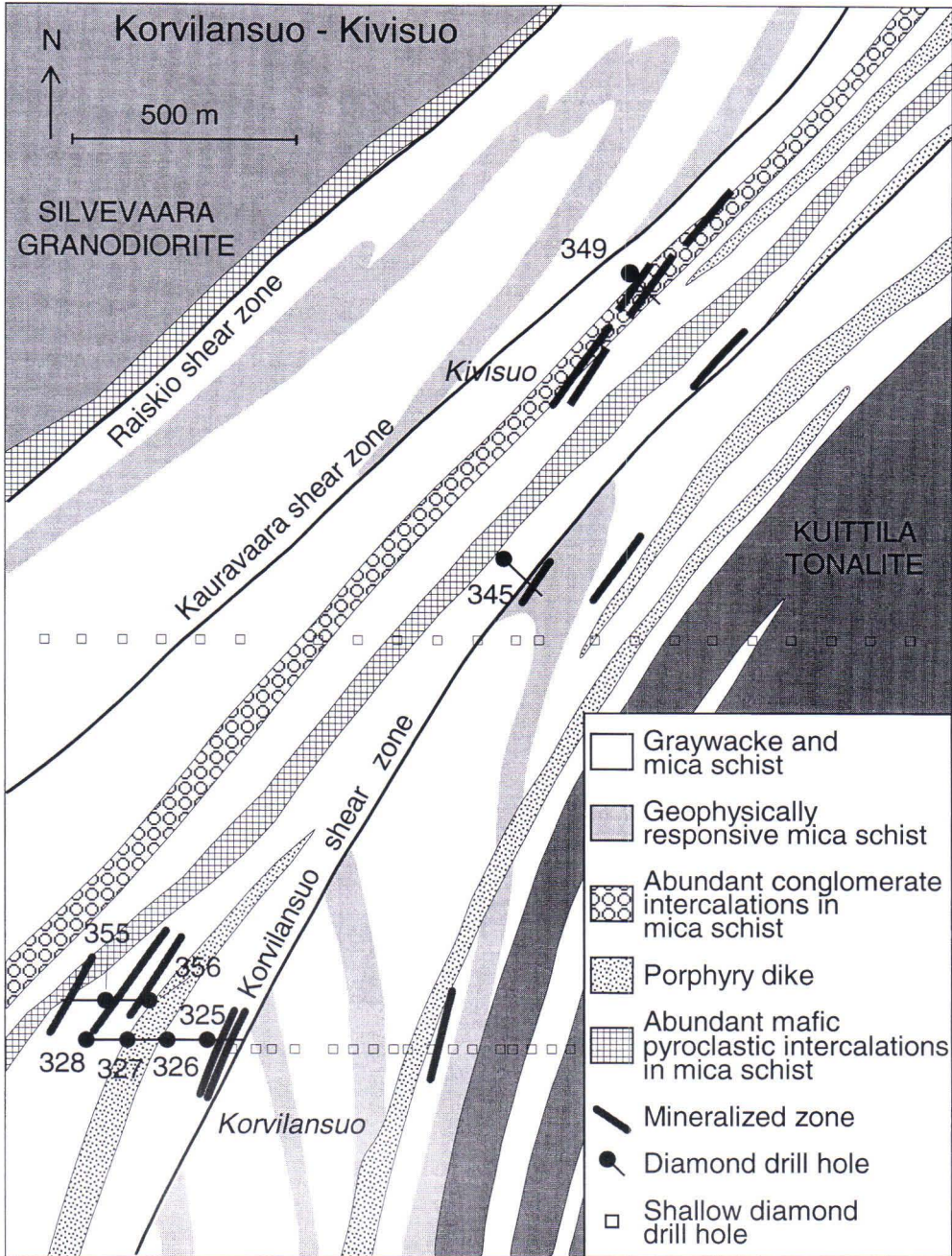


Fig. 23. Simplified geology and locations of sampled diamond drill holes at the Korvilansuo and Kivisuo gold occurrences. The map has been redrawn after Nurmi et al., 1993.

Table 7. Median compositions of the least mineralized ($Au < 100$ ppb) and strongly mineralized ($Au \geq 1000$ ppb) host rocks at the Korvilansuo occurrence. Int volc: intermediate volcanic rocks; Sed: sedimentary rocks; Porp: porphyry dikes. Number of samples is shown in parentheses. For the least mineralized and strongly mineralized sedimentary rocks, Li is based on 58 and 1 samples, respectively.

	Least mineralized			Strongly mineralized
	Int volc (2)	Sed (88)	Porp (27)	Sed (13)
SiO ₂ %	63.25	64.95	66.50	64.50
TiO ₂ %	0.76	0.59	0.36	0.54
Al ₂ O ₃ %	15.80	16.05	15.70	16.00
Fe ₂ O ₃ %	6.08	5.59	3.45	5.68
MnO %	0.09	0.08	0.06	0.09
MgO %	3.69	2.38	1.84	2.29
CaO %	3.84	2.30	3.60	2.15
Na ₂ O %	2.86	2.63	4.41	2.74
K ₂ O %	2.14	2.58	2.37	1.80
P ₂ O ₅ %	0.29	0.14	0.15	0.14
LOI %	1.04	1.70	0.85	1.31
Ag ppm	0.12	0.20	0.16	0.73
As ppm	3.6	5.6	4.8	6.4
Au ppb	50	20	10	2940
B ppm	40	175	49	3780
Ba ppm	670	866	1040	830
Bi ppm	0.13	0.3	0.1	4.1
Co ppm	23	22	15	19
CO ₂ %	0.02	0.01	0.58	<0.01
Cr ppm	176	150	62	102
Cu ppm	38	46	28	35
Li ppm	71	43	34	47
Mo ppm	3	2	3	1
Ni ppm	90	65	30	46
Pb ppm	9	11	13	9
Rb ppm	102	93	81	67
S %	0.26	0.48	0.39	0.64
Sr ppm	642	468	730	720
Te ppb	165	220	100	3120
W ppm	3.3	3	2	<1
Zn ppm	95	78	63	56
Zr ppm	215	122	91	125

samples from drill holes 355 and 356 represent 0.7 to 3 m of core (average 2 m). Only limited sections of drill core including the mineralized zones were analyzed for all elements from drill holes 355 and 356.

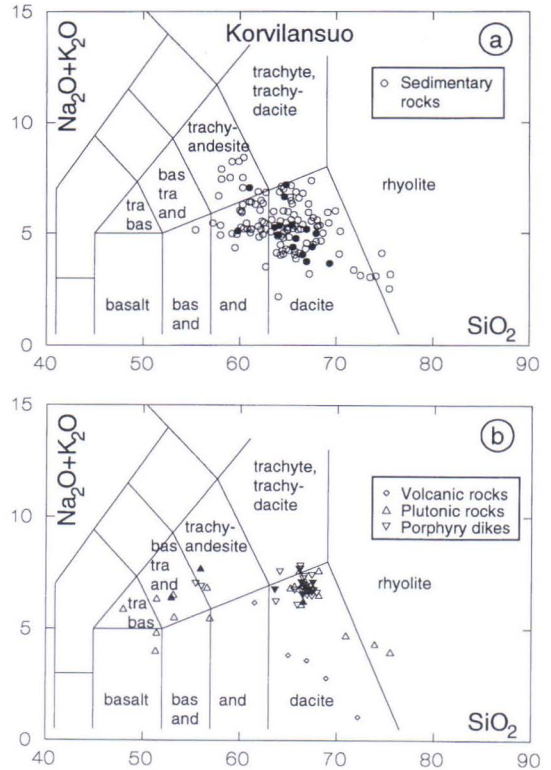


Fig. 24. SiO₂ - Na₂O+K₂O diagram for the Korvilansuo sedimentary (a) and igneous (b) rocks. The least altered samples are shown as filled symbols. The sedimentary rocks are plotted to facilitate comparison with the igneous rocks. bas and: basaltic andesite, and: andesite, tra bas: trachybasalt, bas tra and: basaltic trachyandesite.

Geochemical alteration

Calculated mobilities of selected elements in rocks intersected by diamond drill hole 356 are shown in Fig. 25. The contrasting behavior of certain elements in various mineralized zones is well summarized in this drill hole. The abundances of CO₂ in the least altered sedimentary rocks are below the detection limit of 0.01% and because CO₂ abundances are mostly below the detection limit for altered samples at Korvilansuo as well, calculating mass transfer of CO₂ was possible for only a few samples. Disregarding drill hole 325 and a few anomalous samples from other drill holes, Mo and W also have low contents

Drill hole 356 at Korvilansuo

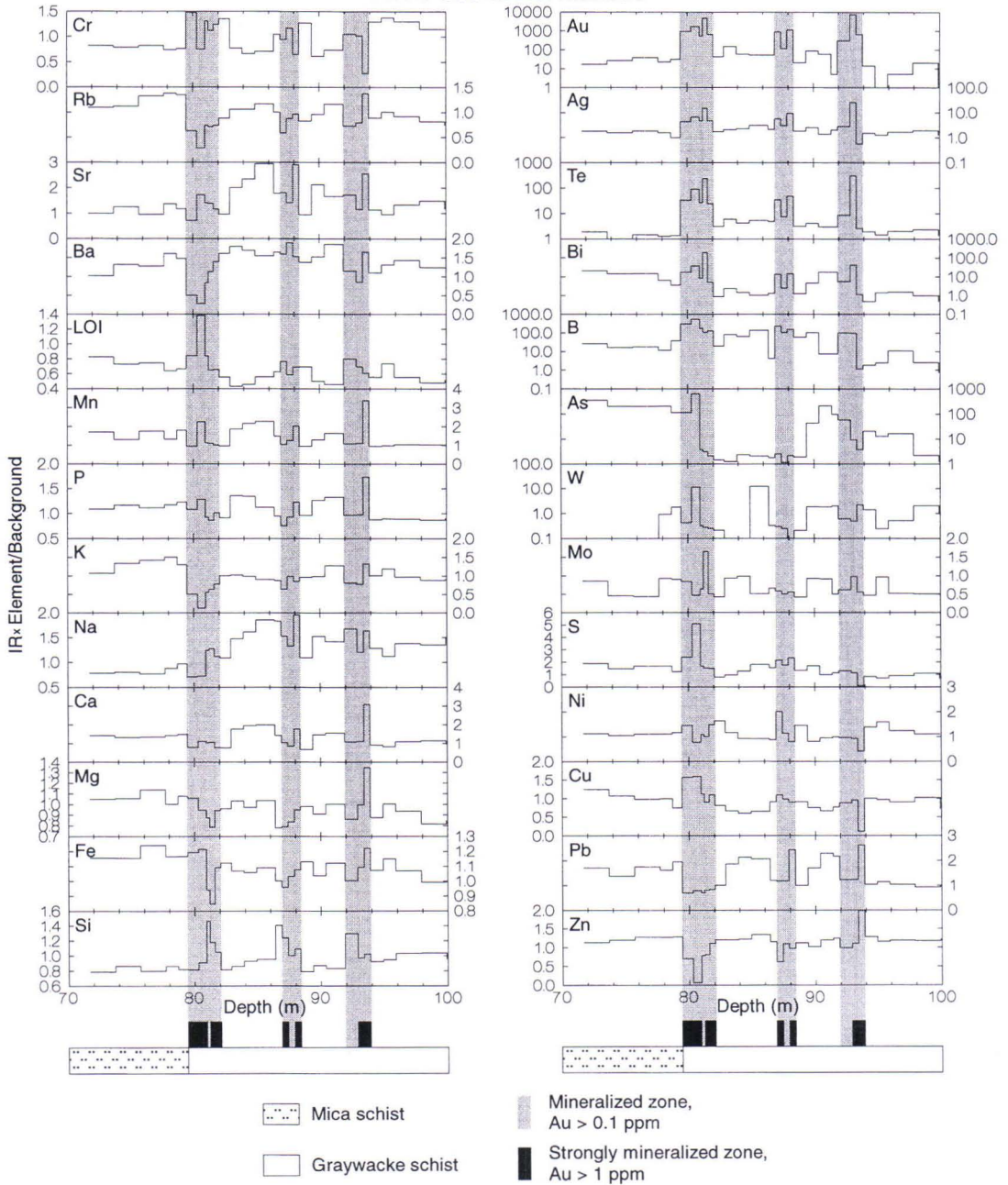


Fig. 25. Mobility versus depth for selected elements within diamond drill hole 356 at Korvilansuo. Mobility is expressed as $IR \times c^b/c^a$, where IR is the immobile element ratio and c^a and c^b are the concentrations of component c before and after alteration, respectively.

near or below the detection limits.

Silver, B, and Te are enriched along the whole 150 m length of drill hole 325, but the enrichments fall within the limits of background variation. Gold values commonly lie below the detection limit of 10 ppb in the upper part of the drill hole. The analyzed section (80–132 m) of drill hole 355 shows overall enrichments in Ag, Au, and B, and Te, and depletions in Na and Cr. Within the completely analyzed interval (70–100 m) of drill hole 356, Ag, As, Au, B, and Te are enriched and LOI has decreased (Fig. 25). However, only Au enrichment exceeds the limits of background variation in these drill holes. The altered zones contain narrow highly mineralized ($\text{Au} \geq 1 \text{ ppm}$) zones usually less than 1 m wide. A summary of mass changes within the strongly mineralized and contiguous less min-

eralized ($0.1 \text{ ppm} \leq \text{Au} < 1 \text{ ppm}$) rocks is given in Fig. 26.

For most of the major elements, mass change does not exceed the limits of background variation. The only exceptions to this are the slight increases of LOI and K, and the slight depletion of Ti, all of which occur within the less intensely mineralized rocks (Fig. 26). The decreases of Na, LOI, and K within the strongly mineralized zones, as well as the depletions of Na, Mg and Ca, and enrichment of Mn within the less intensely mineralized rocks are all within the limits of background variation. It is noteworthy that major element mobility seems to be stronger within the less intensely mineralized zones, and that LOI and K show contradictory behavior in the highly and less mineralized zones. The average increases of K and LOI within the

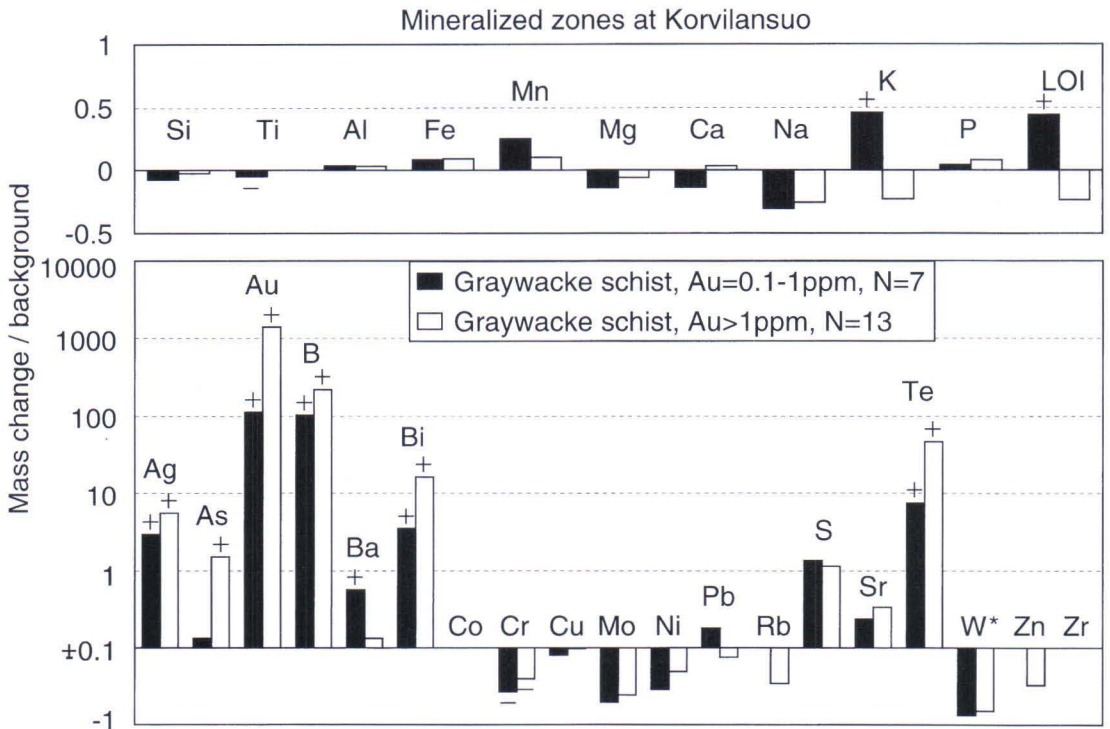


Fig. 26. Summary of relative mass changes within the mineralized zones intersected by diamond drill holes 325, 355, and 356 at Korvilansuo. Relative changes less than or equal to $\pm 10\%$ have been omitted for the trace elements. To make comparisons of gains and losses easier, the scale for the depletions in the lower diagram is also logarithmic.

less intensely mineralized rocks result from 4 samples from an approximately 20 m wide positive anomaly surrounding the highly mineralized zones in drill hole 355 (not shown). On average, Au, B, Te and Bi are intensely enriched, Ag and As are strongly enriched, and Cr is slightly depleted within the strongly mineralized zones (Fig. 26). The enrichments of S and Sr, and the depletions of W, Mo, Zn, Rb, Ni, and Pb are within the limits of background variation. Of all the 20 mineralized samples, it only proved possible to calculate

mass change of CO₂ for 3 analyses, in which CO₂ is strongly enriched. Of the trace elements, Ba, Cr, Cu, Mo, Ni, Pb, S, and W seem to be more mobile within the less intensely mineralized zones (Fig. 26). Many major and trace elements vary from depleted in one mineralized zone to enriched in another (Fig. 25). Only Ag, B, Bi, S, and Te tend to be consistently enriched within the mineralized zones, with positive anomalies coinciding with the Au anomalies.

Kivisuo

The Kivisuo gold occurrence is located approximately 1.5 km northeast along strike from Korvilansuo (Figs. 2 and 23), and the host rocks belong to the same lithic units as those described for the Korvilansuo occurrence (Fig. 27). However, especially the volcanic rocks differ geochemically from the host rocks at Korvilansuo (Figs. 24 and 27), reflecting both alteration and large primary compositional variations of the rock types. Gold occurs as disseminations in silicified, chloritized, and sericitized tourmaline-bearing mica schists and to a lesser degree in narrow quartz-tourmaline veins. Disseminated sulfides are predominantly pyrrhotite, chalcopyrite and pyrite; arsenopyrite and various tellurides occur in the quartz-tourmaline veins (Kojonen et al., 1993). The highest gold grade analyzed was 9.5 ppm over a 2 m interval but typically the rocks containing disseminated gold show gold values of 1–4 ppm over several meters of drill core. Average chemical compositions of least mineralized and strongly mineralized host rocks are given in Table 8.

The Kivisuo samples were taken from two separate diamond drill holes (345 and 349) spaced approximately 700 m apart along a NE trending Au-bearing zone (Fig. 23). Drill core sample length varies from 0.35 m to 3.5 m with an average of 2.0 m. Only samples from

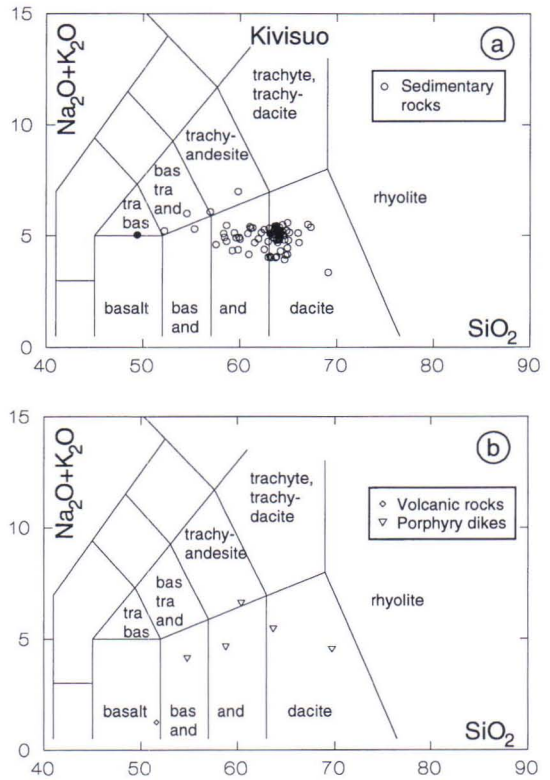


Fig. 27. SiO₂ - Na₂O+K₂O diagram for the Kivisuo sedimentary (a) and igneous (b) rocks. The least altered samples are shown as filled symbols. The sedimentary rocks are plotted to facilitate comparison with the igneous rocks. bas and: basaltic andesite, and: andesite, tra bas: trachybasalt, bas tra and: basaltic trachyandesite.

Table 8. Median compositions of the least mineralized ($Au < 100$ ppb) and strongly mineralized ($Au \geq 1000$ ppb) host rocks at the Kivisuo occurrence. Maf volc: mafic volcanic rocks; Sed: sedimentary rocks; Porp: porphyry dikes; -: not analyzed. Number of samples is shown in parentheses. For the least mineralized sedimentary rocks, Li and W are based on 2 and 35 samples, respectively. For the strongly mineralized sedimentary rocks, W is based on only 1 sample.

	Least mineralized		Strongly mineralized	
	Sed (48)	Porp (3)	Maf volc (1)	Sed (3)
SiO ₂ %	63.60	58.80	51.60	64.20
TiO ₂ %	0.72	0.81	0.66	0.64
Al ₂ O ₃ %	15.90	15.60	13.60	15.60
Fe ₂ O ₃ %	6.91	8.06	10.60	6.92
MnO %	0.08	0.10	0.21	0.09
MgO %	3.24	3.94	9.29	3.16
CaO %	1.83	3.37	7.38	2.78
Na ₂ O %	2.75	2.87	0.91	3.20
K ₂ O %	2.21	1.30	0.33	1.85
P ₂ O ₅ %	0.12	0.17	0.36	0.10
LOI %	2.20	1.47	1.70	1.54
Ag ppm	0.18	0.15	0.58	0.22
As ppm	44	36	70	110
Au ppb	20	20	2200	4410
B ppm	56	219	10700	66
Ba ppm	601	524	79	656
Bi ppm	0.4	0.6	21	0.5
Co ppm	32	24	30	34
CO ₂ %	<0.01	<0.01	0.05	<0.01
Cr ppm	239	252	557	195
Cu ppm	66	69	49	72
Li ppm	58	-	-	-
Mo ppm	2	2	12	2
Ni ppm	113	66	172	100
Pb ppm	9	13	7	13
Rb ppm	83	77	26	71
S %	0.53	0.47	0.32	0.45
Sr ppm	308	451	370	411
Te ppb	160	170	7530	140
W ppm	<1	30	-	9
Zn ppm	95	96	26	103
Zr ppm	139	133	120	128

limited intervals covering the mineralized zones were analyzed for all elements. With the exception of a few porphyry dikes and one mafic dike, the sampled intervals are located within sedimentary rocks.

Geochemical alteration

Calculated mobilities of selected elements in rocks intersected by diamond drill hole 345 are shown in Fig. 28 as representative of the Kivisuo occurrence. Abundances of CO₂ are very commonly below the detection limit of 0.01%. Because CO₂ contents in the least altered sedimentary rocks are also below 0.01%, calculating mass transfer of CO₂ was possible for only a few samples. The detection limit for W for the core samples from drill hole 345 is 10 ppm. Since W concentrations in the least altered rocks and in the rocks intersected by drill hole 345 are below that, it follows that mass change of W could not be calculated for drill hole 345. For most of the samples from drill hole 349, the contents of W are below the detection limit of 1 ppm.

The whole analyzed interval (84–158 m) of drill core from drill hole 345 is enriched in Ag, As, Au, B, Bi, Pb, and S, but only the enrichments of Au and Ag are strong enough to exceed the limits of background variation. Within the analyzed interval (3–90 m) of core from drill hole 349, only Ag, Au, S, and Te are consistently enriched but only Au enrichment exceeds the limits of background variation. The altered zones include narrow (less than or equal to 2 m) zones containing more than 1 ppm Au. One of the highly mineralized zones is hosted by a mafic dike, the others by graywacke schist (Fig. 28). A summary of mass changes within these highly mineralized zones, and within contiguous less mineralized ($0.1 \text{ ppm} \leq Au < 1 \text{ ppm}$) rocks, is shown in Fig. 29.

The mineralized zones within the graywacke schist are characterized by strong enrichment of Ca and slight enrichments of Mn and Fe (Fig. 29). The weak enrichment of Na and slight decreases of LOI and K do not exceed the limits of background variation. Within the highly mineralized zones, Au and As are intensely enriched, Bi is strongly enriched, and Sr and Pb are moderately enriched. Chromium shows slight depletion. The

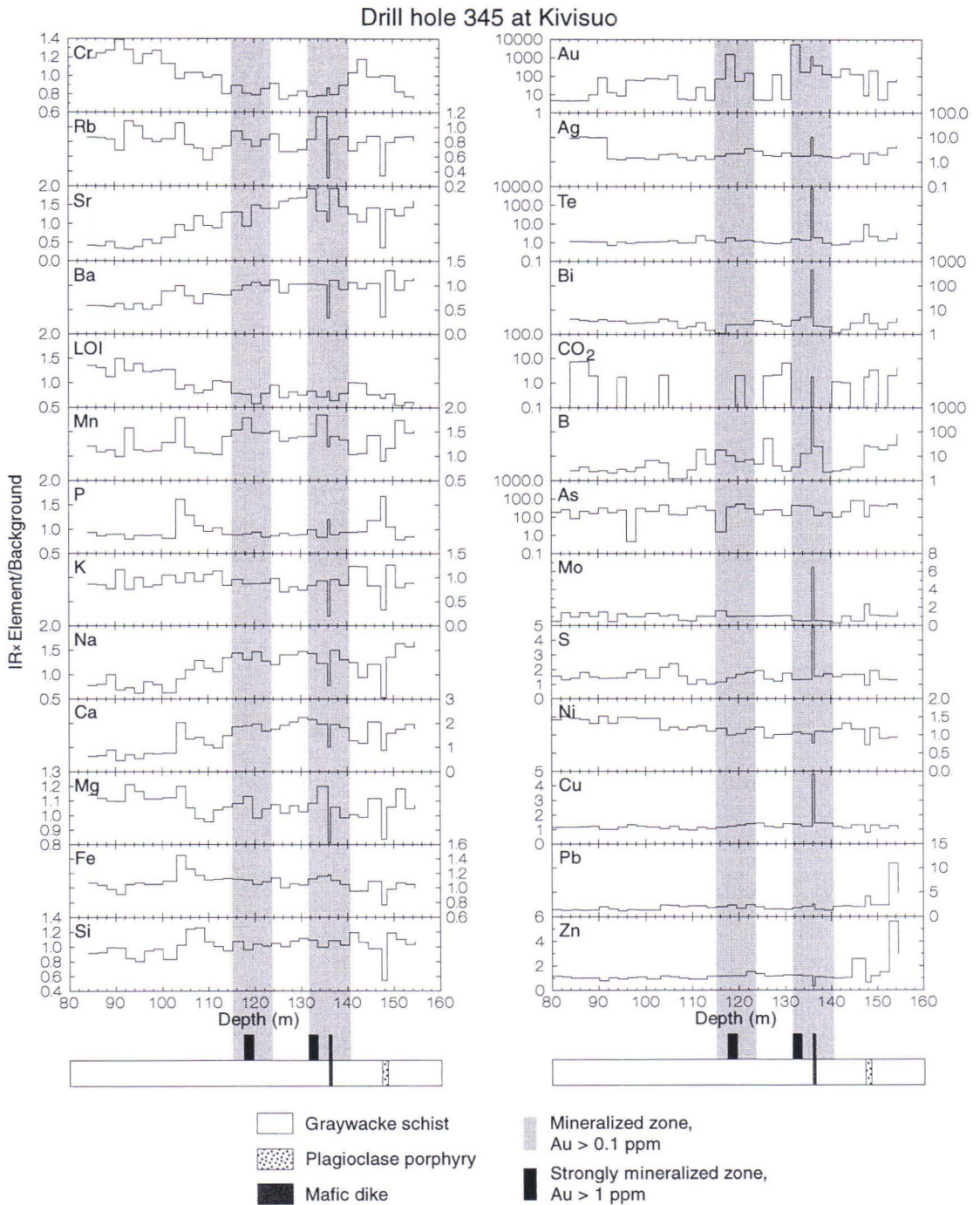


Fig. 28. Mobility versus depth for selected elements within diamond drill hole 345 at Kivisuo. Mobility is expressed as $IR \times c^a/c^b$, where IR is the immobile element ratio and c^b and c^a are the concentrations of component c before and after alteration, respectively.

enrichments of B, Ag, Te, S, Cu, Zn, and Co, and the depletion of Rb, are within the limits of background variation. Mass changes of CO₂ and W could not be calculated for the mineralized graywacke schist samples. The low level of enrichment of Ag, Bi, and Te is noteworthy, as well as the fact that no elements show distinct anomalies above local background that coincide with the Au anomalies (Fig. 28). A few elements, however, display a broad halo covering all the mineralized zones, in particular Ca, Na, Mn, Sr (positive halo), and Cr (negative halo). Moreover, Ag, Bi, CO₂, Cu, Mo, S, Te, and W each show at least a narrow anomaly coinciding with the Au peak in rocks intersected by drill hole 349.

Major element mobility within the mafic dike is characterized by strong K depletion.

Slight enrichments are shown by Al, P, Mn, and Fe, and slight depletions by Mg and Ti. The decreases of Na and LOI are within the limits of background variation. Of the trace elements, Au, Te, B, Bi, and As are intensely enriched, Ag, Mo, Cu, and Pb are strongly enriched, Rb, Ba, and Zn are moderately depleted, and Ni is slightly depleted. The enrichments of S and CO₂, and the depletion of Cr, do not exceed the limits of background variation. Most of the elements that show enrichment or depletion also exhibit local anomaly peaks coinciding with the mineralized zone within the mafic dike (Fig. 28). Only As, Cr, Fe, LOI, Ni, and Pb have either a very small peak or no peak at all. The anomaly due to CO₂ within the dike does not differ from its other, seemingly random anomalies.

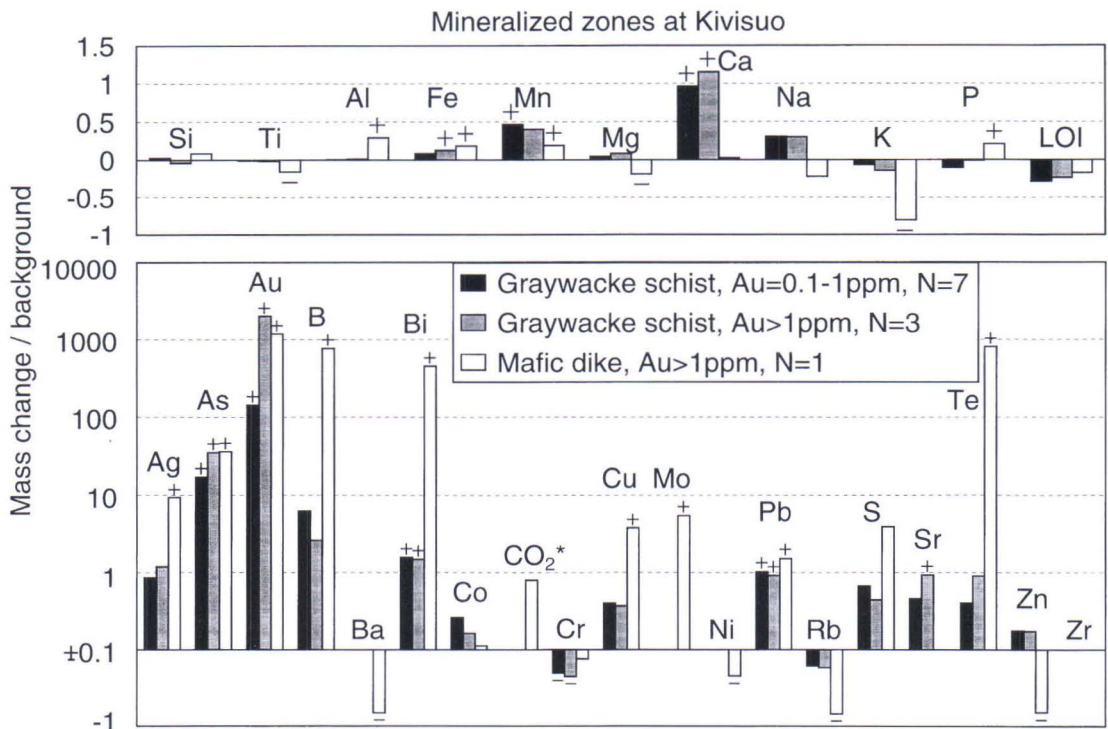


Fig. 29. Summary of relative mass changes within the mineralized zones intersected by diamond drill holes 345 and 349 at Kivisuo. Relative changes less than or equal to $\pm 10\%$ have been omitted for the trace elements. To make comparisons of gains and losses easier, the scale for the depletions in the lower diagram is also logarithmic. A plus sign above the bar or a minus sign below the bar indicates that the value is outside the limit of background variation. CO₂*: Graywacke schist, Au=0.1–1 ppm, N=2, not shown; Graywacke schist, Au>1 ppm, N=0.

Muurinsuo

The Muurinsuo gold occurrence is located within the schists adjacent to the northern end of the Kuittila Tonalite (Figs. 2 and 30). A 300-m-long and approximately 10-m-wide

NE-trending mineralized zone, and several additional subparallel horizons have been delineated within the schist belt, about 200 m from the northwestern contact of the Kuittila

Table 9. Median compositions of the least mineralized ($Au < 100$ ppb) and strongly mineralized ($Au \geq 1000$ ppb) host rocks at the Muurinsuo occurrence. Maf volc: mafic volcanic rocks; Int volc: intermediate volcanic rocks; Sed: sedimentary rocks; Porp: porphyry dikes; -: not analyzed. Number of samples is shown in parentheses. For the least mineralized sedimentary rocks, least mineralized porphyry dikes, strongly mineralized mafic volcanic rocks, and strongly mineralized sedimentary rocks, Li is based on 155, 30, 1, and 3 samples, respectively. For the least mineralized sedimentary rocks, least mineralized porphyry dikes, and strongly mineralized sedimentary rocks, W is based on 180, 46, and 10 samples, respectively.

	Least mineralized				Strongly mineralized		
	Maf volc (5)	Int volc (18)	Sed (195)	Porp (51)	Maf volc (5)	Sed (14)	Porp (1)
SiO ₂ %	51.60	65.20	65.90	61.50	50.60	63.45	59.70
TiO ₂ %	0.84	0.58	0.65	0.59	0.86	0.66	0.66
Al ₂ O ₃ %	11.40	15.10	15.10	15.80	11.20	15.40	19.00
Fe ₂ O ₃ %	9.67	5.83	6.16	6.18	10.00	6.42	5.55
MnO %	0.19	0.06	0.05	0.10	0.27	0.06	0.05
MgO %	12.10	2.51	2.80	3.40	11.20	3.18	2.20
CaO %	7.51	1.61	1.32	4.29	7.26	1.36	3.40
Na ₂ O %	1.25	2.84	2.42	3.61	0.56	2.13	3.94
K ₂ O %	1.91	2.38	2.37	2.04	1.74	2.31	0.79
P ₂ O ₅ %	0.31	0.12	0.11	0.17	0.33	0.13	0.18
LOI %	2.00	1.77	2.08	1.23	2.39	2.47	2.62
Ag ppm	0.06	0.21	0.19	0.20	0.65	0.28	0.66
As ppm	9.1	5	4.6	6.2	912	15	18
Au ppb	5	10	10	20	1800	1400	1550
B ppm	25	75	70	30	1320	162	7340
Ba ppm	307	669	650	753	225	578	420
Bi ppm	0.4	0.3	0.2	0.2	1.8	0.5	5.3
Co ppm	29	26	27	28	53	35	22
CO ₂ %	0.04	0.01	<0.01	0.14	0.02	0.01	0.03
Cr ppm	668	227	252	136	752	255	104
Cu ppm	15	57	59	53	32	62	133
Li ppm	-	51	52	62	43	40	-
Mo ppm	3	3	3	3	4	3	28
Ni ppm	243	87	96	52	402	114	46
Pb ppm	3	12	7	9	4	6	5
Rb ppm	88	81	85	79	64	86	36
S %	0.07	0.70	0.61	0.77	0.97	0.71	1.99
Sr ppm	443	384	289	674	410	287	879
Te ppb	90	300	240	380	2100	685	3620
W ppm	<1	4.5	3	2.5	<1	<1	<1
Zn ppm	83	84	69	68	76	87	30
Zr ppm	126	122	125	111	129	130	152

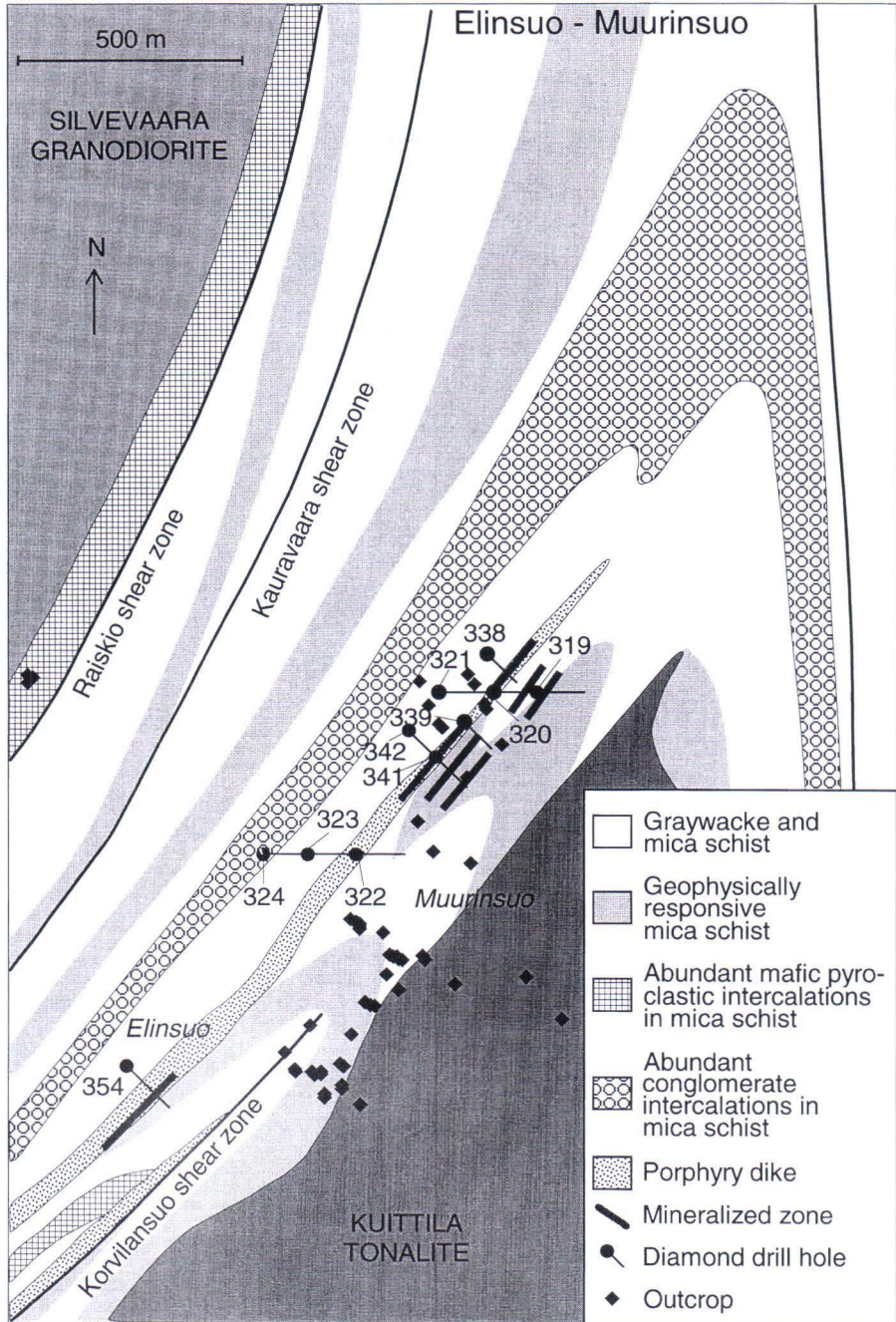


Fig. 30. Simplified geology and location of sampled diamond drill holes at the Muurinsuo and Elinsuo gold occurrences. The map has been redrawn after Nurmi et al., 1993.

Tonalite (Nurmi et al., 1993). However, the ore grades seem to be discontinuous and probably represent many separate lenses or elongate lodes. Disseminated gold occurs in altered mica schists, mafic volcanic rocks, and porphyry dikes. Average chemical compositions of least mineralized and strongly mineralized host rocks are given in Table 9.

Rock types in the Muurinsuo area comprise tightly foliated mica schists and graywackes, with thin conglomeratic and mafic tuffaceous intercalations. The samples have been plotted on a $\text{SiO}_2 - \text{Na}_2\text{O} + \text{K}_2\text{O}$ diagram to enable comparison with the other gold occurrences (Fig. 31). Sheared quartz-plagioclase porphyry dikes con-

taining disseminated sulfides are abundant, especially in the southwestern part of the mineralized zone. The porphyry dikes commonly contain thin quartz-siderite and quartz-tourmaline veins (Nurmi et al., 1993). Tourmaline also occurs as an accessory mineral in all rock types (Kojonen et al., 1993). The mica schists and graywackes have been extensively altered to sericite and sericite-chlorite schists, containing quartz, muscovite, plagioclase, chlorite, and biotite as major components. Disseminated sulfides include pyrite, pyrrhotite, chalcopyrite, minor arsenopyrite, pentlandite and galena, and rare molybdenite. Ilmenite and rutile also occur as disseminations (Kojonen et al., 1993). The mafic volcanoclastic interbeds are characterized by abundant chlorite and actinolite (Sorjonen-Ward, 1993).

Native gold occurs with Bi, Au, and Ag tellurides and disseminated sulfides. Gold grades of 1–3 ppm over 2–5 m are typical, and the best assays reported by Nurmi et al. (1993) are 2.5–4.9 ppm Au over 5 m. The highest gold grade in the present data is 6 ppm over an interval of 2 m.

The Muurinsuo samples were taken from 51 outcrops and 10 diamond drill holes within the schist belt near the northwestern margin of the Kuittila Tonalite (Fig. 30). Samples from drill holes 319, 320, 321, 322, 323, and 324 represent 0.4–8.6 m of core (average 5.0 m) while samples from drill holes 338, 339, 341, and 342 represent 0.7–2.7 m of core (average 2.0 m). For drill holes 339 and 342, only samples within limited intervals covering the mineralized zones were analyzed for all elements. The outcrop samples usually have less than 100 ppb Au, and drill holes 322, 323, 324, and 339 do not intersect mineralized zones in which Au values exceed 1 ppm.

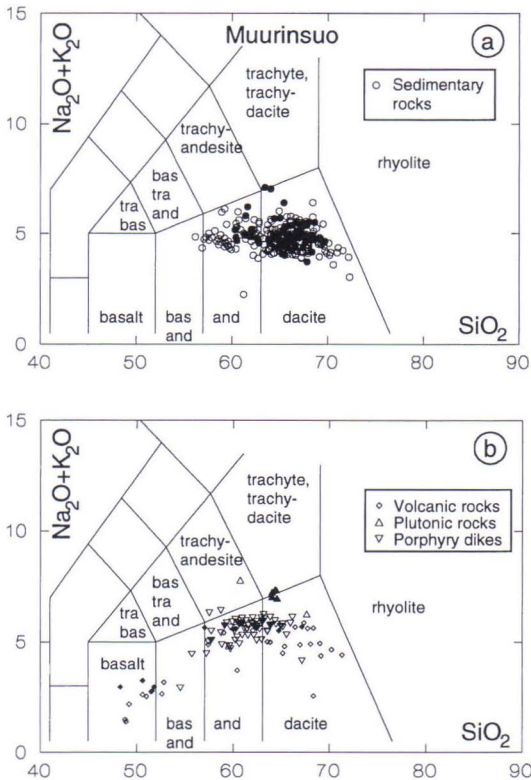


Fig. 31. $\text{SiO}_2 - \text{Na}_2\text{O} + \text{K}_2\text{O}$ diagram for the Muurinsuo sedimentary (a) and igneous (b) rocks. The least altered samples are shown as filled symbols. The sedimentary rocks are plotted to facilitate comparison with the igneous rocks. bas and: basaltic andesite, and: andesite, tra bas: trachybasalt, bas tra and: basaltic trachyandesite.

Geochemical alteration

Calculated mobilities of selected elements in rocks intersected by diamond drill hole 342 are

Table 10. Mass transfer within, and minimum width of, zones of hydrothermal alteration at Muurinsuo. Drill holes not intersecting strong mineralization ($Au \geq 1$ ppm) are shown in parentheses. Elements in parentheses are consistently enriched or depleted, but some values fail to exceed the limits of background variation. Lithium was not analyzed and the detection limit for W was 10 ppm for drill holes 338, 339, 341, and 342, and 1 ppm for the other drill holes.

Drill hole	Minimum width of alteration (m)	Enriched	Depleted
319	144.90	(Ag, B, Co, S, Te, W)	
320	141.90	Au, (As, B, S, Te, W)	
321	145.10	(B, S, Te, W)	(Zn)
338	104.90	Au, (Ag, B, LOI, S)	(Mo)
341	95.25	(Ag, B, S, Te)	
342	50.50	Au, (Ag, B, Bi, S, Te)	
(322)	139.80	(Ag, B, S, Te, W)	(Zn)
(323)	137.60	(Ag, B, Mo, S, Te, W)	
(324)	134.70	Au, Te, (Ag, As, B, Bi, S)	(Li, Mn)
(339)	56.85	Au, (Ag, S, Te)	(Sr)

shown in Fig. 32 as representative of the Muurinsuo occurrence. The analytical detection limit of W for core samples from drill holes 338, 339, 341, and 342 is 10 ppm. Tungsten concentrations in both the least altered rocks and in the rocks intersected by these drill holes are below 10 ppm, and mass transfer of W could not be calculated for these drill holes.

All the 10 drill holes intersect hydrothermal alteration haloes within which Ag, B, S, and Te are usually enriched, and Au and W are commonly enriched (Table 10). However, excluding Au, and Te in drill hole 324, mass changes of these elements are within the limits of primary variation. Where Au is not indicated as enriched in Table 10, its concentration mostly falls below the detection limit of 10 ppb, and calculating mass change for it has therefore not been possible for these samples. The minimum width of these alteration haloes (length of drill hole or analyzed interval) varies from 50.5 m in drill hole 342 to 145.1 m in drill hole 321. The lack of W enrichment in core samples from drill holes 338, 339, 341, and 342 may be due to the high detection

limit (10 ppm) used in analyzing these samples. The hydrothermally altered rocks intersected by drill holes 319, 320, 321, 338, 341, and 342 contain narrow (0.9–5 m) highly mineralized zones with more than 1 ppm Au. A summary of mass changes within these zones, and the contiguous less mineralized ($0.1 \text{ ppm} \leq Au < 1 \text{ ppm}$) rocks, is shown in Fig. 33.

Major element mobility within the sedimentary rocks is characterized by slight increase of LOI (Fig. 33), while slight depletions of Ca and Na do not exceed the background variation. Some major elements do not behave consistently between the various mineralized zones. In particular, Ca and Na can occasionally show enrichment (Fig. 32). Of the trace elements, Au is intensely enriched within the highly mineralized zones, and Te, As, and Bi are strongly enriched. Enrichments of B, W, Ag, S, CO_2 , Ni, Mo, and Co, and depletions of Pb, Li, Ba, and Zn are within the limits of background variation. None of the elements studied show enrichment or depletion anomalies corresponding to all of the mineralized zones within the sedimentary rocks, and most have no anomalies at all. The best coenrichment with Au is shown by Te, B, Ag, and As.

The mafic volcanic rocks show slight Mn enrichment, moderate to slight Na depletion, and slight Mg depletion (Fig. 33). The increase of LOI exceeds the limit of background variation only within the less intensely mineralized rocks. The behavior of K varies from common slight depletion to moderate enrichment within one mineralized zone. Trace element mobility within the highly mineralized zones is characterized by intense enrichments of Au, As, Te, B, Bi, and S, strong enrichments of Ag and Cu, moderate enrichments of Ni and Co, and slight depletion of Rb. The enrichments of W, Mo, and Pb, and the depletions of CO_2 and Ba are within the limits of background variation. Although CO_2 is on average depleted, it is enriched within some mineralized zones (Fig. 32). The W enrichment shown in Fig. 33 is based on only one

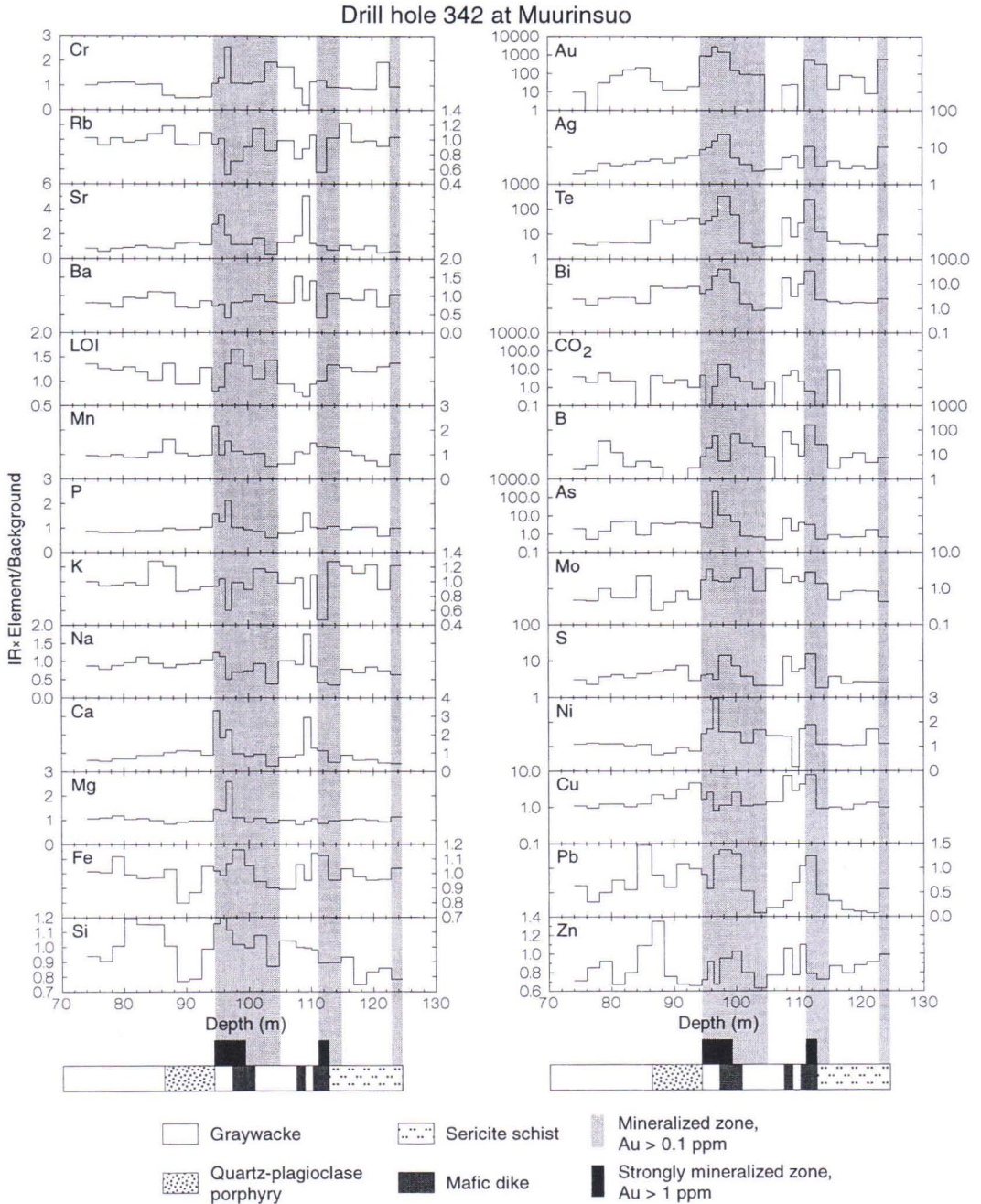


Fig. 32. Mobility versus depth for selected elements within diamond drill hole 342 at Muurinsuo. Mobility is expressed as $IR \times c^1/c^0$, where IR is the immobile element ratio and c^0 and c^1 are the concentrations of component c before and after alteration, respectively.

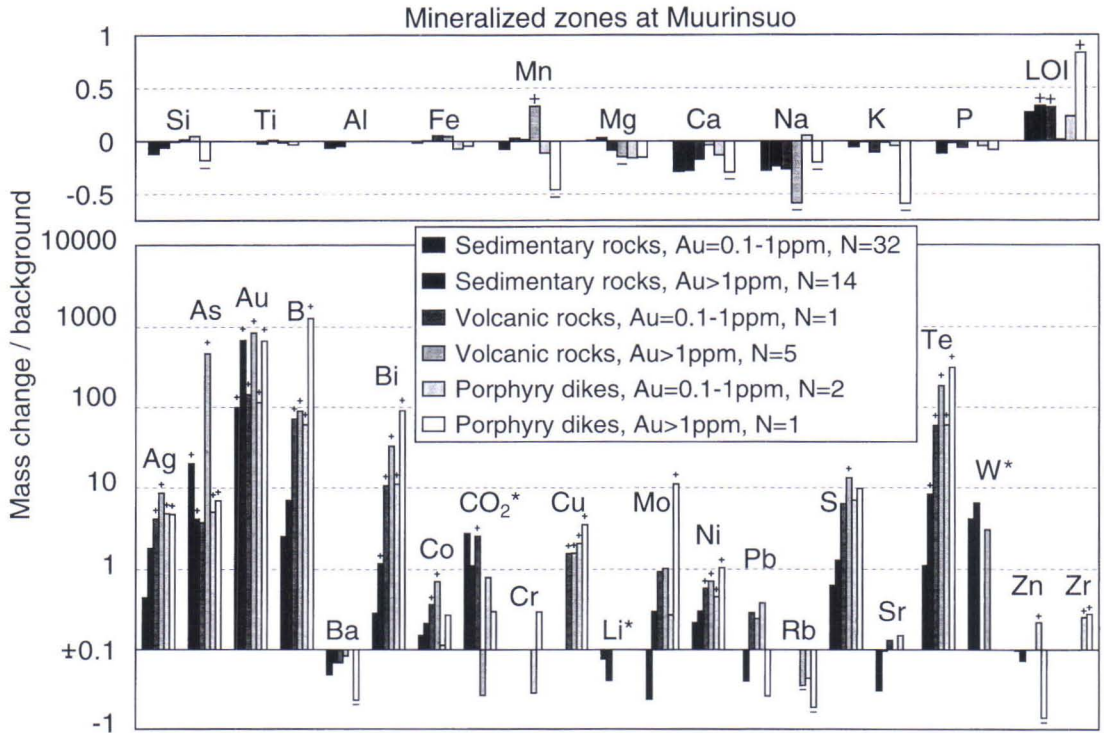


Fig. 33. Summary of relative mass changes within the mineralized zones intersected by diamond drill holes 319, 320, 321, 338, 341, and 342 at Muurinsuo. Relative changes less than or equal to $\pm 10\%$ have been omitted for the trace elements. To make comparisons of gains and losses easier, the scale for the depletions in the lower diagram is also logarithmic. A plus sign above the bar or a minus sign below the bar indicates that the value is outside the limit of background variation. CO_2^* : Sedimentary rocks, Au=0.1–1 ppm, N=19; Sedimentary rocks, Au>1 ppm, N=9. Li^* : Sedimentary rocks, Au=0.1–1 ppm, N=5; Sedimentary rocks, Au>1 ppm, N=3; Volcanic rocks and porphyries, not analyzed. W^* : Sedimentary rocks, Au=0.1–1 ppm, N=5; Sedimentary rocks, Au>1 ppm, N=3; Volcanic rocks, Au=0.1–1 ppm, N=0; Volcanic rocks, Au>1 ppm, N=1; Porphyries, N=0.

sample because W abundances of the other strongly mineralized volcanic samples are below the detection limit of 10 ppm. Lithium was not analyzed for the volcanic samples. Only Ag, As, B (excluding one highly mineralized zone), Bi, Na, S, and Te exhibit distinct anomaly peaks above or below the local background coinciding with all the mineralized zones.

Major element mobility within the porphyries is characterized by moderate increase of LOI, moderate K depletion, and slight Mn, Ca, Na, and Si depletions (Fig. 33). The slight Mg depletion does not exceed the limits of background variation. Of the trace elements,

B, Au, Te, Bi, and Mo are intensely enriched, As, Ag, Cu, and Ni are strongly enriched, Zr is slightly enriched, Zn and Rb are moderately depleted, and Ba is slightly depleted. Enrichments of S, CO_2 , Co, and Cr, and depletion of Pb, are within the limits of background variation. Lithium was not analyzed for the porphyry samples, and the detection limit of W (10 ppm) is too high. All of the altered elements, except Mg, Ca, P, As, Co, CO_2 , Cr, and Pb, show local anomaly peaks coinciding with the highly mineralized zone.

Elinsuo

The Elinsuo gold occurrence is situated about 1 km southwest of Muurinsuo (Figs. 2 and 30). Host rocks (Figs. 31 and 34) and mineralized zones are analogous to those at Muurinsuo and the two targets obviously belong to the same mineralizing system. However, disseminated Fe sulfides are more abundant and tourmalinization is more prominent at Elinsuo (Nurmi et al., 1993). Gold occurs within sheared and altered porphyry dikes as intergrowths within pyrite or Ag and Bi tellurides, and within tourmaline-quartz±sericite±biotite schists as inclusions within pyrite, intergrown

with Ag-Au and Bi tellurides (Kojonen et al., 1993). Typical gold grades are 1–3 ppm over 1–2 m, the highest value being 3.1 ppm Au over 2 m. Average chemical compositions of least mineralized and strongly mineralized host rocks are given in Table 11.

Table 11. Median compositions of the least mineralized (Au<100 ppb) and strongly mineralized (Au≥1000 ppb) host rocks at the Elinsuo occurrence. Sed: sedimentary rocks; Porp: porphyry dikes; -: not analyzed. Number of samples is shown in parentheses.

	Least mineralized		Strongly mineralized
	Sed (18)	Porp (1)	Sed (5)
SiO ₂ %	64.40	62.10	65.50
TiO ₂ %	0.69	0.63	0.71
Al ₂ O ₃ %	15.25	16.40	14.90
Fe ₂ O ₃ %	6.57	5.88	6.64
MnO %	0.07	0.05	0.04
MgO %	3.08	1.89	2.88
CaO %	1.38	4.32	1.04
Na ₂ O %	2.56	4.14	2.29
K ₂ O %	2.56	1.63	0.50
P ₂ O ₅ %	0.12	0.20	0.11
LOI %	2.31	1.62	2.47
Ag ppm	0.25	0.38	0.54
As ppm	2.1	10	34
Au ppb	45	90	1300
B ppm	93	84	9230
Ba ppm	663	671	193
Bi ppm	0.4	0.4	1.7
Co ppm	34	22	33
CO ₂ %	<0.01	0.02	0.03
Cr ppm	262	35	270
Cu ppm	88	283	83
Li ppm	-	-	-
Mo ppm	7	54	6
Ni ppm	124	13	89
Pb ppm	10	10	7
Rb ppm	92	70	23
S %	0.96	2.08	1.76
Sr ppm	282	884	368
Te ppb	280	410	2550
W ppm	<1	<1	<1
Zn ppm	81	71	6
Zr ppm	139	138	134

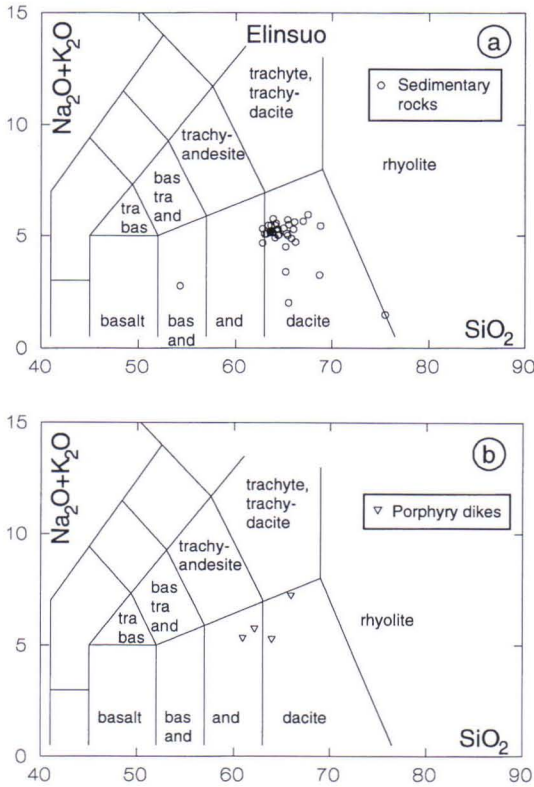


Fig. 34. SiO₂ - Na₂O+K₂O diagram for the Elinsuo sedimentary rocks (a) and porphyry dikes (b). The least altered samples are shown as filled symbols. The sedimentary rocks are plotted to facilitate comparison with the igneous rocks. bas and: basaltic andesite, and: andesite, tra bas: trachybasalt, bas tra and: basaltic trachyandesite.

All of the Elinsuo samples are from diamond drill hole 354, which intersects a NE-trending mineralized zone within the schist belt approximately 200 m from the northwestern margin of the Kuittila Tonalite (Fig. 30). Drill core sample lengths vary from 0.50 to 3.30 m with an average of 2 m. Only a 72 m wide interval including the mineralized zone was analyzed for all elements. Excepting four narrow porphyry dikes, the sampled interval is composed of variably sericitized and chloritized mica schists and graywackes, which in the mineralized zones have altered to quartz-tourmaline rocks (Kojonen et al., 1993).

Geochemical alteration

Calculated mobilities of selected elements in rocks intersected by diamond drill hole 354 are shown in Fig. 35. Abundances for W are mostly below the detection limit of 1 ppm, as are its background values. Consequently, mass transfer of W could only be calculated for a few samples, and it is not shown in Fig. 35. The CO₂ contents are also often below the detection limit of 0.01%, thus precluding mass transfer calculations.

The analyzed interval (32–105 m) is within a zone of hydrothermally altered sericitic schists in which Ag, Au, B, S, and Te are enriched. However, only Au enrichments exceed the limits of background variation. The altered zone contains three narrow (0.55–1.6 m) zones of quartz-tourmaline rock that contain more than 1 ppm gold. A summary of mass changes within these highly mineralized zones, and within contiguous rocks with at least 0.1 ppm Au, is shown in Fig. 36.

Major element mobility within the strongly mineralized zones is characterized by moder-

ate depletion of K, moderate increase of LOI and slight enrichment of Fe (Fig. 36). The slight depletions of Ca, Na, and Mn (except within the less intensely mineralized zone) are within the limits of background variation. Most of the major elements behave differently in the first highly mineralized zone compared with the other two zones (Fig. 35). Within the first zone, Si, Fe, Mg, and LOI have increased, and Ca, Na, P, and Mn have depleted, while within the other two zones the changes of these elements are either very small or even slightly reversed (Ca). Manganese depletion defines a negative anomaly persisting for about 12 m into the hanging-wall rocks. Trace element mobility within the strongly mineralized zones consists of intense enrichments of Au, B, Te and As, strong enrichments of Bi, S, and Ag, moderate enrichments of Co and Cu, strong depletion of Zn, and moderate depletions of Rb and Ba. The enrichments of CO₂, Mo, and Cr within the highly mineralized zones do not exceed the limits of background variation, unlike the enrichments of Mo and Cr within the less intensely mineralized rocks. Although many elements display an anomaly peak above or below local background that coincides spatially with the first highly mineralized zone, only Ag, As, B, Bi, CO₂, and Te show clear positive anomalies. Conversely, Ba, K, Rb, and Zn exhibit distinctive negative anomalies that coincide precisely with each of the highly mineralized zones.

None of the four porphyry dikes on the hanging-wall side of the mineralized zones are strongly mineralized, although they typically have more than 100 ppb Au, and show slight negative anomalies of Mg, Mn, K, and Ni, and distinct positive anomalies of Ag, As, Bi, Te, and S (Fig. 35). For the remaining elements, both positive and negative anomalies are present.

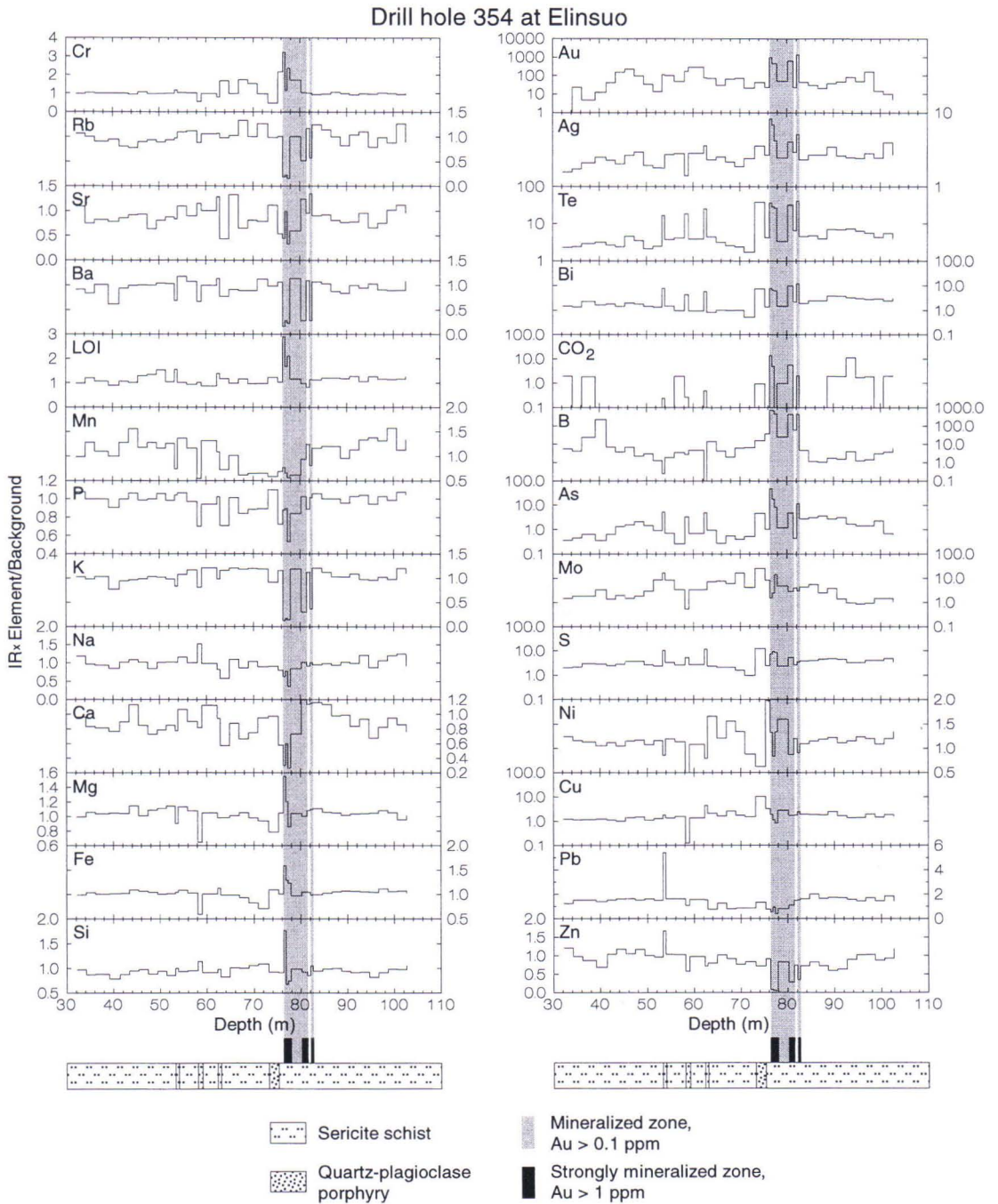


Fig. 35. Mobility versus depth for selected elements within diamond drill hole 354 at Elinsuo. Mobility is expressed as $IR \times c^b/c^a$, where IR is the immobile element ratio and c^b and c^a are the concentrations of component c before and after alteration, respectively.

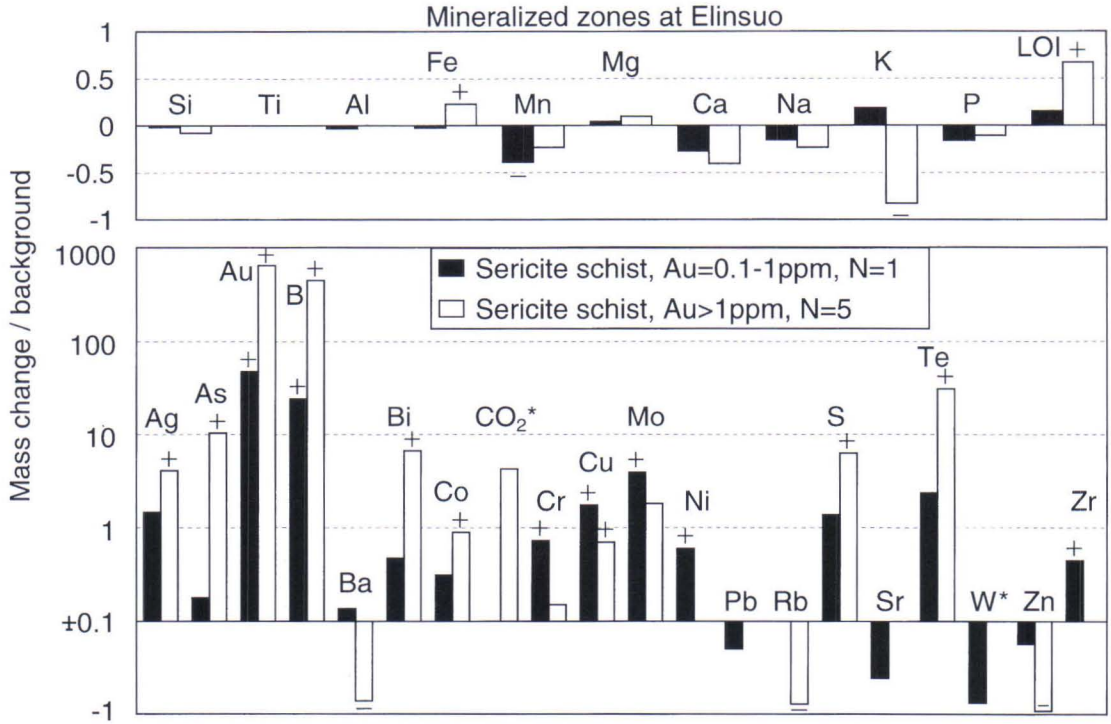


Fig. 36. Summary of relative mass changes within the mineralized zones intersected by diamond drill hole 354 at Elinsuo. Relative changes less than or equal to $\pm 10\%$ have been omitted for the trace elements. To make comparisons of gains and losses easier, the scale for the depletions in the lower diagram is also logarithmic. A plus sign above the bar or a minus sign below the bar indicates that the value is outside the limit of background variation. CO_2^* : Au>1 ppm, N=4. W^* : Au>1 ppm, N=2, not shown.

Rämepuro

The Rämepuro gold occurrence is located about 8 km to the north of Muurinsuo, at the eastern contact of the Hattu schist belt (Fig. 1). The occurrence has been drilled and evaluated by Outokumpu Finmines Ltd. (Pekkarinen, 1988).

The rock types at Rämepuro (Figs. 37 and 38) comprise intermediate volcanoclastic rocks at the western contact of the Viluvaara granodiorite, overlain to the west by graywackes with some conglomeratic and felsic pyroclastic intercalations (Ojala, 1988; Ojala et al., 1990). A quartz-plagioclase porphyry dike up to 30 m thick has intruded the contact between the graywackes and volcanoclastic rocks. A few thin banded iron formation ho-

rizons occur within both the volcanoclastic rocks and the graywackes. Average chemical compositions of least mineralized and strongly mineralized host rocks are given in Table 12.

The graywacke is lepidoblastic and has plagioclase, quartz, biotite, and occasionally also muscovite and chlorite, as principal minerals (Ojala, 1988; Kojonen et al., 1993). The volcanoclastic rocks are fine-grained and more homogenous than the graywackes, and consist mainly of plagioclase, quartz, biotite, chlorite, actinolite, and muscovite (Ojala, 1988). The quartz-plagioclase porphyry is fine- to medium-grained and has quartz and albite phenocrysts. Other principal minerals are bi-

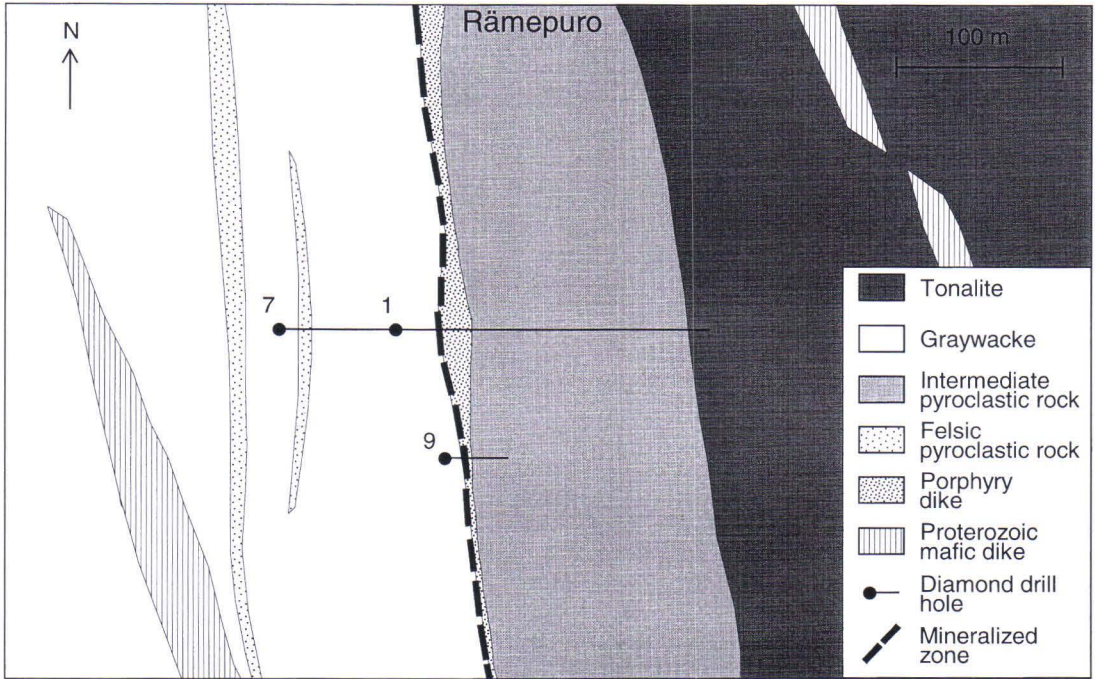


Fig. 37. Simplified geology and location of sampled diamond drill holes at the Rämepuro gold occurrence. Modified after Ojala et al., 1990.

otite and muscovite. Pyrite, pyrrhotite, chalcopyrite and ilmenite occur as disseminations within all the rock types (Ojala, 1988; Kojonen, 1993).

Gold is hosted by narrow, strongly sheared zones within the quartz-plagioclase porphyry dike and adjacent schists. The mineralized zone is 1.5 to 10 m wide, about 500 m long on the surface, and dips steeply to the west. Gold occurs mainly within semiconcordant quartz-tourmaline veins that are a few centimeters to several tens of centimeters thick, but also as disseminations within the altered host rocks, which are mainly composed of quartz, sericite, biotite, albite, chlorite, and tourmaline (Nurmi et al., 1993). The quartz-tourmaline veins contain zoned blue-green-orange tourmaline, quartz, plagioclase, mica, and chlorite as principal minerals. Pyrrhotite, pyrite, chal-

copyrite, sphalerite, and ilmenite are common (Kojonen et al., 1993). Fine-grained native gold occurs between quartz and tourmaline grains, as well as intergrown with sulphides, commonly associated with metallic bismuth and hedleyite (Kojonen et al., 1993). Estimated mineral resources down to a 50–70 m depth are about 250 000 t of ore grading 5 ppm Au (Pekkarinen, 1988).

The Rämepuro samples were taken from three diamond drill holes (1, 7, and 9) adjacent to the eastern contact of the Hattu schist belt (Fig. 37). Drill core sample length varies from 2.75 m to 15.85 m with an average of 10.5 m. Most of the samples (30) are from the profile comprising drill holes 1 and 7, which were sampled from beginning to end. The mineralized zone intersected by drill hole 9 is represented by three samples.

Table 12. Median compositions of the least mineralized ($Au < 100$ ppb) and strongly mineralized ($Au \geq 1000$ ppb) host rocks at the Rämepuro occurrence. Maf volc: mafic volcanic rocks; Int volc: intermediate volcanic rocks; Sed: sedimentary rocks; Porp: porphyry dikes; -: not analyzed. Number of samples is shown in parentheses. Smaller number of samples for the least mineralized mafic volcanic rocks: Bi 1, Mo 1; for the least mineralized intermediate volcanic rocks: Bi 2, Mo 1; for the least mineralized sedimentary rocks: Bi 1; for the least mineralized tonalites: Bi 3, Mo 1; for the strongly mineralized sedimentary rocks: Mo 1; for the strongly mineralized porphyry dikes: Ag 1, Mo 1.

	Least mineralized				Strongly mineralized	
	Maf volc (2)	Int volc (11)	Sed (9)	Ton (4)	Sed (2)	Porp (2)
SiO ₂ %	61.00	60.20	65.20	67.15	63.85	69.75
TiO ₂ %	0.57	0.78	0.59	0.35	0.63	0.51
Al ₂ O ₃ %	13.70	17.10	15.80	15.40	15.95	14.25
Fe ₂ O ₃ %	13.10	8.71	6.45	3.04	7.32	6.48
MnO %	0.16	0.08	0.10	0.06	0.11	0.05
MgO %	3.12	3.81	2.09	1.45	2.38	1.71
CaO %	2.75	1.83	2.75	3.09	2.21	0.82
Na ₂ O %	1.79	2.37	3.78	5.80	2.67	2.28
K ₂ O %	2.65	2.10	2.20	2.38	2.98	2.08
P ₂ O ₅ %	0.13	0.10	0.12	0.13	0.12	0.06
LOI %	1.16	2.54	1.08	0.89	1.89	1.77
Ag pp	-	-	-	-	-	4.1
As ppm	12	62	5	1.5	11	11
Au ppb	32	3	9	1	4940	11000
B ppm	660	100	110	30	980	2915
Ba ppm	445	440	590	750	680	695
Bi ppm	0.5	0.5	0.5	1	33	351
Co ppm	25	34	21	8.5	25	28
CO ₂ %	0.04	<0.01	0.01	0.16	0.01	<0.01
Cr ppm	195	260	140	84	185	130
Cu ppm	78	75	58	92	150	378
Li ppm	70	80	50	30	65	43
Mo ppm	7	5	-	12	5	0.5
Ni ppm	84	120	64	26	68	93
Pb ppm	8	10	8	8	4	2
Rb ppm1	45	120	90	95	130	68
S %	0.74	0.28	0.33	0.17	0.58	0.96
Sr ppm	320	270	540	865	390	345
Te ppb	130	47	31	12	625	6400
W ppm	8	4	5	7	8	11
Zn ppm1	10	120	91	65	115	145
Zr ppm	75	110	100	90	100	74

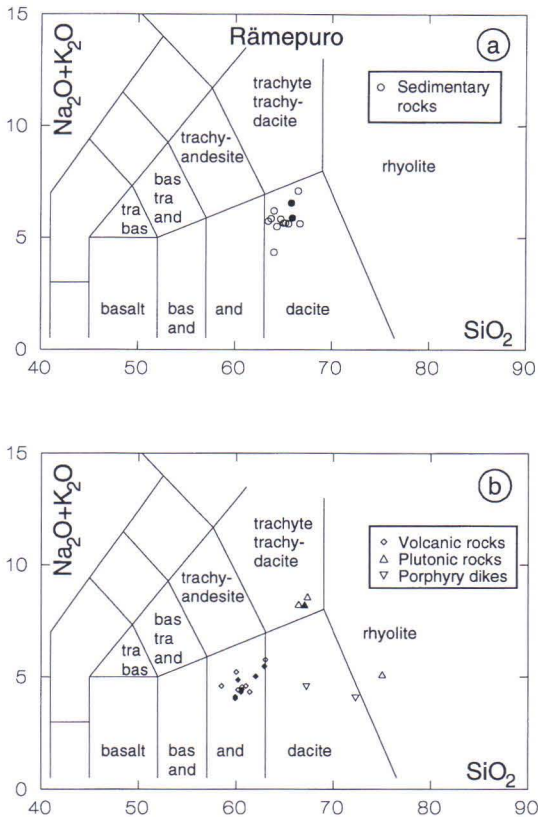


Fig. 38. SiO_2 - $\text{Na}_2\text{O} + \text{K}_2\text{O}$ diagram for the Rämepuro sedimentary (a) and igneous (b) rocks. The least altered samples are shown as filled symbols. The sedimentary rocks are plotted to facilitate comparison with the igneous rocks. bas and: basaltic andesite, and: andesite, tra bas: trachybasalt, bas tra and: basaltic trachyandesite.

The length of drill core samples from Rämepuro is distinctly greater than that from the other occurrences, which complicates direct comparisons. Furthermore, such long samples easily mask narrow anomalies of Au and related elements. The Rämepuro data have nevertheless been included, to permit documentation of the broad geochemical features of the occurrence.

Geochemical alteration

Calculated mobilities of selected elements in rocks intersected by diamond drill hole 1

are shown in Fig. 39 as representative of the Rämepuro occurrence. The detection limits for Ag, Bi, and Mo (0.5 ppm, 0.5 ppm, and 5 ppm, respectively) are higher for Rämepuro than for the other occurrences. The contents of these elements in the least altered samples are always below the detection limit, and because their abundances at Rämepuro are also generally below the detection limit, their mass transfer could be calculated for only a few samples. For a similar reason, mass transfer of CO_2 could only be calculated for a minority of the intermediate tuff samples.

Throughout the entire length of drill hole 1 (200 m), S and W are consistently enriched, and As, B, and Te are enriched, though not as consistently (Fig. 39). Only B and W show systematic enrichments over the whole length (152 m) of drill hole 7. However, none of the elements show consistent mass changes outside the limits of primary variation. Drill hole 9 is represented by only three samples. All three drill holes intersect a highly mineralized 1.5–10 m wide shear zone, containing more than 1 ppm gold, at the contact between the graywacke and the intermediate tuff. A summary of mass changes within this highly mineralized zone, and within contiguous less mineralized ($0.1 \text{ ppm} \leq \text{Au} < 1 \text{ ppm}$) rocks, is given in Fig. 40.

Major element mobility within the mineralized sedimentary rocks is characterized by moderate K and Mn enrichments. Iron, Al, and Si are slightly enriched, while Mg is slightly depleted. Enrichments of Ca, Na, and P do not exceed the limits of background variation. Of the trace elements, Au, Bi, and B are intensely enriched within the highly mineralized zone, Te, As, and Cu are strongly enriched, and Sr, Li, and Rb are moderately enriched. The enrichments of W, Mo, S, Zn, CO_2 , and Ba, and the depletions of Ni and Cr all lie within the limits of background variation. Despite the relative length of the samples (usually 10–15 m), a number of elements display a distinct

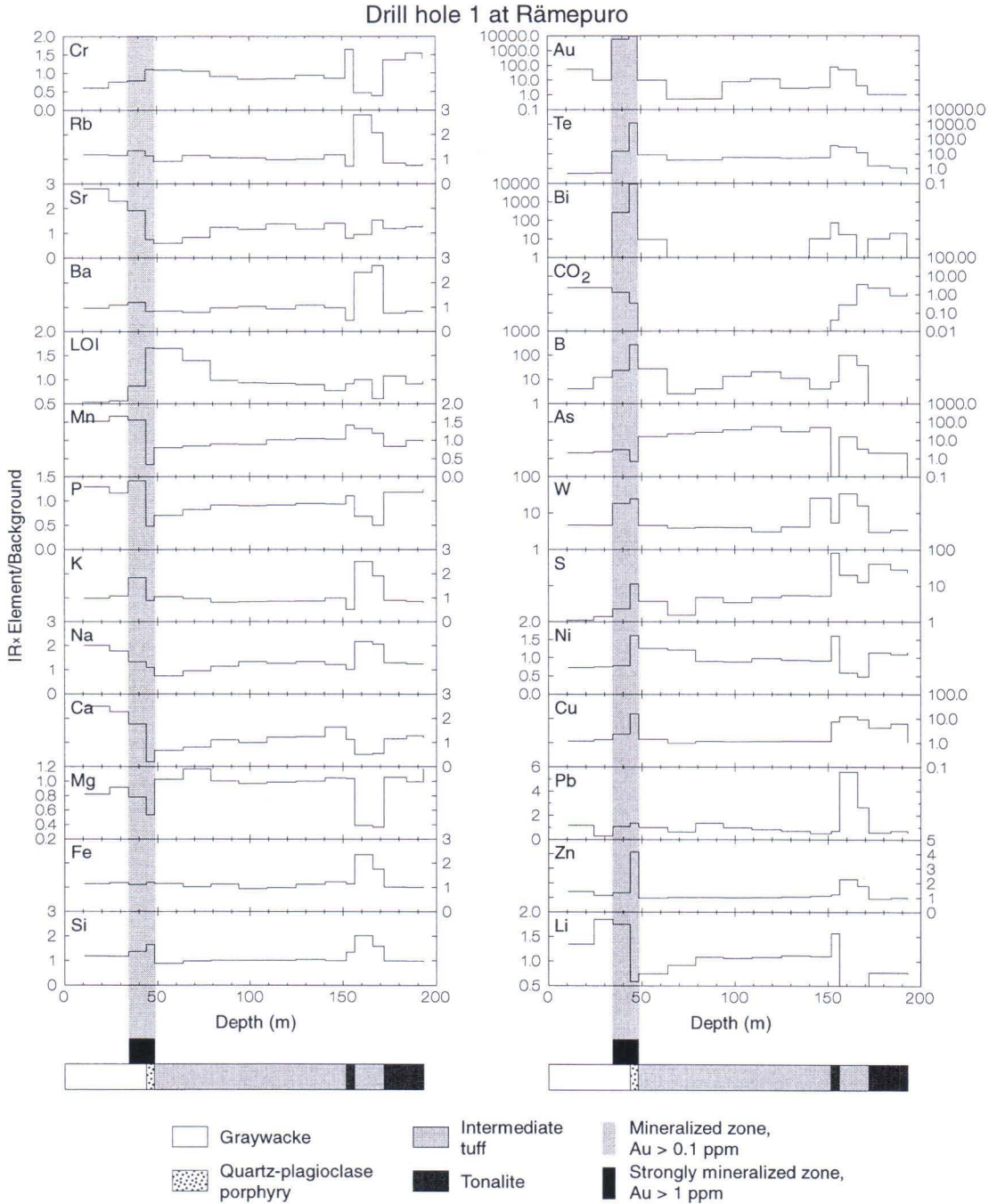


Fig. 39. Mobility versus depth for selected elements within diamond drill hole 1 at Rämepuro. Mobility is expressed as $IR \times \frac{c^a}{c^b}$, where IR is the immobile element ratio and c^a and c^b are the concentrations of component c before and after alteration, respectively.

local anomaly peak coinciding with the mineralized zone intersected by drill hole 1 (Fig. 39). In contrast, only a few elements show such an anomaly in the rocks penetrated by drill hole 7. Elements that consistently exhibit anomaly peaks that coincide with the mineralized zones are K, LOI, B, Ba, Bi, Cu, Li, Rb, S, and Te. Calcium, Na, Mn, and Sr display a positive anomaly that continues for approximately 35 m into the hanging-wall graywackes (Fig. 39). Loss on ignition has an approximately 25 m wide negative anomaly in the hanging-wall graywackes, and a 30-m-wide positive anomaly in the footwall tuffs.

Major element mobility within the mineralized porphyry dikes is characterized by mod-

erate increase of LOI, slight enrichments of Si, Fe and Al, strong depletion of Ca, moderate depletions of P and Mn, and slight depletion of Mg (Fig. 40). The slight depletion of Na does not exceed the limits of background variation. Of the trace elements, Bi, Au, Te, B, Ag, W, and Cu are intensely enriched, As and Zn are strongly enriched, and Ni is moderately enriched, while Sr, Li and Zr are slightly depleted. The enrichment of S, and the depletions of Mo and CO₂ are within the limits of background variation. Except for Fe, Na, Ba, and Sr, all elements that are either enriched or depleted within the mineralized zone also display a local anomaly which coincides with the Au anomaly (Fig. 39).

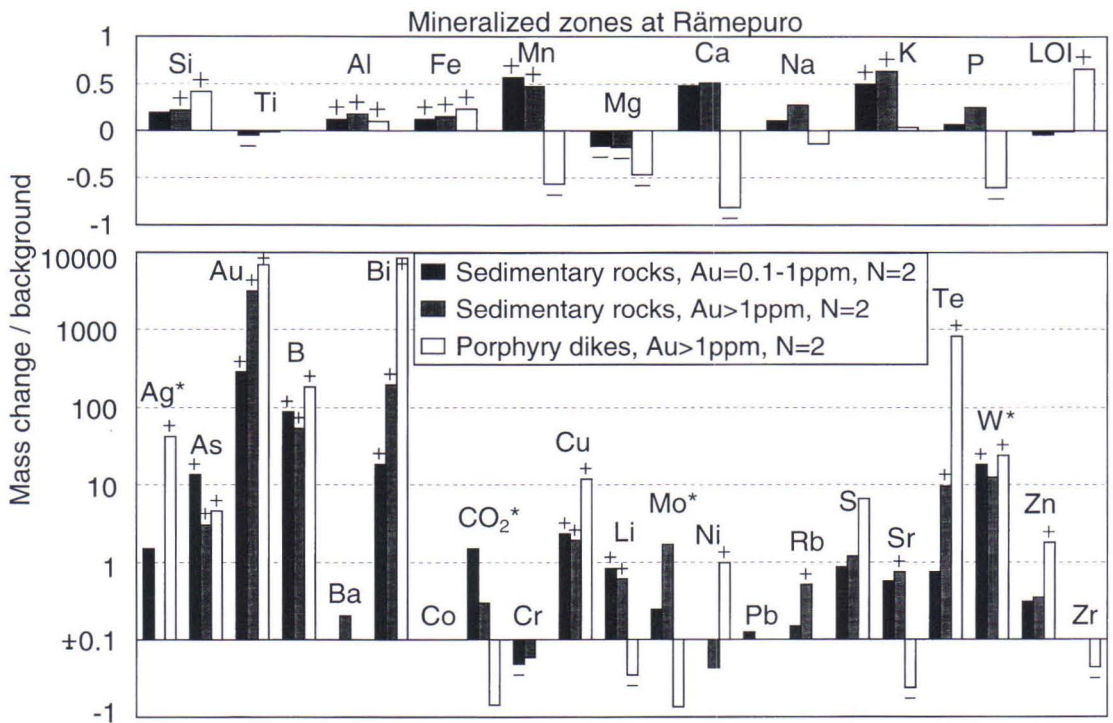


Fig. 40. Summary of relative mass changes within the mineralized zones intersected by diamond drill holes 1, 2, and 9 at Rämepuro. Relative changes less than or equal to $\pm 10\%$ have been omitted for the trace elements. To make comparisons of gains and losses easier, the scale for the depletions in the lower diagram is also logarithmic. A plus sign above the bar or a minus sign below the bar indicates that the value is outside the limit of background variation. Ag*: Sedimentary rocks, Au=0.1–1 ppm, N=1; Sedimentary rocks, Au>1 ppm, N=0; Porphyries, N=1. CO₂*: Sedimentary rocks, Au=0.1–1 ppm, N=1; Sedimentary rocks, Au>1 ppm, N=1. Mo*: Sedimentary rocks, Au=0.1–1 ppm, N=1; Sedimentary rocks, Au>1 ppm, N=1; Porphyries, N=1. W*: Sedimentary rocks, Au=0.1–1 ppm, N=1.

SUMMARY OF GEOCHEMICAL ALTERATION

Wallrock alteration features for the individual gold occurrences are summarized below according to rock type and characteristics of the main rock types are compared with each other and across the gold occurrences. Such

comparisons are complicated because not all the main rock types are mineralized within every gold occurrence. Some general mineralogical interpretations are also given.

Tonalites

The tonalites form the most coherent group among the mineralized main rock types. This is largely due to the fact that all the highly mineralized zones within tonalitic rocks are hosted by the Kuittila Tonalite, which is quite homogenous in composition. The results of the mass transfer calculations can be regarded as reasonably reliable, since a good estimate exists

for the unaltered composition of the tonalite (Appendix 3). All the strongly mineralized tonalite samples come from two occurrences, Kelokorpi and Kuittila. Alteration characteristics at both occurrences, and within the various alteration styles at Kuittila, are quite similar, and differ mostly in intensity (Fig. 41).

Slight to strong increases of Mn, Mg, K,

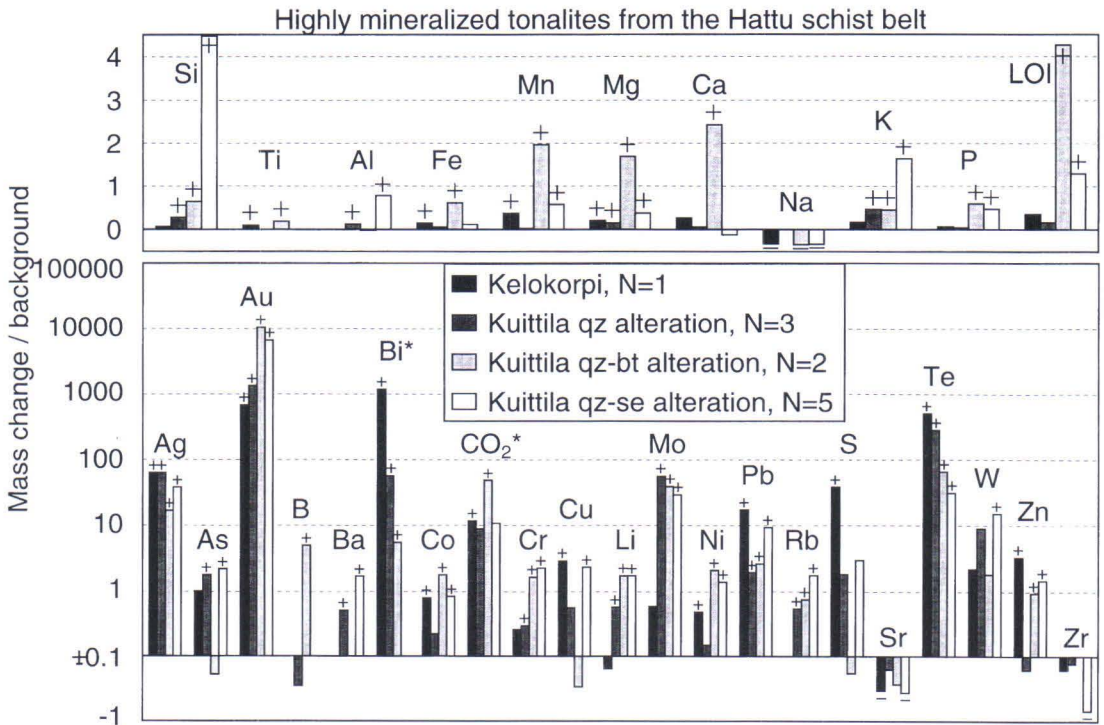


Fig. 41. Summary of relative mass changes within highly mineralized tonalites. Relative changes less than or equal to $\pm 10\%$ have been omitted for the trace elements. To make comparisons of gains and losses easier, the scale for the depletions in the lower diagram is also logarithmic. A plus sign above the bar or a minus sign below the bar indicates that the value is outside the limit of background variation. qz: quartz, bt: biotite, se: sericite. Bi*: Kuittila, qz alteration, N=2; Kuittila, qz-se alteration, N=2, not shown.

and LOI, and slight Na depletion are common to both occurrences, although at Kelokorpi K and LOI exceed the limits of background variation only within the less mineralized rocks surrounding the highly mineralized zone (Figs. 17 and 18). Slight Ti and slight to moderate Fe enrichments occur both at Kelokorpi and within the quartz-biotite alteration zone at Kuittila. Slight to strong Si enrichment and slight to moderate enrichments of P and Al were documented only at Kuittila. Calcium mobility varies considerably at each occurrence, but on average, Ca is significantly enriched only within the quartz-biotite alteration zone at Kuittila. Titanium shows the most immobile behavior, but Al (excluding the quartz-sericite alteration at Kuittila) and Fe (excluding the quartz-biotite alteration at Kuittila) also show very limited mobility.

Intense and consistent enrichments of Au, Te, and Ag, and strong to intense enrichment of Pb are common to both occurrences (Fig.

41). Bismuth is intensely enriched at Kelokorpi, and intensely to strongly enriched within the quartz and quartz-biotite alteration zones at Kuittila, but mostly below detection limit within the quartz-sericite alteration zone. Mass changes among the remaining trace elements do not always exceed the limits of background variation. Carbon dioxide and W are intensely to strongly enriched, and As, Co, Cr, Cu, Ni, S, and Zn are usually strongly to moderately enriched, while Sr and Zr are typically weakly to moderately depleted at both occurrences. Molybdenum is intensely enriched at Kuittila, but only moderately enriched at Kelokorpi. Moderate to strong Ba, Li, and Rb enrichments occur only at Kuittila, while Bi and S show much stronger enrichments at Kelokorpi. Changes in Zr and B are usually small, excluding the moderate depletion within the quartz-sericite alteration zone and the strong enrichment within the quartz-biotite alteration zone at Kuittila, respectively.

Porphyry dikes

Highly mineralized porphyry dikes occur at two occurrences, Muurinsuo and Rämepuro. Compared with the tonalites, the porphyries have more variance in their background compositions, and since the estimate is based on fewer samples, it is more susceptible to errors caused by atypical or altered compositions. The average geochemical behavior during alteration of the porphyries is broadly similar at both occurrences.

Major element mobility is characterized by moderate LOI increase, slight to strong Ca depletion and slight to moderate Mn depletion (Fig. 42). Magnesium, Na, and P are also slightly to moderately depleted, although the depletion exceeds the background variation at only one occurrence. Silicon and Fe are slightly enriched at Rämepuro, but show slight to insignificant depletions at Muurinsuo. Potassium is moderately depleted at

Muurinsuo only. Titanium and Al show mostly immobile behavior, although Al is slightly enriched in one sample from Rämepuro, which raises its average enrichment above the limit of background variation.

Trace element mobility is characterized by consistent, intense enrichments (in diminishing order) of Bi, Au, Te, and B, strong to intense enrichments of Ag and Cu, and strong enrichments of As and Ni (Fig. 42). Barium is slightly depleted, Rb and Zn are moderately depleted, Mo is intensely enriched and Zr is slightly enriched at Muurinsuo. Strontium and Zr are slightly depleted and Zn is strongly enriched at Rämepuro. Tungsten and Li were only analyzed from Rämepuro, where they are intensely enriched and insignificantly depleted, respectively. Variations in Co, CO₂, Cr, Pb, and S in altered samples nowhere exceed the limits of background variation.

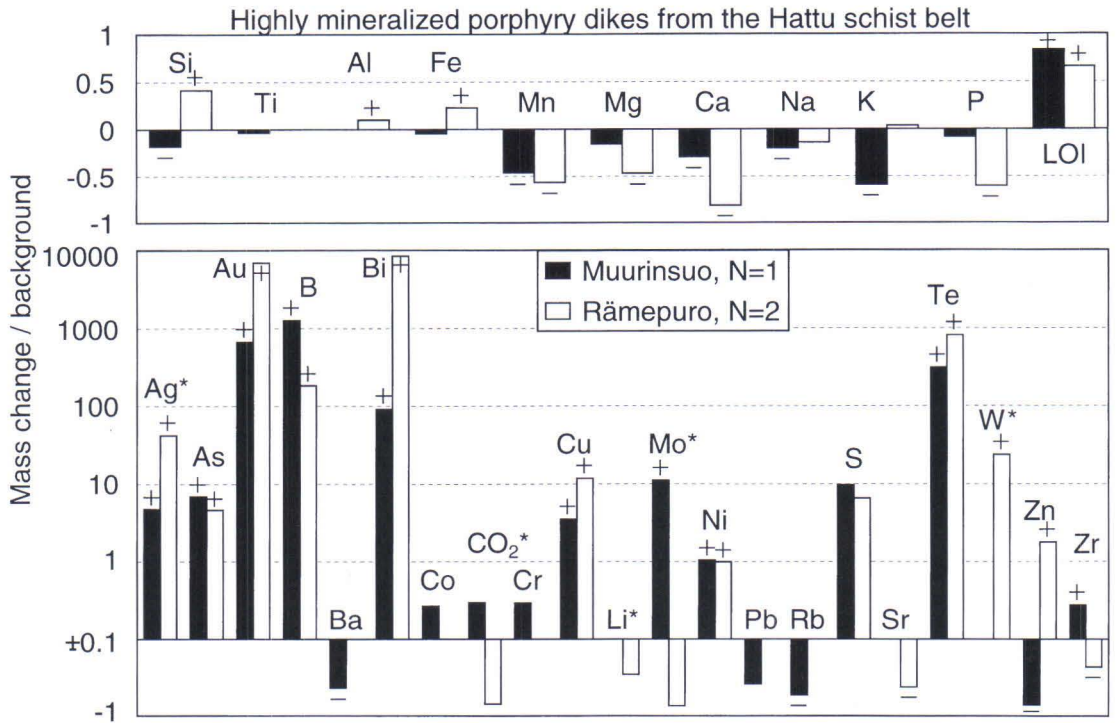


Fig. 42. Summary of relative mass changes within highly mineralized porphyry dikes. Relative changes less than or equal to $\pm 10\%$ have been omitted for the trace elements. To make comparisons of gains and losses easier, the scale for the depletions in the lower diagram is also logarithmic. A plus sign above the bar or a minus sign below the bar indicates that the value is outside the limit of background variation. Ag*: Rämepuro, N=1. Li*: Muurinsuo, not analyzed. Mo*: Rämepuro, N=1. W*: Muurinsuo, N=0.

Volcanic rocks

Volcanic rocks host strongly mineralized zones at Kelokorpi, Kivisuo, and Muurinsuo. The spread in unaltered background compositions is even larger than for the porphyries. Consequently, at least some of the apparent variability in the alteration behavior of the major elements between occurrences is probably due to primary compositional variations.

The least altered samples of mafic and intermediate (subtype 1) volcanic rocks are altered, at least with respect to Na and K. The data points for the mafic and intermediate volcanic rocks on the Hughes diagram (Fig. 11) plot horizontally away from the fields of unaltered basalts and andesites, respectively. This could indicate that K has been added and Na has been removed, while the sum of alkali-

lies has remained unchanged. If this is the case, then the calculated depletions of Na and enrichments of K for the gold occurrences are smaller than in reality and can be taken to represent minimum values of mass change. The calculated enrichments of Na and depletions of K are probably overestimated for the same reason.

Of the major elements, only Mn is consistently and slightly enriched at every occurrence (Fig. 43). Slight Mg depletion occurs at Kivisuo and Muurinsuo, and slight Ti depletion occurs at Kelokorpi and Kivisuo. Sodium is moderately depleted at Muurinsuo. The slight depletion of Na at Kivisuo (within the limits of background variation) can be taken as a minimum estimate, and it is possible that the actual value is significant. Each occurrence

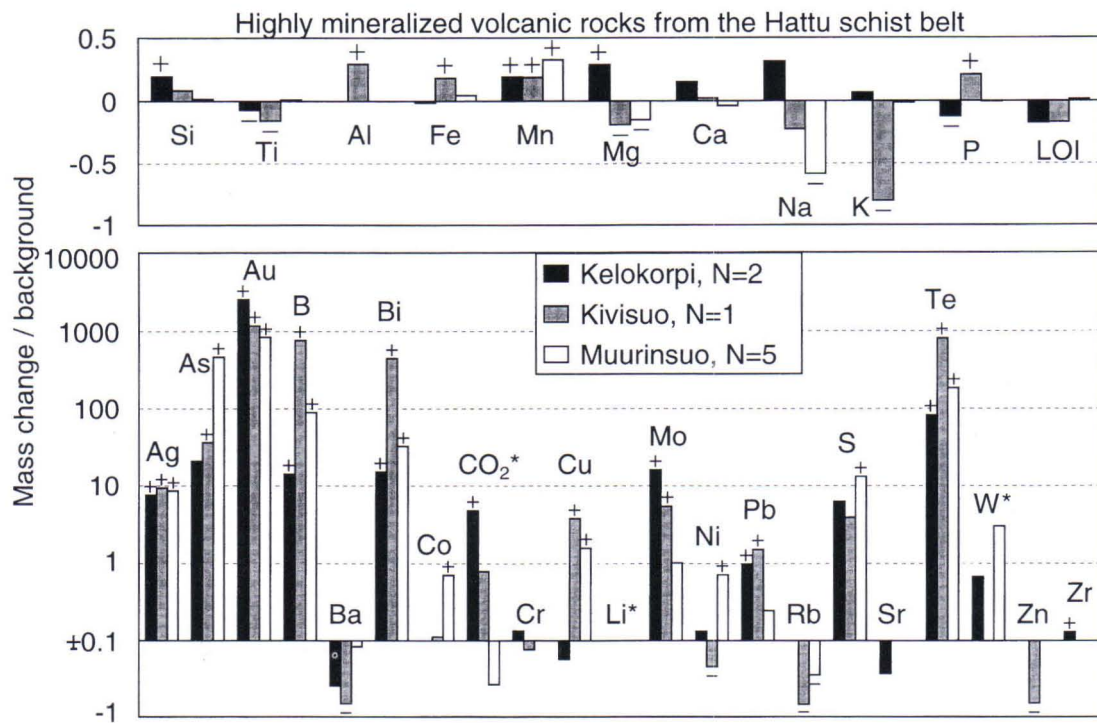


Fig. 43. Summary of relative mass changes within highly mineralized volcanic rocks. Relative changes less than or equal to $\pm 10\%$ have been omitted for the trace elements. To make comparisons of gains and losses easier, the scale for the depletions in the lower diagram is also logarithmic. A plus sign above the bar or a minus sign below the bar indicates that the value is outside the limit of background variation. Li*: Kivisuo, Muurinsuo, not analyzed. W*: Kivisuo, N=0; Muurinsuo, N=1.

has its own characteristic features. Slight but significant Si and Mg enrichments and P depletion only occur at Kelokorpi, where Na and Ca also exhibit slight enrichments, albeit within the limits of background variation. Kivisuo is characterized by intense K depletion and slight Al, P, and Fe enrichments. Again, the K depletion has probably been overestimated. Titanium is immobile only at Muurinsuo.

Patterns of trace element mobility are more coherent between the occurrences. Consistent, and marked increases are shown (in decreasing order) by Au, Te, B, and Bi (Fig. 43). Silver is strongly enriched at every occurrence. Arsenic is consistently intensely enriched, S and Mo are strongly to intensely enriched and Pb is slightly to strongly enriched, although enrichments do not exceed

the limits of background variation at every occurrence. Barium is slightly to moderately depleted at every occurrence, but exceeds the limits of background variation only at Kivisuo. Significant, strong enrichment of CO_2 and slight enrichment of Zr occur only at Kelokorpi. The strong Cu enrichment and slight to moderate Rb depletion present at other occurrences are absent from Kelokorpi. Moderate, but significant enrichments of Co and Ni occur only at Muurinsuo. Kivisuo differs from the other occurrences in having moderate Zn depletion and slight Ni depletion. Chromium, Sr, and Zr are consistently the most immobile elements. Lithium was only analyzed from Kelokorpi, where it shows insignificant depletion. The enrichment of W falls within the limits of background variation.

Sedimentary rocks

Intensely mineralized sedimentary rocks occur at Korvilansuo, Kivisuo, Elinsuo, Muurinsuo, and Rämepuro. The sedimentary rocks are by far the most heterogeneous of the main rock types, and it is difficult to estimate how much of the variability in the alteration characteristics between the occurrences is due to fluctuations in primary composition and inaccuracies in defining the chemical subtype of the precursor.

Due to widespread hydrothermal alteration within the Hattu schist belt, the least altered sedimentary rocks used to estimate the background chemical compositions are most prob-

ably altered. This alteration, combined with the variations induced by primary compositional variations within and between graded beds, can account for the contrasting alteration behavior between the occurrences, and also between alteration zones within a single occurrence.

No major element shows consistent enrichment or depletion across all the occurrences. Slight Fe enrichment is quite common, and LOI shows significant slight to moderate increase within the Muurinsuo-Elinsuo area (Fig. 44). Titanium is immobile at every occurrence. Disregarding the small mobility at

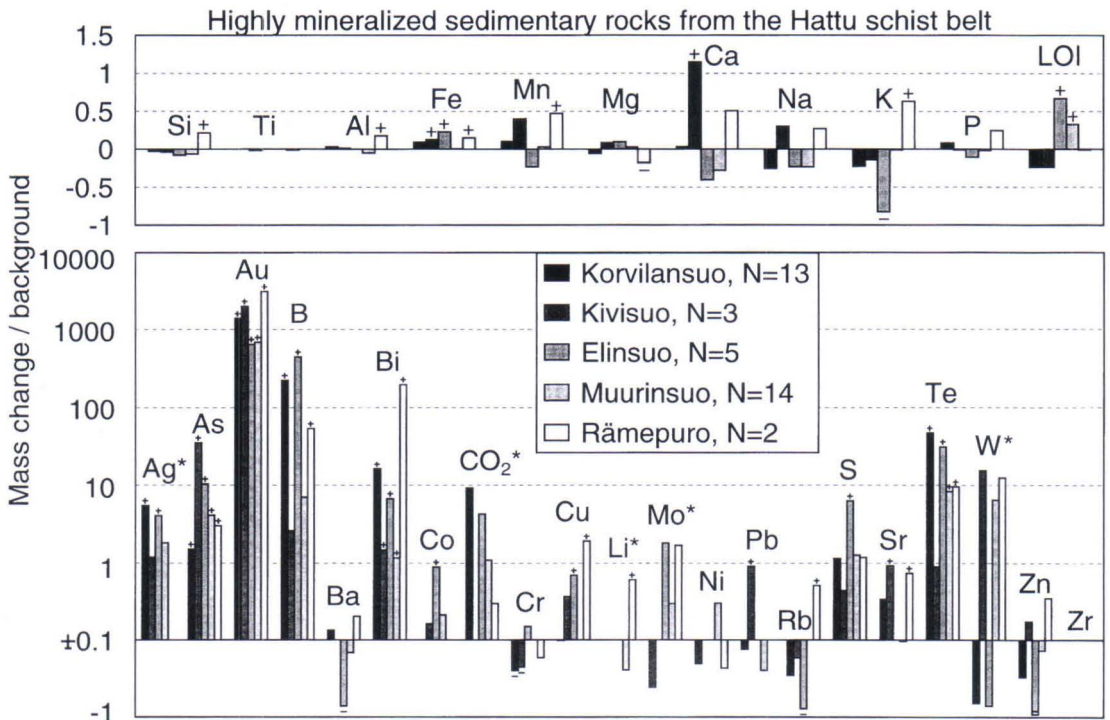


Fig. 44. Summary of relative mass changes within highly mineralized sedimentary rocks. Relative changes less than or equal to $\pm 10\%$ have been omitted for the trace elements. To make comparisons of gains and losses easier, the scale for the depletions in the lower diagram is also logarithmic. A plus sign above the bar or a minus sign below the bar indicates that the value is outside the limit of background variation. Ag*: Rämepuro, N=0. CO₂*: Korvilansuo, N=3; Kivisuo, N=0; Elinsuo, N=4; Muurinsuo, N=9; Rämepuro, N=1. Li*: Korvilansuo, N=1; Kivisuo, Elinsuo, not analyzed; Muurinsuo, N=3. Mo*: Rämepuro, N=1. W*: Korvilansuo, N=11; Kivisuo, N=1; Elinsuo, N=2; Muurinsuo, N=3.

Rämepuro, Al is also immobile, and gains and losses of Si, Mg, and P are negligible. No two occurrences have similar alteration characteristics for all the major elements, and all but Korvilansuo and Muurinsuo record erratic behavior with respect to at least one major element. The strong K enrichment, slight Si and Al enrichments, and slight Mg depletion, which are characteristic of, and exclusive to Rämepuro, might reflect differences in the primary chemical composition of the sedimentary rocks in the northern part of the Hattu schist belt. Kivisuo is distinguished from the other occurrences by strong Ca enrichment, and Elinsuo by intense K depletion (Fig. 44).

Trace element mobility is characterized by consistent, intense increase of Au, and strong to intense increases of Bi and As (Fig. 44). Boron is invariably strongly to intensely enriched, Te is moderately to intensely enriched, Ag is strongly enriched, and S is slightly to strongly enriched, although the enrichments do not exceed the limits of back-

ground variation at every occurrence. Mass transfer of Ag could not be calculated for Rämepuro due to the poor quality of analytical data. Mass transfer of CO₂ could not be calculated for Kivisuo, but at all other occurrences CO₂ is slightly to strongly enriched, although it does not exceed the limits of primary variation. Zirconium is always immobile, and the mobility of Ni is also small. Lead is significantly (moderately) enriched only at Kivisuo, where the strongest enrichment of As and the weakest Ag, B, S, and Te enrichments are also found. Significant, strong depletion of Zn, moderate depletions of Rb and Ba, strong enrichment of S, and moderate enrichment of Co are restricted to Elinsuo. Only Rämepuro shows significant, moderate Rb and Li enrichments; Li was not analyzed from Kivisuo and Elinsuo, though. Bismuth enrichment at Rämepuro is an order of magnitude greater than that recorded elsewhere. Neither Korvilansuo nor Muurinsuo exhibits particularly distinctive alteration signatures.

Comparisons between the main rock types

For each of the rock types, trace element mobility is commonly much stronger than major element mobility. Moreover, excluding a few exceptions, the direction (enrichment or depletion) and magnitude of trace element changes are similar for each rock type. Major element gains and losses are more variable, but can yield information on significant mineralogical changes caused by the interaction of the hydrothermal fluid with the host rocks.

Sodium depletion is common to all the main rock types and is consistent with the typical alteration of plagioclase. The average magnitude of the depletion (-20% to -32%) is similar for all the main rock types (Figs. 41-44), although for the volcanic and sedimentary rocks it is within the limits of background variation. This might be the result of wider primary compositional variations within the

volcanic and sedimentary rocks compared with the tonalites and porphyry dikes. However, because hydrothermal alteration is very widespread within the Hattu schist belt, Na depletion may have affected even the least altered parts of the probably more permeable supracrustal rocks. Slight Fe enrichment is common to all the main rock types, although it does not exceed the limit of background variation at every occurrence. There is no significant Fe or Al depletion in the highly mineralized zones within any main rock type. Titanium and Al are the least mobile major components, but even they show slight changes within some occurrences and host rock types.

Only the tonalites show invariably slight to moderate Mg enrichment. Potassium and Si are also most strongly and consistently en-

riched within the tonalites, although the K enrichment at Kelokorpi exceeds the limit of background variation only in the slightly mineralized rocks adjoining the highly mineralized zone. All other rock types show significant K depletion at one gold occurrence, and no enrichment in K, except within the graywackes at Rämepuro (Figs. 41–44). The porphyry dikes differ from the other rocks in showing consistent, slight to strong depletions in Ca, Mn, and Mg. Only the volcanic rocks show slight, but significant Ti depletion, although not at every occurrence. No major element mass change features are entirely restricted to the sedimentary rocks.

The trace elements display quite similar behavior for all the main rock types. Strongest (more than 100%) average enrichments, when combining data from all the highly mineralized zones are shown by Au, Te, B, Bi, Ag, CO₂, W, As, and S. Only Au, however, shows enrichments that exceed the limit of background variation for all the rock types and occurrences (Figs. 41–44). Silver and Te are consistently significantly enriched within the igneous host rocks, and Bi within the volcanic rocks, porphyry dikes, and sedimentary rocks.

Mineralogical interpretations

The mineralogical interpretations presented are very general in character. No detailed petrographical investigations have been done for this study, and exact chemical compositions of the minerals are usually not known. Moreover, the length of the drill core samples an-

Arsenic enrichment invariably exceeds the limits of background variation within mineralized zones hosted by porphyry dikes or sedimentary rocks. Boron is significantly enriched within all mineralized zones hosted by porphyry dikes or volcanic rocks. Copper and Ni are consistently enriched above the limits of background variation only within the porphyry dikes, and Pb and Rb only within the tonalites. None of the other elements are consistently significantly enriched or depleted within any main rock type, although many of them do exceed the limits of background variation at some occurrences.

The tonalites show the highest average Mo (excluding Kelokorpi) and CO₂ enrichments, smallest average enrichments in B and As, and the most consistent slight enrichments in Ba, Co, Cr, Li, Rb, and Zn. However, none of these elements exceeds the limits of background variation at every mineralized zone. The porphyry dikes have the highest average enrichments in Au, B, Bi, Cu, Te, and W, while the volcanic rocks have the highest average enrichment in As, and the sedimentary rocks show the smallest average enrichments in Ag, Bi, and Te.

alyzed (1–2 m) could easily incorporate more than one mineralogical alteration zone. The suggested mineralogical reactions are qualitative and are presented only as examples of the many potential reactions possible.

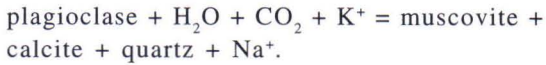
Tonalites

The unaltered Kuittila tonalite contains plagioclase, quartz, biotite, and muscovite as major minerals. Accessory minerals include potassium feldspar, calcite, epidote, zircon,

apatite, and tourmaline (Kojonen et al., 1993; Ojanen, 1993; Sorjonen-Ward, 1993). Alteration around the quartz lodes is visible as sheared and bleached zones several meters wide, with typical mineral assemblages containing quartz, albite, sericite, calcite, potas-

sium feldspar, biotite, and epidote (Nurmi et al., 1993). The most intensely altered zones are dominated by quartz, sericite, and carbonate (Kojonen et al., 1993).

Plagioclase destruction is reflected in the common Na depletion, and sericite formation in the common increase of K and LOI. These changes can be described for example, by the following general reaction:



Simple calculations show that if all the Al in the quartz-sericite altered tonalite were in muscovite, it would require a K enrichment of about 180%. Binding all the Al to either biotite or potassium feldspar would require approximately 730% enrichment of K. Average K enrichment within the quartz-sericite alteration zone at Kuittila is 164%, which is in good agreement with a quartz-sericite-carbonate-albite assemblage. Similar calculations for the Kelokorpi occurrence and for the quartz and quartz-biotite alteration zones at Kuittila indicate that binding all the Al in the altered tonalite to muscovite would result in K enrichment of about 53-75%, and binding it to biotite or potassium feldspar would result in K enrichment of about 360-425%. Because K enrichment at these occurrences is on the average 16-46%, a larger part of Al must have been retained in plagioclase, especially in the quartz-biotite alteration zone.

The strong Ca and CO₂ co-enrichment within the quartz-biotite alteration zone at Kuittila is probably due to carbonate formation. According to Kojonen et al. (1993) the carbonate at both Kuittila and Kelokorpi is invariably calcite. The very good correlation between Ca and the volatile phases within the drill hole 309 at Kuittila (Fig. 21) indicates that most of the Ca in the altered zone is in calcite. This is also supported by the observation that pla-

gioclase in the altered tonalite is almost pure albite (Kojonen et al., 1993). Binding all the Ca to calcite in the highly mineralized zone at Kelokorpi, and in the quartz, quartz-biotite, and quartz-sericite alteration zones at Kuittila would result in average CO₂ enrichments of approximately 2155%, 1790%, 6000%, and 1480%, respectively. These values are larger than the respective calculated CO₂ enrichments of 1167%, 883%, 4848%, and 1073% (Fig. 41), indicating that not all the Ca resides in calcite.

The co-enrichment of Fe, Mn, and Mg can be explained by biotite formation, especially within the quartz-biotite alteration zone at Kuittila, but probably also elsewhere. The enrichment of these elements varies from one mineralized zone to another according to a similar pattern, which is taken to support the interpretation that they all occur within the same mineral. Silicification and quartz veining and brecciation is reflected by the Si enrichment, which is significant only at Kuittila.

Porphyry dikes

The least altered quartz-plagioclase porphyry dikes have quartz, plagioclase, biotite, and muscovite as major minerals, and potassium feldspar, chlorite, epidote, apatite, zircon, titanite, carbonate, and tourmaline as accessory minerals (Ojala, 1988; Kojonen et al., 1993; Ojanen, 1993). Within the mineralized zone at Rämepuro, biotite is in places totally absent and muscovite is present only in trace amounts, while plagioclase is partly altered to potassium feldspar (Ojala, 1988). The increase of LOI, depletions of Ca, Na, Mg, and Mn, and the variable behavior of K, Fe, and Si could all be explained by reactions involving the breakdown of plagioclase and biotite, and formation of muscovite, chlorite, quartz, and potassium feldspar. A general reaction for Rämepuro could be:

biotite + plagioclase + $\text{SiO}_2(\text{aq}) + \text{H}^+ + \text{Fe}^{2+} =$
chlorite + muscovite + potassium feldspar +
quartz + $\text{Mg}^{2+} + \text{Ca}^{2+} + \text{Na}^+$,

and a general reaction for Muurinsuo could be:

biotite + plagioclase + $\text{H}^+ =$ chlorite +
muscovite + $\text{SiO}_2(\text{aq}) + \text{Mg}^{2+} + \text{Ca}^{2+} + \text{Na}^+ + \text{K}^+$.

It is possible that Ca was removed from the rock because there was not enough CO_2 to bind it all within carbonate; CO_2 is only slightly enriched at Muurinsuo and moderately depleted at Rämepuro (Fig. 42). Some of the Fe liberated from biotite (or added by the fluid, as at Rämepuro) has probably reacted with S to form pyrrhotite or pyrite, although the sulfide phase is not considered in the reactions above. In fact a simple calculation shows that if all the Fe in the mineralized porphyries at Muurinsuo and Rämepuro were in pyrrhotite, S enrichments of 1106% and 1825%, respectively, would be required. Since sulfur enrichment at Muurinsuo is 977% (Fig. 42), this does indeed indicate that a considerable proportion of Fe in the mineralized porphyry dikes at Muurinsuo occurs within sulfide minerals.

Volcanic rocks

Detailed descriptions of the mineralogy of the least altered mafic volcanic rocks within the Hattu schist belt are not available. According to O'Brien et al. (1993), all the basaltic rocks have been metamorphosed to hornblende-plagioclase assemblages. The intermediate tuff at Kelokorpi contains biotite, quartz, muscovite, potassium feldspar, and plagioclase (andesine-labradorite) as major components and chlorite, tourmaline, epidote, titanite, zirconium, ilmenite, and rutile as accessory components (Kojonen et al., 1993). The mafic volcanic rocks at Kivisuo and Muurinsuo have more basaltic compositions.

Major minerals at Kivisuo are amphibole, plagioclase (albite-oligoclase), biotite, and chlorite, while at Muurinsuo hornblende, biotite, tourmaline, chlorite, plagioclase (andesine), and quartz occur as major minerals, and sericite, potassium feldspar, calcite, titanite, rutile, apatite, garnet, and epidote form accessory minerals (Kojonen et al., 1993; Ojanen, 1993).

Major element changes in the mafic volcanic rocks at Muurinsuo could be explained by partial breakdown of amphibole and plagioclase to form chlorite and epidote according to the following general reaction:

amphibole + albite + $\text{H}^+ =$ chlorite + epidote +
quartz + $\text{H}_2\text{O} + \text{Mg}^{2+} + \text{Na}^+$.

The primary K-bearing mineral in the mafic volcanic rocks is biotite. Consequently, the K depletion at Kivisuo requires that most of the biotite has been destroyed, for example according to the following general reaction:

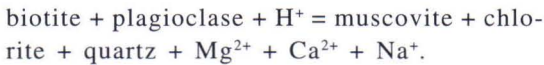
biotite + albite + $\text{Al}^{3+} + \text{Fe}^{2+} + \text{H}^+ =$
chlorite + muscovite + quartz + $\text{H}_2\text{O} + \text{Mg}^{2+} +$
 $\text{Na}^+ + \text{K}^+$.

The Si increase at Kelokorpi was probably consumed in the formation of the quartz-carbonate-tourmaline veins found throughout the mineralized zone (Kojonen et al., 1993). The Mg enrichment could be related to the alteration of Fe-rich biotite to a more Mg-rich variety according to the following general reaction:

(Fe, Mg)-biotite + $\text{H}_2\text{S} + \text{Mg}^{2+} =$ (Mg, Fe)-
biotite + pyrrhotite + H^+ .

Sericitization of plagioclase is common within the intermediate tuff (Kojonen et al., 1993; Nurmi et al., 1993). The lack of Na depletion at Kelokorpi could simply reflect the altered character of the least altered sam-

ples of the intermediate subtype 1 used in mass transfer calculations. In fact, the alteration characteristics at Kelokorpi could easily be explained by a slightly less altered composition within the mineralized zone compared with the least altered samples, according to the following general reaction:

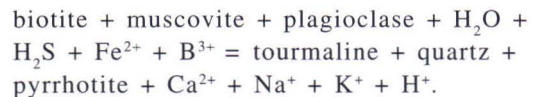


Detailed petrographical studies of both the mineralized zones and the least altered rocks would be needed to verify the above interpretations.

Sedimentary rocks

According to Ojala (1988), major minerals within the graywackes at Rämepuro comprise quartz, plagioclase and biotite, and commonly muscovite and chlorite as well. There are no detailed petrographical descriptions of unaltered graywackes and mica schists available for the other occurrences. Major components of the sedimentary rocks within and surrounding the highly mineralized zones comprise sericite, biotite, chlorite, plagioclase, potassium feldspar, and quartz in varying proportions. Accessory minerals include tourmaline, epidote, carbonate, titanite, rutile, apatite, zircon, and garnet (Kojonen et al., 1993). Proportions of the major minerals in the altered sedimentary rocks vary due to primary depositional factors, such as grading, and hydrothermal alteration. Consequently, some of the heterogeneity in the alteration characteristics between the gold occurrences is at-

tributed to variations in primary mineralogical composition. It is possible to construct generalized reactions that result in the major element gains and losses characteristic of the various occurrences by altering the proportions of plagioclase, quartz, biotite, muscovite, chlorite, and epidote between the precursor and the mineralized rock. Without detailed mineralogical and petrographical studies it is however impossible to decide which gains and losses are caused by hydrothermal alteration and which are due to variable mineralogical compositions in the precursor rocks. For example, the strong Ca enrichment at Kivisuo could be due to epidotization, but more likely it reflects a more plagioclase-rich initial composition for the precursor rock, especially considering that the whole succession intersected by drill hole 345 from 103 m onwards shows consistent enrichments in both Ca and Na (Fig. 28). Carbonatization is precluded at Kivisuo by the very low CO₂ abundances. At Elinsuo the mineralized zones consist of a quartz-tourmaline rock with strong Fe sulfide dissemination, and writing the following general reaction to characterize the mineralogical changes is possible:



If all of the Fe in the mineralized zones were bound in pyrrhotite, it would require enrichment of S of about 590–900%. Sulfur enrichment at Elinsuo is on average 630% (Fig. 44), which indicates that a large part of Fe does indeed reside in sulfide minerals.

LARGE ION LITHOPHILE ELEMENT GEOCHEMISTRY

Potassium enrichment is a typical feature of many lode gold deposits (Colvine et al., 1988; Groves and Foster, 1991). Rubidium readily substitutes for K in potassic minerals, due to similarities in their ionic radii ($K^+=1.33\text{\AA}$, $Rb^+=1.47\text{\AA}$) and they behave coherently in magmatic systems; deviations from this be-

havior can therefore be useful petrogenetic indicators. The K/Rb signature of gold-related alteration can thus potentially provide information on the source processes that generate ore fluids, provided that the effects of mineral-mineral partitioning, fluid-rock ratio, and host rock composition can be estimated

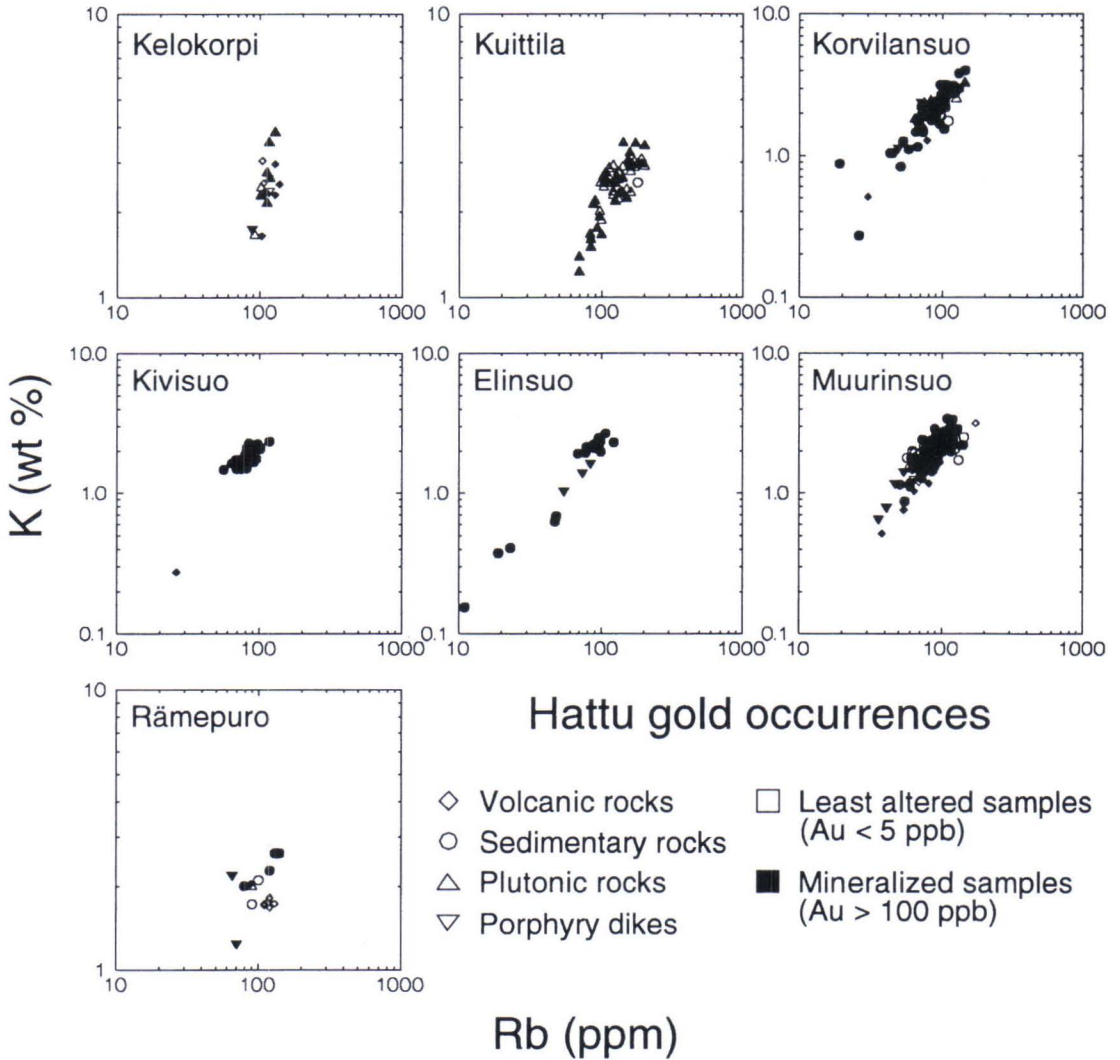


Fig. 45. K-Rb plots of mineralized and least altered rocks for the Hattu gold occurrences.

Table 13. Average K_2O and Rb contents and K-Rb ratios of mineralized ($Au \geq 100$ ppb) and least altered ($Au 5 \leq$ ppb) rocks from the gold occurrences of the Hattu schist belt. N: number of samples; *: the least altered values are averages for the whole rock type.

Deposit	Mineralized				Least altered			
	K_2O wt %	Rb ppm	K/Rb	N	K_2O wt %	Rb ppm	K/Rb	N
Kelokorpi	2.83	112	216	13	2.86	104	223	9
volcanic rocks	2.81	120	197	6	3.14	106	234	4
plutonic rocks	3.24	114	236	6	2.47	97	209	2
porphyry dikes	2.10	88	198	1	2.86	116	205	1
Kuittila tonalites	2.80	126	195	28	3.17	130	200	32
Korvilansuo	2.72	87	249	60	2.5	88	245	26
volcanic rocks*	1.37	57	169	3	2.14	108	169	20
sedimentary rocks	2.75	90	248	47	2.49	92	238	17
plutonic rocks	2.73	79	283	6	3.06	106	255	3
porphyry dikes	2.55	70	289	4	2.42	82	259	6
Kivisuo	2.11	79	225	34	2.08	82	222	6
volcanic rocks*	0.33	26	105	1	2.14	108	169	20
sedimentary rocks	2.11	79	226	31	2.14	84	235	5
porphyry dikes*	2.05	74	231	2	2.15	83	226	19
Elinsuo	2.49	85	233	22	2.49	97	213	1
sedimentary rocks	2.61	87	241	19	2.49	97	213	1
porphyry dikes*	1.69	73	192	3	2.15	83	226	19
Muurinsuo	2.39	87	228	126	2.34	86	230	95
volcanic rocks	1.74	82	195	13	1.97	88	172	9
sedimentary rocks	2.50	88	231	95	2.37	85	236	73
porphyry dikes	2.19	87	221	18	1.99	75	220	7
Rämepuro	2.65	88	204	7	2.14	115	154	10
volcanic rocks	2.46	88	232	1	2.09	120	151	7
sedimentary rocks	2.98	125	198	4	2.33	95	203	2
porphyry dikes*	2.08	68	258	2	2.15	83	226	19

(Perring and Barley, 1990). For this study, the systematics of the large ion lithophile elements K, Rb, and Ba were studied for both the mineralized and the least altered rocks of the Hattu schist belt gold occurrences.

Potassium and Rb are strongly correlated within mineralized rocks at every occurrence (Fig. 45) and the K-Rb ratios for each of the main rock types vary between 105 and 289 (Table 13). Excluding one volcanogenic sam-

ple from Kivisuo, the K-Rb ratios are near, but usually slightly lower than, the average crustal value of 285 (Taylor and McLennan, 1985). With the exception of Rämepuro, the volcanic rocks show a slight tendency for having lower K-Rb ratios than the other rocks. However, considering the amount of data available, there is no significant lithologic control over the K-Rb covariation or the magnitude of the K-Rb ratio. Apart from the dikes at Elinsuo, no notable differences exist in the K/Rb values between the least altered and the most strongly mineralized samples.

The degree of linear correlation between K and Ba is only moderate for the data as a whole (Fig. 46), and absent altogether for the mineralized tonalites from the Kuittila prospect. The values of the K-Ba ratio vary from 21 (Korvilansuo plutonic rocks and dikes) to 69 (Kelokorpi volcanic rocks), usually being close to, but slightly lower than the average crustal value of 36 (Taylor and McLennan, 1985). The K-Ba ratios for volcanic rocks tend to be somewhat higher than for the other rock types. The altered plutonic rocks from Kelokorpi and sedimentary rocks from

Rämepuro, tend to have somewhat higher K-Ba ratios than the least altered rocks. Considering the amount of data available, there are no other significant differences in the K/Ba values between the least altered and the most strongly mineralized rocks. Linear correlations between Ba and Rb are generally poor, and for plutonic rocks, nonexistent (Fig. 47).

Studies relating to the K-Rb systematics of Archean lode gold deposits have been done in the Abitibi greenstone belt in Canada (Kerrick, 1989a,b) and the Yilgarn block in western Australia (Perring and Barley, 1990), and have also been reported for Archean and early Proterozoic gold deposits in Finland (Nurmi et al., 1991). There are no ultramafic host rocks within that part of the Hattu schist belt under consideration here, and only sporadic mafic units. Consequently, abundances of K, Rb, and Ba are restricted to the upper part of the compositional range shown by the Canadian, Australian, and Finnish Proterozoic deposits (Fig. 48). Except for the absence of low abundances of K, Rb, and Ba, the results for the Hattu schist belt deposits are similar to those from the Canadian deposits. The K-Rb

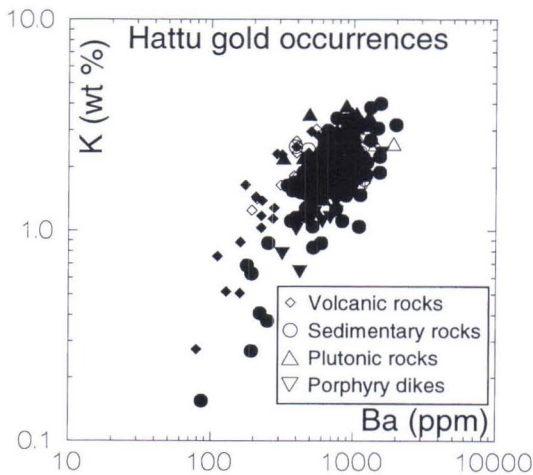


Fig. 46. K-Ba plot of mineralized and least altered rocks from the Hattu gold occurrences.

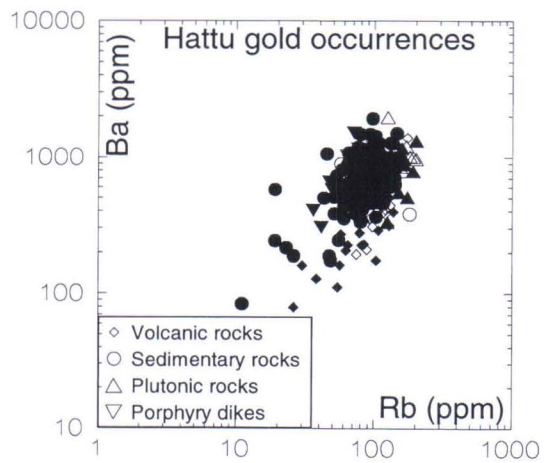


Fig. 47. Ba-Rb plot of mineralized and least altered rocks from the Hattu gold occurrences.

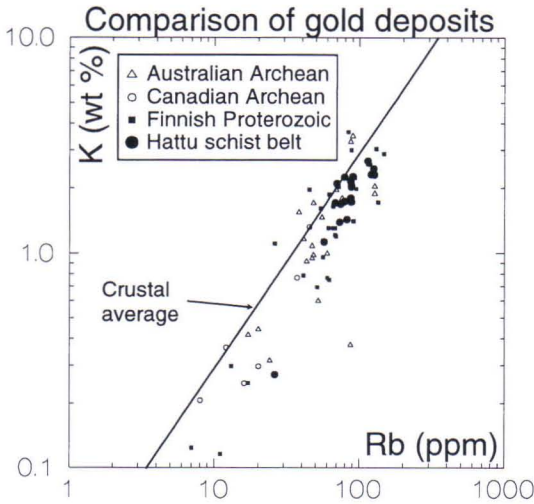


Fig. 48. K-Rb plot comparing the Hattu gold occurrences with Australian and Canadian Archean and Finnish Proterozoic deposits. Data for the mineralized rocks from the Hattu occurrences is from Table 13, for the Canadian deposits from Kerrich, 1989a and b, for the Australian deposits from Perring and Barley, 1990, and for the Finnish early Proterozoic deposits from Nurmi et al., 1991.

ratios have a restricted range close to the crustal average, and there is no significant lithologic control on K-Rb covariation or the magnitude of the K-Rb ratio. The Australian and Finnish Proterozoic deposits show a larger spread of K-Rb ratios. Moreover, for the Australian deposits, different mineralized

rock types within a single deposit can have dissimilar K-Rb ratios, and differences exist in the K-Rb ratios of mineralized and least altered rocks (Perring and Barley, 1990).

According to Kerrich (1989a,b), the coherent trends of K, Rb, and Ba in Archean lode gold deposits are unlike those observed in several classes of magmatic-related or massive base metal sulfide deposits, or those expected from granulitization reactions. Instead, they would best be explained by dehydration reactions in lithologically complex source regions, such as the root zones of terrane boundary structures along which different greenstone terrains were juxtaposed (Wyman and Kerrich, 1988). Perring and Barley (1990) showed that K-Rb systematics alone cannot provide an unequivocally diagnostic fingerprint of the source processes responsible for Archean gold mineralization. According to Groves and Foster (1991) the K-Rb ratios for Archean lode gold deposits are typical crustal values, and suggest less fractionation than is normally recorded from magmatic-hydrothermal mineral deposits. The similarity of the K-Rb-Ba systematics in the Hattu schist belt compared with the pattern common to Archean lode gold deposits worldwide is consistent with an analogous origin for the ore fluids, even though the precise nature of the process remains to be fully ascertained.

DISCUSSION

Comparison with previous work

One of the main goals of this study has been to study major element mass transfer during gold mineralization and hydrothermal alteration. Bornhorst and Rasilainen (1993) studied mass transfer associated with mineralization, but their results indicated either limited mobility or immobility for most major elements, except for K in all rock types, and Na and Si in felsic igneous rocks. However, their work did indicate that major element mobility could have been masked by large primary variation. This study has shown that all of the major elements can be mobile, and that Fe, Mn, Mg, Ca, and P, which Bornhorst and Rasilainen (1993) regarded as mostly immobile, are in fact quite often mobile within every main rock type in the Hattu schist belt. The differences in results are due to more refined and accurate mass transfer calculations enabled by dividing the main rock types into a larger number of chemical subtypes; this has reduced the primary igneous and sedimentary variation in the chemical compositions of the subtypes and facilitated more accurate determination of mass transfer due to hydrothermal alteration. Moreover, Bornhorst and Rasilainen (1993) used a much larger set of samples, most of which were only slightly mineralized, while this study concentrates on strongly mineralized samples within and immediately adjacent to highly mineralized zones. However, the intensity of mineralization does not seem crit-

ical, because the results of mass transfer calculations do not change much when larger sample sets, similar to those of Bornhorst and Rasilainen (1993), are used.

Strong average enrichments within all the mineralized zones are shown by Au, Te, B, Bi, Ag, CO₂, W, As, and S. Earlier work (Bornhorst and Rasilainen, 1993) also placed Au, Te, B, Bi, CO₂, W, As, and S among the most mobile elements, although in a slightly different order. Furthermore, Cr, Zn, Mo, Li, and Cu were interpreted to have played a significant role in the hydrothermal system. This study shows however that the significance of these elements is restricted to certain rock types. Igneous rocks are significantly enriched in Cu and Mo, whereas only tonalites are invariably enriched in Cr, Zn, and Li. Moreover, the direction of mass change for these elements varies, so that their average mobility is quite small. Earlier work indicated that Ag mobility is restricted to tonalites, but this study shows that Ag is among the most strongly and consistently mobile elements within all the main rock types. The failure of previous work to reveal Ag mobility is probably due to the use of unrealistically large limits for primary variation, which in turn result from poor analytical quality of much of the Ag data from the northern part of the Hattu schist belt; these data have accordingly been excluded from this study.

Comparisons with Archean lode gold deposits in Australia and Canada

Figs. 49–51 show host rock alteration in the Hattu occurrences compared against alteration reported in the literature for Archean lode gold deposits in Australia and Canada. Due to the large primary variations of major element abundances for common igneous and sedi-

mentary rocks, local background concentrations are essential to obtaining reliable results in mass transfer calculations. More general background concentration estimates are acceptable for gold-related trace elements, because their enrichments are usually many or-

ders of magnitude greater than their background abundances. To minimize the effects of primary variation, only studies that report element abundances both for the altered rocks and for the precursor rocks adjacent to the Australian and Canadian deposits were used (Appendix 5). Except for one deposit (Rundle), mass changes are not given in numerical form in the publications, and recalculating them was therefore necessary. The isocon method of Grant (1986) was used, and the isocon was based on one or more of Al, Ti, and Zr. Results for some of the Australian deposits are based on calculations using quite general background estimates for mafic, felsic and sedimentary rocks, and are probably not accurate with respect to major element mobility. However, the data as a whole provides a general picture of the alteration characteristics of Archean lode gold deposits, including major elements. Background abundances of Ag, As, CO₂, Cu, Mo, Pb, and S were not available for the Hemlo deposits but were estimated instead using average background concentrations for intermediate and felsic igneous rocks and sedimentary rocks in the data set collected from literature. For a few deposits, no background values of Si, P, and LOI have been published; instead of estimating these, smaller numbers of samples were used for these components.

Many authors have pointed out that host rock composition affects alteration mineralogy (e.g., Colvine et al., 1988; Böhlke, 1989; Mikucki et al., 1990), and therefore also alteration chemistry. Consequently, the volcanic, sedimentary, and felsic igneous host rocks in the Hattu occurrences were compared to corresponding host rocks in Australian and Canadian deposits.

Tonalites and porphyry dikes

Highly mineralized (Au \geq 1 ppm) tonalitic host rocks from the Hattu occurrences were compared with felsic igneous host rocks from

11 lode gold deposits in Australia and Canada (Fig. 49). For most of the Australian and Canadian deposits very limited trace element data is available, and the trace element results can only be considered as rough approximations. The deposits in Australia and Canada show clear average increases in LOI and K, and depletion in Na. Average major element mass changes for the Hattu tonalites agree well with those for the felsic igneous host rocks in the Australian and Canadian deposits, although the Hattu data display somewhat larger ranges for many elements, and slightly higher average enrichments in Si, Mn, Mg, and P. Manganese, Mg, Ca, and K are clearly more depleted in porphyry dikes in the Hattu occurrences than in felsic host rocks in the deposits in Australia and Canada.

The Australian and Canadian deposits display intense average enrichments in Au, Ag, Te, Bi, W, S, As, and CO₂, strong average enrichments in Mo, Cu, Li, and Pb, and moderate average enrichment in Rb. For the Hattu tonalites, Ag, As, S, and W display smaller average enrichments, whereas Ba, Co, Cr, Mo, Ni, Pb, and Zn tend to have somewhat higher average enrichments. For the porphyry dikes, Ag, CO₂, Li, and Pb have smaller average enrichments, whereas Bi has an appreciably greater average enrichment compared with the Australian and Canadian deposits, due to its very intense enrichment in Rämepuro. The only other porphyry sample from Muurinsuo agrees well with the Australian and Canadian Bi data. Nurmi et al. (1991) report B concentrations of 9–508 ppm, with a median of 14 ppm, for five felsic host rocks in Canadian and Australian lode gold deposits. Calculating mass transfer using these B values, without mass change correction, and using the same background estimate as for the Hattu felsic rocks (20 ppm), gives a relative B enrichment range from -0.55 to +24.4, with a median of -0.3. This is rather similar to the range for the Hattu tonalites. In contrast, the Hattu porphyries are clearly strongly enriched in B.

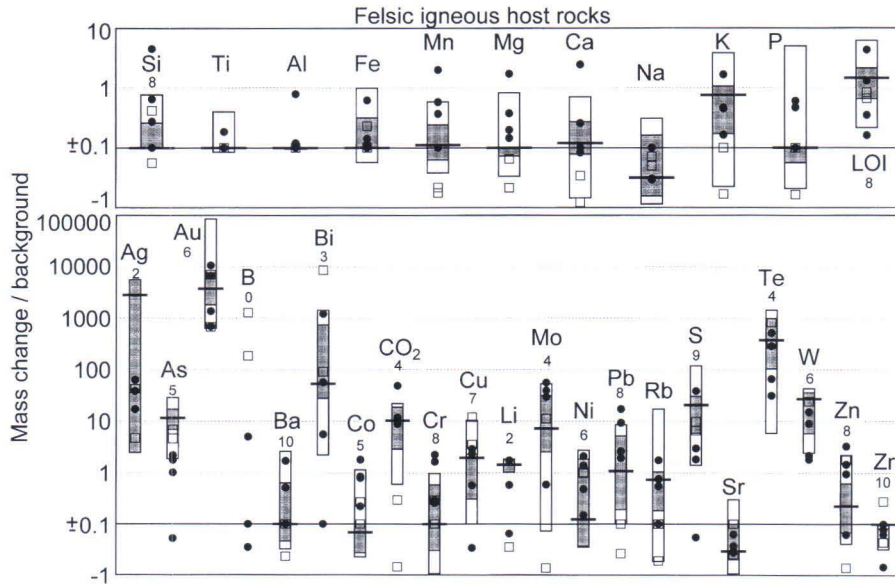


Fig. 49. Mass changes for felsic igneous host rocks with $Au \geq 1$ ppm in the Hattu occurrences (filled circles; tonalites, open squares: porphyry dikes) and in 11 Australian and Canadian lode gold deposits. The bars represent ranges, the shaded areas interquartile ranges (from 25th to 75th percentile), and the horizontal lines median values, for the Australian and Canadian deposits. Data for the Hattu occurrences is combined from Figs. 41 and 42. References for the Australian and Canadian data are given in Appendix 5. Number of Australian and Canadian deposits, if less than 11, is given below the element symbol.

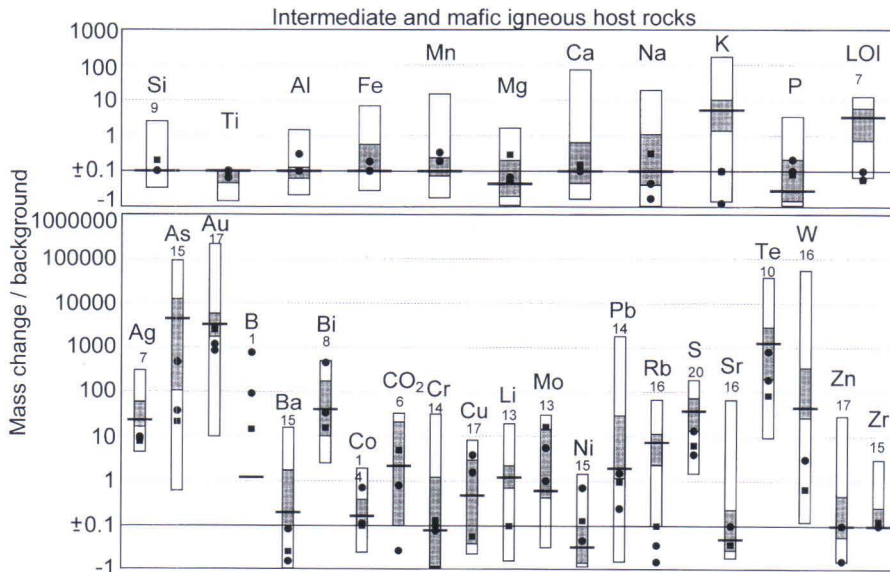


Fig. 50. Mass changes for intermediate (filled squares) and mafic (filled circles) igneous host rocks with $Au \geq 1$ ppm in the Hattu occurrences and for mafic host rocks in 21 Australian and Canadian lode gold deposits. The bars represent ranges, the shaded areas interquartile ranges (from 25th to 75th percentile), and the horizontal lines median values, for the Australian and Canadian deposits. Data for the Hattu occurrences is from Fig. 43. References for the Australian and Canadian data are given in Appendix 5. Number of Australian and Canadian deposits, if less than 21, is given below the element symbol.

Lode gold deposits are characterized by close association of Ag, As, B, Bi, S, Te, and W with Au (e.g., Kerrich, 1983; Groves and Foster, 1991). Smaller enrichments of some of these elements in the Hattu occurrences are probably related to lower average Au enrichments in these occurrences. Consequently, available data do not support the existence of significant differences in geochemical alteration characteristics between tonalitic host rocks in the Hattu schist belt and felsic host rocks in Archean lode gold deposits in Australia and Canada. The Hattu porphyry dikes differ both from the Hattu tonalites and from the Australian and Canadian host rocks mainly in lacking K, CO₂, Rb, Li, and Pb enrichments, and in showing intense enrichments in B and Bi (Rämepuro) and generally larger depletions in Mn, Mg, and Ca. However, the very limited amount of data available for the

Hattu porphyries and on many trace element concentrations for Australian and Canadian deposits renders these results uncertain.

Volcanic rocks

Highly mineralized (Au ≥ 1 ppm) mafic and intermediate volcanic rocks from the Hattu occurrences were compared with mafic host rocks from 22 Australian and Canadian lode gold deposits (Fig. 50). The Australian and Canadian deposits show distinct average increases in K and LOI, and slight average depletions in Mg and P. The most obvious difference in major element mobility between the Hattu occurrences and the Australian and Canadian deposits is the lack of K and LOI increases in the former. For other major elements, the Hattu data are consistent with data from the Australian and Canadian deposits.

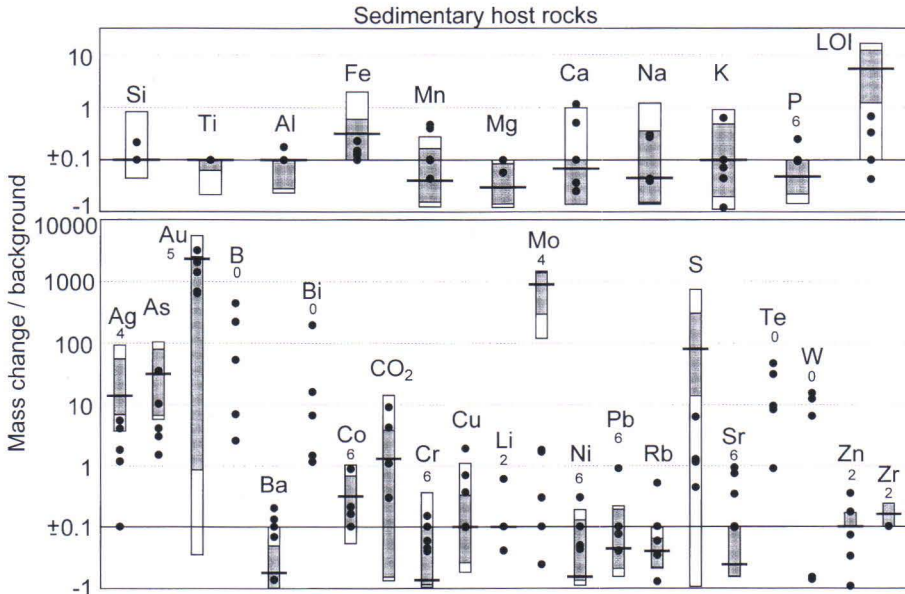


Fig. 51. Mass changes for sedimentary host rocks with Au ≥ 1 ppm in the Hattu occurrences (filled circles) and in 8 Australian and Canadian lode gold deposits. The bars represent ranges, the shaded areas interquartile ranges (from 25th to 75th percentile), and the horizontal lines median values, for the Australian and Canadian deposits. Data for the Hattu occurrences is from Fig. 44. References for the Australian and Canadian data are given in Appendix 5. Number of Australian and Canadian deposits, if less than 8, is given below the element symbol.

The Australian and Canadian deposits display intense average enrichments in As, Au, Te, W, Bi, S, and Ag, and strong average enrichments in Rb, CO₂, Pb, Li, and B. Most of the Hattu trace element data fall within the ranges of the Australian and Canadian data, but some obvious differences occur. Average enrichments of As, Li, and W are lower, and average enrichment of B is higher, for the Hattu occurrences. Moreover, Ag, Au, Pb, S, and Te are somewhat less enriched, and Mo and Ni are slightly more enriched, for the Hattu occurrences. In contrast to the Australian and Canadian data, Rb and Ba are depleted, evidently reflecting the behavior of K in the Hattu occurrences. The results concerning Li and B are uncertain because only two Li analyses for the Hattu occurrences and only one B analysis for the Australian and Canadian deposits were available. Nurmi et al. (1991) report B contents of 7.7–86.8 ppm, with a median of 53.1 ppm, for five mafic host rocks in Canadian and Australian lode gold deposits. Calculating mass transfer using these B values, without mass change correction, and using the same background estimate as for the Hattu volcanic rocks (15 ppm), gives a relative B enrichment range from -0.49 to +4.79, with a median of 2.54. Boron enrichment for the Hattu volcanic rocks is consistently greater than the upper limit of this range (Fig. 50).

Consequently, the mafic and intermediate volcanic host rocks in the Hattu occurrences differ from mafic host rocks in Australian and Canadian deposits mainly due to their lack of K, LOI, Ba, or Rb increases, and probably in their being more intensely enriched in B.

Sedimentary rocks

Highly mineralized (Au \geq 1 ppm) sedimentary rocks from the Hattu occurrences were compared with sedimentary host rocks from 8 Australian and Canadian lode gold deposits

(Fig. 51). For most of these deposits very limited trace element data are available, and the trace element results are therefore only rough approximations. The Australian and Canadian deposits show a distinct average increase in LOI, slight average enrichment in Fe, and slight average depletions in Mg, Mn, Na, P, and Ca. With a few exceptions, the Hattu major element data fall within the ranges of the Australian and Canadian data, the most significant difference being the weaker increase of LOI for the Hattu occurrences. Iron is invariably slightly less enriched, and Mn, Mg, and P are consistently slightly less depleted, or even slightly enriched, for the Hattu occurrences.

The Australian and Canadian deposits display intense enrichments in Au, Mo, S, As, and Ag, strong enrichment in CO₂, and moderate depletions in Cr, Ni, and Ba. Unfortunately, no B, Bi, Te, and W abundances are reported in the available published data. For most trace elements, the Hattu data cover a wider range. Obvious differences between the Hattu occurrences and the deposits in Australia and Canada are the markedly smaller Mo and S enrichments for the former. Furthermore, Ag, As, and Au have generally somewhat lower enrichments, while Ba, Cr, Cu, Ni, and Sr tend to have slightly higher enrichments for the Hattu occurrences.

Based on the very limited data available, the sedimentary host rocks in the Hattu occurrences differ from sedimentary host rocks in the Australian and Canadian deposits mainly with respect to smaller Mo enrichments, and possibly also smaller Ag, S, and LOI enrichments. All the Australian and Canadian sedimentary samples are from the Hemlo camp, which is known for its high Mo abundances; this therefore renders the representativeness of the intense Mo enrichment in Australian and Canadian sedimentary host rocks questionable.

Summary of comparisons with Archean lode gold deposits in Australia and Canada

Wallrock alteration in Archean lode gold deposits usually involves large additions of H₂O, CO₂, S, and K, together with introduction or redistribution of Si (Kerrick, 1983; Groves and Foster, 1991; Groves, 1993). Rubidium, Li, and Ba are also usually enriched, and localized introduction of Na or Ca is common. Aluminium, Ti, V, Y, and Zr are normally immobile, and Fe, Mg, Cr, Ni, and Sc are relatively immobile. Gold is strongly enriched, normally 10³–10⁴ times background, and Ag, As, and W are consistently enriched. Variable enrichments are also shown by Bi, Sb, Te, B, and Pb, whereas Cu and Zn contents are usually low. Although these characteristics describe lode gold deposits as a group, the alteration features of individual deposits can be considerably different.

Strong increases of Au, Ag, As, S, and LOI are common to those Australian and Canadian deposits for which mass changes were calculated in this study. Tellurium, Bi, W, and K are invariably enriched in igneous host rocks but there are no data for Te, Bi, and W for sedimentary host rocks. The modest relative enrichment of CO₂ for the Australian and Canadian mafic, and possibly also sedimentary, host rocks suggests that rocks used to estimate background concentration of CO₂ have been to some degree affected by carbonatization. Disregarding the lack of K enrichment in sedimentary host rocks, the present data for Australian and Canadian deposits agrees with the general characteristics of lode gold-related alteration described above.

Although alteration characteristics for tonalitic host rocks in the Hattu occurrences and felsic igneous host rocks in the Australian and Canadian deposits are similar, differences exist for the other rock types. The most common discrepancy is in the generally weaker enrichment or lack of enrichment of one or more of K, Rb, Ba, LOI, and CO₂ for the Hattu

schist belt, indicating that gold mineralization for most of the belt was accompanied by weaker hydration, carbonatization, and K-metasomatic reactions than in Archean lode gold deposits in general. The difference in the amount of carbonate alteration between the Hattu occurrences and the deposits in Australia and Canada is actually greater than indicated by Figs. 49–51. Disregarding the tonalites, the Hattu rocks are virtually devoid of CO₂, with average abundances from less than 0.01% to 0.03%, more than one order of magnitude smaller than for the Australian and Canadian deposits. The similarity of relative enrichments of CO₂ between the Hattu occurrences and the Australian and Canadian deposits is thus due to the very low background abundances used for the Hattu occurrences.

Silver, As, S, and W are regularly, and Au and Te are very often, slightly less enriched for the Hattu deposits than for the Australian and Canadian deposits. Nurmi et al. (1993) reported generally higher Te, Bi, and B abundances, and lower Ag, As, S, and W abundances for highly mineralized host rocks in the Hattu deposits than for host rocks in nine Archean lode gold deposits in Australia and Canada. A close association of Ag, As, S, Te, and W with Au is common to lode gold deposits (e.g., Kerrich, 1983; Groves and Foster, 1991), and is also evident at the Hattu occurrences (Rasilainen et al., 1993). Therefore, the behavior of Ag, As, S, Te, and W is attributed to the fact that Au enrichments are also somewhat smaller in the Hattu occurrences and is not considered to represent a significant difference between the deposit groups.

The present data do not support the generally higher Bi and Te enrichments in the Hattu host rocks suggested by Nurmi et al. (1993). Nevertheless, felsic porphyry dikes at Rämepuro are more enriched in Bi than either tonalitic host rocks in the Hattu occurrences or felsic host rocks in the Australian and Canadian deposits. Porphyry dikes and mafic and intermediate volcanic rocks in the Hattu

occurrences seem to be more enriched in B than corresponding host rocks in the Australian and Canadian deposits. However, more

data on B abundances in various host rocks in Archean lode gold deposits would be needed to confirm this result.

Implications for wallrock alteration and gold deposition

Some aspects relating to K and CO₂ metasomatism, and the implications of wallrock alteration characteristics for gold deposition are briefly considered below in the light of the data presented in this study.

A problematic feature of the Hattu occurrences is that, CO₂ and K only seem to be commonly strongly enriched within tonalitic host rocks. Some mobility may have been masked by the quite large variations in primary abundances within the other rock types. On the other hand, primary variation could be expected to produce essentially random variation in mass transfer calculations, whereas the tendency toward K depletion within the sedimentary, volcanic, and porphyritic host rocks does not seem random. In the Hattu rocks, K resides mostly in muscovite and biotite, and to a smaller extent in K-feldspar. Because sericitization of plagioclase is common for all altered rocks, the lack of K enrichment seems to indicate simultaneous or later chloritization or sericitization of biotite, or chloritization of muscovite. Chloritization is actually more common in the host rocks in the Hattu occurrences than previously realized (Sorjonen-Ward, pers. comm.). On the other hand, sedimentary host rocks do not show average K enrichment in Australia and Canada, either (Fig. 51). This could be due to errors in the mass transfer calculations caused by large variations in the primary abundances of K, due to the use of unrepresentative precursors for the altered sedimentary rocks, or the consequence of mineral reactions similar to those proposed for the Hattu rocks.

The common lack of K enrichment at the Hattu occurrences might also be related to the lack of carbonate alteration. In alteration as-

sociated with lode gold deposits, reaction of a H₂O-CO₂ fluid with Ca, Fe, and Mg-bearing silicates in the wall rocks causes carbonate precipitation. Aluminium released as a consequence of these reactions removes K from the fluid. The K-Na ratios of such fluids usually favor muscovite formation (Kerrick, 1983). In the Hattu schist belt, there are practically no carbonate minerals in the highly mineralized rocks, excluding the tonalites. Consequently, if there was no carbonate precipitation, less Al would have been available to react with K in the fluid, leading to weaker K enrichment.

The only significant enrichments of CO₂ in the Hattu occurrences included in this study occur in the tonalitic host rocks at Kuittila and Kelokorpi, where calcite is the only carbonate mineral present (Kojonen et al., 1993). Abundances of CO₂ in other rock types are very low, and excluding a few modest enrichments in porphyry dikes, there is virtually no CO₂ enrichment in mineralized zones in other host rocks. Moreover, the weak and sporadic enrichments in the other rock types do not correlate with Au enrichments. This agrees with the finding of Bornhorst and Rasilainen (1993) that CO₂ enrichment is correlated with Mo and W enrichment, but not with Au enrichment.

Although calcite solubility probably decreases with falling temperature at high temperatures and high salinities, and in strongly alkaline solutions, changes in fluid pH and boiling are usually considered among the more likely mechanisms for calcite precipitation (Holland and Malinin, 1979). Wallrock-fluid reactions involving H⁺ metasomatism can have a critical role in controlling calcite precipitation. Loss of H⁺ from the fluid leads

to an increase in the CO_3^{2+} concentration at any given total carbon species concentration, which can cause carbonate minerals to precipitate (Holland and Malinin, 1979). Concurrent gains of Ca^{2+} , Mg^{2+} , Na^+ , K^+ , and other cations to the solution reinforce this effect.

In the Hattu schist belt, mineralized zones often crosscut different lithologic units in the same occurrence, indicating that the physical conditions of mineralization (T, P) and the chemical properties of the hydrothermal fluid were similar for all rock types. For the presumed ore-forming conditions in the Hattu schist belt, 250–400°C and 3 kb (Nurmi, 1993), boiling of the fluid does not seem likely. More probably therefore, calcite precipitation was caused by fluid-wallrock reactions. Consequently, the selective calcite precipitation was controlled by the different chemical, and possibly physical, properties of the host rocks, manifested in their different mineralogical compositions.

Gold precipitation in lode gold deposits is caused by a change in the physicochemical conditions of the fluid, which tends to destabilize gold complexes. This destabilization can be accomplished in a variety of ways, including cooling, oxidation, or reduction of the fluid, increasing the pH of the fluid, or decreasing the total sulfur content of the fluid (McCuaig and Kerrich, 1994). One or more of the following processes are commonly invoked to explain the modification of fluid chemistry: large-scale pressure and temperature gradients, fluid-wallrock reactions, pressure decreases inducing phase separation in the fluid, and fluid mixing (Mikucki and Groves, 1990; McCuaig and Kerrich, 1994).

Fluid immiscibility is considered to be mostly responsible for the formation of rich vein deposits (Groves and Foster, 1991). It was previously believed that phase separation rarely occurs above the greenschist-amphibolite transition, but recent experimental and theoretical studies (e.g., Naden and Shepherd, 1989; Johnson, 1991; Ho et al., 1992) have

shown that phase immiscibility may be more common than formerly thought under moderate to high temperature and pressure conditions. Phase separation could conceivably explain the scarcity of carbonate minerals in the volcanic and sedimentary host rocks in the Hattu occurrences. However, the greater abundance of carbonates in the tonalitic host rocks, and the absence of rich quartz-gold veins conflict with phase separation as the major gold precipitating mechanism. Phase immiscibility as the cause of gold precipitation in the Hattu occurrences cannot therefore be ruled out based on the available data, but it is considered less likely than fluid-wallrock reactions.

The intimate association between bulk gold and wallrock alteration in most Archean lode gold deposits has led many authors to suggest that fluid-wallrock reactions were the primary cause for gold deposition (e.g., Groves and Phillips 1987; Neall and Phillips, 1987; Clark et al., 1989; Mikucki and Groves, 1990;). This seems also to be the case in the Hattu occurrences, where most of the gold occurs in the altered host rocks, and the importance of vein gold is small. Sulfidation reactions in host rocks with large $\text{Fe}/(\text{Fe}+\text{Mg})$ values have been proposed as the mechanism that induced instability of the reduced sulfur complexes in the fluid and caused gold precipitation in many deposits (Groves and Foster, 1991). Other fluid-wallrock reactions that can cause gold deposition are intense K and CO_2 metasomatism (Kishida and Kerrich, 1987). These processes release H_2 into the hydrothermal fluid, which causes pH to decrease, potentially inducing gold precipitation.

There is good correlation between sulfur enrichment and gold abundance in the mafic host rocks in the Hattu occurrences (Kivisuo and Muurinsuo, see Figs. 28 and 32). For the other rock types, this correlation is weaker and not as consistent. Both S enrichment and absolute S abundances are lower in the Hattu occurrences than in the Australian and Canadian deposits used as a reference in this study.

Consequently, sulfidation could have caused gold precipitation in the mafic volcanic rocks, but in the other host rocks different reactions

are considered more likely. Detailed petrographical and isotopic studies are needed to determine the precise nature of these reactions.

CONCLUSIONS

Major and trace element mobility has been studied within seven Archean lode gold occurrences in the Hattu schist belt. Relative major element mobility is always much weaker than trace element mobility, even for the most strongly altered major elements. Due to large variations in primary abundances of the major elements, and their usually modest mass changes, great care is required in selecting background samples for use in mass transfer calculations. Subdividing the rock types into chemically defined subtypes is vital for attaining the required accuracy in mass transfer calculations to reveal major element mobility.

Average Na depletion is common for all main rock types hosting gold at the Hattu occurrences, although for volcanic and sedimentary rocks the magnitude of depletion remains within the limits of background variation. Slight Fe enrichment is also common to all the main rock types. Titanium and Al are the least mobile components. Tonalitic rocks are characterized by significant average enrichments of Mn and Mg, and depletion of Na. Significant increases of K and LOI are also common. Porphyry dikes display significant average depletions in Ca and Mn, and increase in LOI. Average Na and Mg depletion is ubiquitous, although not always significant. Both intermediate and mafic volcanic rocks invariably display average Mn enrichment; intermediate compositions are characterized by significant average Mg enrichment, whereas mafic volcanic rocks show average Mg depletion. Slight average Fe enrichment is the most frequent characteristic of sedimentary host rocks, but there is no average major element change common to every occurrence. Potassium has a tendency for average, but usually not

significant, depletion, and LOI has significantly increased in the Muurinsuo-Elinsuo area.

All the main rock types display generally similar alteration patterns with respect to the trace elements. Strongest average enrichment (more than 100%) is shown by Au, Te, B, Bi, Ag, CO₂, W, As, and S, but only Au enrichment exceeds the limit of background variation consistently for every rock type and in every occurrence. The tonalites show the strongest average CO₂ enrichment, the weakest average As enrichment, and no average B enrichment.

The major element mobility characteristics, specially the common tendency toward K depletion in mineralized sedimentary, volcanic, and porphyritic felsic dike host rocks, suggest that chloritization may be more common than realized in the field.

Excluding the tonalites, the host rocks in the Hattu occurrences have suffered less intense potassium metasomatism, hydration, and carbonatization than is common for lode gold deposits in general. They commonly show slightly less intense relative average enrichments in Ag, As, S, Te, and W, probably reflecting the often slightly smaller average Au enrichment. Conversely, the available data suggest stronger B enrichment in the mineralized volcanic and porphyritic dike host rocks in the Hattu occurrences than in lode gold deposits in general.

The similarity of the K-Rb-Ba systematics in the Hattu occurrences compared with the pattern common to Archean lode gold deposits worldwide favors a similar source and origin for the ore fluids. For the mafic rocks, sulfidation of the wall rocks may have caused gold precipitation, but for the other rock types, some other fluid-wallrock reactions were probably critical.

ACKNOWLEDGMENTS

Discussions with Peter Sorjonen-Ward have been very informative concerning many aspects of the geology and mineralization within the Hattu schist belt. Many valuable comments on the manuscript by Theodore Bornhorst, Pekka Nurmi, and Tapani Rämö are

gratefully acknowledged. The manuscript benefited greatly from the constructive reviews of James Grant and Ari Luukkonen. Peter Sorjonen-Ward is also thanked for correcting the English of the manuscript.

REFERENCES

- Allen, C. A., 1987.** The nature and origin of the Porphyry gold deposit, western Australia. In: Ho, S. E. & Groves, D. I. (eds.) Recent advances in understanding Precambrian gold deposits. Geology Department and University Extension, The University of Western Australia, Publication 11, 137–145.
- Ames, D. E., Franklin, J. M. & Froese, E., 1991.** Zonation of hydrothermal alteration at the San Antonio gold mine, Bisset, Manitoba, Canada. *Economic Geology* 86, 600–619.
- Anhaeusser, C. R., Fritze, K., Fyfe, W. S., & Gill, R. C. O., 1975.** Gold in "primitive" Archean volcanics. *Chemical Geology* 16, 129–135.
- Binns, R. A. & Eames, J. C., 1989.** Geochemistry of wall rocks at the Clunes gold deposit, Victoria. In: Keays, R. R., Ramsay, W. R. H. & Groves, D. I. (eds.) The geology of gold deposits: the perspective in 1988. *Economic Geology Monograph* 6, 310–319.
- Bornhorst, T.J. & Rasilainen, K., 1993.** Mass transfer during hydrothermal alteration associated with Au mineralization within the late Archean Hattu schist belt, Ilomantsi, eastern Finland. In: Nurmi, P. & Sorjonen-Ward, P. (eds.) Geological development, gold mineralization and exploration methods in the late Archean Hattu schist belt, Ilomantsi, eastern Finland. Geological Survey of Finland, Special Paper 17, 273–289.
- Bornhorst, T.J., Rasilainen, K. & Nurmi, P.A., 1993.** Geochemical character of lithologic units in the late Archean Hattu schist belt, Ilomantsi, eastern Finland. In: Nurmi, P. & Sorjonen-Ward, P. (eds.) Geological development, gold mineralization and exploration methods in the late Archean Hattu schist belt, Ilomantsi, eastern Finland. Geological Survey of Finland, Special Paper 17, 133–145.
- Böhlke, J. K., 1989.** Comparison of metasomatic reactions between a common CO₂-rich vein fluid and diverse wall rocks: intensive variables, mass transfers, and Au mineralization at Alleghany, California. *Economic Geology* 84, 291–327.
- Cassidy, K.F. & Bennett, J. M., 1993.** Gold mineralization at the Lady Bountiful mine, Western Australia: an example of a granitoid-hosted Archean lode gold deposit. *Mineralium Deposita* 28, 388–408.
- Clark, M. E., Carmichael, D. M., Hodgson, C. J., & Fu, M., 1989.** Wall-rock alteration, Victory gold mine, Kambalda, Western Australia: processes and P-T-X_{CO₂} conditions of metasomatism. In: Keays, R. R., Ramsay, W. R. H. & Groves, D. I. (eds.) The geology of gold deposits: the perspective in 1988. *Economic Geology Monograph* 6, 445–459.
- Colvine, A.C., Fyon, J.A., Heather, K.B., Marmont, S., Smith, P.M., & Troop, D.G., 1988.** Archean lode gold deposits in Ontario. Ontario Geological Survey, Miscellaneous Paper 139, 136 p.
- Crocket, J. H., 1991.** Distribution of gold in the Earth's crust. In: Foster, R. P. (ed.) *Gold Metallogeny and Exploration*. Glasgow: Blackie, 1–36.
- Downes, M. J., Hodges, D. J. & Derweduwen, J., 1984.** A free carbon- and carbonate-bearing alteration zone associated with the Hoyle Pond gold occurrence, Ontario, Canada. In: Foster, R. P. (ed.) *Gold '82: The Geology, Geochemistry and Genesis of Gold Deposits*. Geological Society of Zimbabwe, Special Publication 1, 435–448.
- Govett, G.J.S., 1983.** Rock Geochemistry in Mineral Exploration. *Handbook of Exploration Geochemistry* 3. Amsterdam: Elsevier, 461 p.
- Grant, J. A., 1986.** The isocon diagram — A simple solution to Gresens' equation for metasomatic alteration. *Economic Geology* 81, 1976–1982.
- Groves, D. I., 1993.** The crustal continuum model for late-Archean lode-gold deposits of the Yilgarn Block, Western Australia. *Mineralium Deposita* 28, 366–374.
- Groves, D. I. & Foster, R. P., 1991.** Archean lode gold deposits. In: Foster, R. P. (ed.) *Gold Metal-*

- logeny and Exploration. Glasgow: Blackie, 63–103.
- Groves, D. I. & Phillips, G. N., 1987.** The genesis and tectonic controls on Archean gold deposits of the Western Australian shield: a metamorphic-replacement model. *Ore Geology Reviews* 2, 287–322.
- Harris, D. C., 1989.** The mineralogy and geochemistry of the Hemlo gold deposit, Ontario. Geological Survey of Canada, Economic Geology Report 38, 88 p.
- Hartikainen, A. & Nurmi, P.A., 1993.** Till geochemistry in gold exploration in the late Archean Hattu schist belt, Ilomantsi, eastern Finland. In: Nurmi, P. & Sorjonen-Ward, P. (eds.) Geological development, gold mineralization and exploration methods in the late Archean Hattu schist belt, Ilomantsi, eastern Finland. Geological Survey of Finland, Special Paper 17, 323–352.
- Holland, H. D. & Malinin, S. D., 1979.** The solubility and occurrence of non-ore minerals. In: Barnes, H. L. (ed.) Geochemistry of hydrothermal ore deposits. New York: Wiley & Sons, 461–508.
- Ho, S. E., Groves, D. I., McNaughton, N. J. & Mikucki E. J., 1992.** The source of ore fluids and solutes in Archean lode gold deposits of Western Australia. *Journal of Volcanology and Geothermal Research* 50, 173–196.
- Hughes, C. J., 1973.** Spilites, keratophyres, and the igneous spectrum. *Geological Magazine* 109, 513–527.
- Johnson, E. L., 1991.** Experimentally determined limits for H₂O-CO₂-NaCl immiscibility in granulites. *Geology* 19, 925–928.
- Kerrich, R., 1983.** Geochemistry of gold deposits in the Abitibi greenstone belt. Canadian Institute of Mining and Metallurgy, Special Volume 27, 75 p.
- Kerrich, R., 1989a.** Source processes for Archean Au-Ag vein deposits: evidence from lithophile-element systematics of the Hollinger-McIntyre and Buffalo Ankerite deposits, Timmins. *Canadian Journal of Earth Sciences* 26, 755–781.
- Kerrich, R., 1989b.** Lithophile element systematics of gold vein deposits in Archean greenstone belts: Implications for source processes. In: Keays, R. R., Ramsay, W. R. H. & Groves, D. I. (eds.) *The Geology of Gold Deposits: The Perspective in 1988*. Economic Geology Monograph 6, 508–519.
- Kishida, A. & Kerrich, R., 1987.** Hydrothermal alteration zoning and gold concentration at the Kerr Addison Archean lode gold deposits, Kirkland Lake, Ontario. *Economic Geology* 82, 649–690.
- Kojonen, K., Johanson, B., O'Brien, H. & Pakkanen, L., 1993.** Mineralogy of gold occurrences in the late Archean Hattu schist belt, Ilomantsi, eastern Finland. In: Nurmi, P. & Sorjonen-Ward, P. (eds.) Geological development, gold mineralization and exploration methods in the late Archean Hattu schist belt, Ilomantsi, eastern Finland. Geological Survey of Finland, Special Paper 17, 233–271.
- Kontas, E., Niskavaara, H., & Virransalo, J., 1986.** Flameless atomic absorption determination of gold and palladium in geological reference samples. *Geostandards Newsletter* 10, 169–171.
- Kontas, E., Niskavaara, H., & Virransalo, J., 1990.** Gold, palladium and tellurium in South African, Chinese and Japanese geological reference samples. *Geostandards Newsletter* 14, 477–478.
- Kuhns, R. J., 1986.** Alteration styles and trace element dispersion associated with the Golden Giant deposit, Hemlo, Ontario, Canada. In: Macdonald, A. J. (ed.) *Proceedings of Gold '86*, an international symposium on the geology of gold. Toronto: Gold '86, 340–354.
- Kwong, Y. T. J. & Crocket, J. H., 1978.** Background and anomalous gold in rocks of an Archean greenstone assemblage, Kakagi lake area, northwestern Ontario. *Economic Geology* 73, 50–63.
- Love, D. A. & Roberts, G., 1991.** The geology and geochemistry of gold mineralization and associated alteration at the Rundle gold deposits, Abitibi subprovince, Ontario. *Economic Geology* 86, 644–666.
- McCuaig, T. C. & Kerrich, R., 1994.** P-T-t-deformation-fluid characteristics of lode gold deposits: evidence from alteration systematics. In: Lentz, D. R. (ed.) *Alteration and alteration processes associated with ore-forming systems*. Geological Association of Canada, Short Course Notes Volume 11, 339–379.
- Mikucki, E. J. & Groves, D. I., 1990.** Gold transport and depositional models. In: Ho, S. E., Groves, D. I. & Bennett, J. M. (eds.) *Gold deposits of the Archaean Yilgarn Block, western Australia: nature, genesis and exploration guides*. Geology Department and University Extension, The University of Western Australia, Publication 20, 278–284.
- Mikucki, E. J., Groves, D. I., & Cassidy, K. F., 1990.** Wallrock alteration in sub-amphibolite facies gold deposits. In: Ho, S. E., Groves, D. I. & Bennett, J. M. (eds.) *Gold deposits of the Archaean Yilgarn Block, western Australia: nature, genesis and exploration guides*. Geology Department and University Extension, The University of Western Australia, Publication 20, 60–78.
- Naden, J. & Shepherd, T. J., 1989.** Role of methane and carbon dioxide in gold deposition. *Nature*

342, 793–795.

- Neall, F. B. & Phillips, G. N., 1987.** Fluid-wallrock interaction in an Archean hydrothermal gold deposit: a thermodynamic model for the Hunt Mine, Kambalda. *Economic Geology* 82, 1679–1694.
- Niskavaara, H. & Kontas, E., 1990.** Reductive coprecipitation as a separation method for the determination of gold, palladium, platinum, rhodium, silver, selenium, and tellurium in geological samples by graphite furnace atomic absorption spectrometry. *Analytica Chimica Acta* 231, 273–282.
- Nurmi, P. A., 1993.** Genetic aspects of mesothermal gold mineralization and implications for exploration in the late Archean Hattu schist belt, Iiomantsi, eastern Finland. In: Nurmi, P. & Sorjonen-Ward, P. (eds.) *Geological development, gold mineralization and exploration methods in the late Archean Hattu schist belt, Iiomantsi, eastern Finland*. Geological Survey of Finland, Special Paper 17, 373–386.
- Nurmi, P. A., Lestinen, P., & Niskavaara, H., 1991.** Geochemical characteristics of mesothermal gold deposits in the Fennoscandian Shield, and a comparison with selected Canadian and Australian deposits. *Geological Survey of Finland, Bulletin* 351, 101 p.
- Nurmi, P. A., Damsten, M., & Sorjonen-Ward, P., 1993.** Geological setting, characteristics and exploration history of mesothermal gold occurrences in the late Archean Hattu schist belt, Iiomantsi, eastern Finland. In: Nurmi, P. & Sorjonen-Ward, P. (eds.) *Geological development, gold mineralization and exploration methods in the late Archean Hattu schist belt, Iiomantsi, eastern Finland*. Geological Survey of Finland, Special Paper 17, 193–231.
- Nurmi, P. & Sorjonen-Ward, P., 1993.** Geological development, gold mineralization and exploration methods in the late Archean Hattu schist belt, Iiomantsi, eastern Finland. *Geological Survey of Finland, Special Paper* 17, 386 p.
- O'Brien, H., Huhma, H., & Sorjonen-Ward, P., 1993.** Petrogenesis of the late Archean Hattu schist belt, Iiomantsi, eastern Finland: Geochemistry and Sr, Nd isotopic composition. In: Nurmi, P. & Sorjonen-Ward, P. (eds.) *Geological development, gold mineralization and exploration methods in the late Archean Hattu schist belt, Iiomantsi, eastern Finland*. Geological Survey of Finland, Special Paper 17, 147–184.
- Ojala, V. J., 1988.** Iiomantsin Hattuvaaran Rämepuron Au-mineralisaation geologia. Pohjois-Karjalan malmiprojekti, Raportti 19, Oulun yliopisto. 78 p.
- Ojala, V. J., Pekkarinen, L. J., Piirainen, T., & Tuukkanen, P. A., 1990.** The Archean gold mineralization in Rämepuro, Iiomantsi greenstone belt, Eastern Finland. *Terra Nova* 2, 238–242.
- Ojanen, H., 1993.** Iiomantsin Kuittilan ja Muurinsuon Au- ja Mo-W-mineralisaatioiden petrografia ja malmimineralogia. Unpublished M.Sc. thesis, University of Oulu, Department of Geology. 108 p.
- Pan, Y., Fleet, M. E. & Stone, W. E., 1991.** Geochemistry of metasedimentary rocks in the late Archean Hemlo-Heron Bay greenstone belt, Superior Province, Ontario: implications for provenance and tectonic setting. *Precambrian Research* 52, 53–69.
- Pattison, E. F., Sauerbrei, J. A., Hannila, J. J. & Church, J. F., 1986.** Gold mineralization in the Casa-Berardi area, Quebec, Canada. In: Macdonald, A. J. (ed.) *Proceedings of Gold '86, an international symposium on the geology of gold*. Toronto: Gold '86, 170–183.
- Perring, C. S. & Barley, M. E., 1990.** K/Rb ratios. In: Ho, S. E., Groves, D. I. & Bennett, J. M. (eds.) *Gold deposits of the Archaean Yilgarn Block, western Australia: nature, genesis and exploration guides*. Geology Department and University Extension, The University of Western Australia, Publication 20, 263–267.
- Perring, C. S., Groves, D. I., & Shellbear, J. N., 1990.** Nature and setting of primary gold deposits: ore geochemistry. In: Ho, S. E., Groves, D. I. & Bennett, J. M. (eds.) *Gold deposits of the Archaean Yilgarn Block, western Australia: nature, genesis and exploration guides*. Geology Department and University Extension, The University of Western Australia, Publication 20, 93–101.
- Pekkarinen, L. J., 1988.** The Hattuvaara gold occurrence, Iiomantsi: a case history. *Annales Universitatis Turkuensis C* 67, 79–87.
- Phillips, G. N., 1986.** Geology and alteration in the Golden Mile, Kalgoorlie. *Economic Geology* 81, 779–808.
- Phillips, G. N. & Groves, D. I., 1984.** Fluid access and fluid-wall rock interaction in the genesis of the Archean gold-quartz vein deposit at Hunt mine, Kambalda, western Australia. In: Foster, R. P. (ed.) *Gold '82: The Geology, Geochemistry and Genesis of Gold Deposits*. Geological Society of Zimbabwe, Special Publication 1, 389–416.
- Rasilainen, K., Nurmi, P. A., & Bornhorst, T. J., 1993.** Rock geochemical implications for gold exploration in the late Archean Hattu schist belt, Iiomantsi, eastern Finland. In: Nurmi, P. & Sorjonen-Ward, P. (eds.) *Geological development, gold mineralization and exploration methods in the late Archean Hattu schist belt, Iiomantsi, eastern Finland*. Geological Survey of Finland, Special Paper 17, 353–362.
- Ray, G. E., Shearer, J. T. & Niels, R. J. E., 1986.**

- The geology and geochemistry of the Carolin gold deposits, southwestern British Columbia, Canada. In: Macdonald, A. J. (ed.) Proceedings of Gold '86, an international symposium on the geology of gold. Toronto: Gold '86, 470-487.
- Saager, R. & Meyer, M., 1984.** Gold distribution in Archaean granitoids and supracrustal rocks from southern Africa: a comparison. In: Foster, R. P. (ed.) Gold '82: The Geology, Geochemistry and Genesis of Gold Deposits. Geological Society of Zimbabwe, Special Publication 1, 53-70.
- Sorjonen-Ward, P., 1993.** An overview of structural evolution and lithic units within and intruding the late Archean Hattu schist belt, Ilomantsi, eastern Finland. In: Nurmi, P. & Sorjonen-Ward, P. (eds.) Geological development, gold mineralization and exploration methods in the late Archean Hattu schist belt, Ilomantsi, eastern Finland. Geological Survey of Finland, Special Paper 17, 9-102.
- Studemeister, P. A. & Kiliyas, S., 1987.** Alteration pattern and fluid inclusions of gold-bearing quartz veins in Archean trondhjemite near Wawa, Ontario, Canada. *Economic Geology* 82, 429-439.
- Taylor, S. R. & McLennan, S. M., 1985.** The continental crust: its composition and evolution. Oxford: Blackwell Scientific Publications. 312 p.
- Tilling, R. I., Gottfried, D., & Rowe, J. J., 1973.** Gold Abundance in Igneous Rocks: Bearing on Gold Mineralization. *Economic Geology* 68, 168-196.
- Vaasjoki, M., Sorjonen-Ward, P., & Lavikainen, S., 1993.** U-Pb age determinations and sulphide Pb-Pb characteristics from the late Archean Hattu schist belt, Ilomantsi, eastern Finland. In: Nurmi, P. & Sorjonen-Ward, P. (eds.) Geological development, gold mineralization and exploration methods in the late Archean Hattu schist belt, Ilomantsi, eastern Finland. Geological Survey of Finland, Special Paper 17, 103-131.
- Wyman, D. & Kerrich, R., 1988.** Alkaline magmatism, major structures, and gold deposits: Implications for greenstone belt gold metallogeny. *Economic Geology* 83, 454-461.

Appendix 1. Average chemical compositions for volcanic rocks from the Hattu schist belt. Medians of the least altered samples. Number of samples is shown in parentheses. High concentrations that are likely due to alteration were replaced by values based on published data or abundances in other subgroups, shown in parentheses after the actual concentrations. (): value based on literature (For Au: Tilling et al., 1973; Anhaeusser et al, 1975; Kwong and Crocket, 1978; Saager and Meyer, 1984; Kontas et al., 1986, 1990; Nurmi et al., 1991. For the other elements: Govett, 1983, and references therein), []: value based on other subgroups, <: value below detection limit, -: not analyzed. Detection limit/2 was substituted for values below the detection limit when performing mass transfer calculations.

	Mafic (4)	Intermediate 1 (10)	Intermediate 2 (6)
SiO ₂ %	51.10	60.20	62.45
TiO ₂ %	0.84	0.79	0.57
Al ₂ O ₃ %	11.30	17.00	17.10
Fe ₂ O ₃ %	9.64	8.93	6.23
MnO %	0.19	0.09	0.08
MgO %	12.30	3.93	2.68
CaO %	7.75	1.67	2.17
Na ₂ O %	1.26	1.85	3.32
K ₂ O %	1.81	2.51	2.19
P ₂ O ₅ %	0.32	0.11	0.13
LOI %	2.20	2.78	1.50
Ag ppm	0.06	0.18 [0.06]	0.26 [0.06]
As ppm	8.7 (2)	43. (2)	6.1 (2)
Au ppb	5.0 (2)	5.0 (2)	5.0 (2)
B ppm	15.	100. [15]	30. [15]
Ba ppm	258.	425.	574.
Bi ppm	0.3 (0.05)	0.3 (0.05)	0.25 (0.05)
Co ppm	29.	33.	32.
CO ₂ %	0.03	<0.01	<0.01
Cr ppm	689.	310.	193.
Cu ppm	11.	66.	52.
Li ppm	-	75.	74.
Mo ppm	3.5 (2)	4.0 (2)	3.5 (2)
Ni ppm	237.	134.	80.
Pb ppm	3.0	12.	9.0
Rb ppm	90.	114.	100.
S %	0.07	0.32 [0.07]	0.65 [0.07]
Sr ppm	376.	206.	388.
Te ppb	90.0 (10)	52.5 (10)	230.0 (10)
W ppm	<1.0	3.0 (1)	7.5 (1)
Zn ppm	82.	120.	105.
Zr ppm	129.	112.	116.

Appendix 2. Average chemical compositions for sedimentary rocks from the Hattu schist belt. Medians of the least altered samples. Number of samples is shown in parentheses. High concentrations that are likely due to alteration were replaced by values based on published data or abundances in other subgroups, shown in parentheses after the actual concentrations. (): value based on literature (For Au: Tilling et al., 1973; Anhaeusser et al, 1975; Kwong and Crocket, 1978; Saager and Meyer, 1984; Kontas et al., 1986, 1990; Nurmi et al., 1991. For the other elements: Govett, 1983, and references therein), []: value based on other subgroups, <: value below detection limit, -: not analyzed. Detection limit/2 was substituted for values below the detection limit when performing mass transfer calculations.

	Subgroup 1 (6)	Subgroup 2 (34)	Subgroup 3 (53)	Subgroup 4 (22)
SiO ₂ %	60.95	64.50	66.30	65.85
TiO ₂ %	0.80	0.71	0.64	0.53
Al ₂ O ₃ %	16.65	15.50	15.00	15.60
Fe ₂ O ₃ %	8.46	6.70	5.92	4.88
MnO %	0.10	0.07	0.05	0.08
MgO %	3.67	3.18	2.69	2.38
CaO %	2.05	1.41	1.43	2.77
Na ₂ O %	2.70	2.29	2.44	3.25
K ₂ O %	1.97	2.39	2.37	2.35
P ₂ O ₅ %	0.11	0.11	0.11	0.14
LOI %	2.20	2.23	2.00	1.31
Ag ppm	0.31 (0.1)	0.16 (0.1)	0.19 (0.1)	0.16 (0.1)
As ppm	3.6 [3]	5.5 [3]	3.0	3.3 [3]
Au ppb	2.0	4.0 [2]	5.0 [2]	5.0 [2]
B ppm	20.	53. [20]	80. [20]	47. [20]
Ba ppm	695.	640.	647.	806.
Bi ppm	0.2	0.2	0.2	0.2
Co ppm	36.	29.	29.	18.
CO ₂ %	<0.01	<0.01	<0.01	<0.01
Cr ppm	245.	274.	245.	100.
Cu ppm	67.	55.	59.	38.
Li ppm	52.	44.	54.	44.
Mo ppm	4.0 [2]	4.0 [2]	3.0 [2]	2.0
Ni ppm	105.	104.	100.	49.
Pb ppm	11.	8.0	6.0	11.
Rb ppm	115.	90.	85.	90.
S %	0.48 [0.31]	0.43 [0.31]	0.57 [0.31]	0.31
Sr ppm	300.	232.	305.	629.
Te ppb	73.	140. [73]	200. [73]	125. [73]
W ppm	<1.0	1.0	<1.0	2.0
Zn ppm	109.	93.	87.	76.
Zr ppm	117.	121.	127.	120.

Appendix 3. Average chemical compositions for plutonic rocks from the Hattu schist belt. Medians of the least altered samples. Number of samples is shown in parentheses. High concentrations that are likely due to alteration were replaced by values based on published data or abundances in other subgroups, shown in parentheses after the actual concentrations. (): value based on literature (For Au: Tilling et al., 1973; Anhaeusser et al, 1975; Kwong and Crocket, 1978; Saager and Meyer, 1984; Kontas et al., 1986, 1990; Nurmi et al., 1991. For the other elements: Govett, 1983, and references therein), []: value based on other subgroups, <: value below detection limit, -: not analyzed. Detection limit/2 was substituted for values below the detection limit when performing mass transfer calculations.

	Subgroup 1 (2)	Subgroup 2 (59)	Subgroup 3 (9)	Subgroup 4 (6)
SiO ₂ %	54.40	64.50	68.20	71.00
TiO ₂ %	1.02	0.44	0.35	0.18
Al ₂ O ₃ %	15.60	15.40	15.60	15.60
Fe ₂ O ₃ %	8.27	4.49	3.02	1.54
MnO %	0.13	0.07	0.06	0.04
MgO %	5.31	2.36	1.41	0.73
CaO %	5.66	3.43	2.58	1.77
Na ₂ O %	3.86	3.95	4.63	5.02
K ₂ O %	3.16	3.03	2.88	3.11
P ₂ O ₅ %	0.56	0.15	0.11	0.05
LOI %	0.89	1.70	0.93	1.00
Ag ppm	0.3 [0.1]	0.1	0.1	<0.5 [0.1]
As ppm	9.1 [2]	2.0	1.0	1.0
Au ppb	5.0 [2]	2.0	1.0	2.0
B ppm	157. [20]	20.	20.	10.
Ba ppm	1605.	910.	950.	1075.
Bi ppm	0.15 [<0.1]	<0.1	<0.1	<0.1
Co ppm	28.	13.	10.	4.0
CO ₂ %	0.58 [0.15]	1.07 [0.15]	0.47 [0.15]	0.15
Cr ppm	173.	81.	60.	21.
Cu ppm	134.	19.	18.	20.
Li ppm	50.	44.	39.	39.
Mo ppm	16. [2]	20. [2]	2.0	3.5 [2]
Ni ppm	62.	30.	22.	10.
Pb ppm	23.	12.	14.	24.
Rb ppm	116.	120.	120.	135.
S %	0.79 [0.01]	0.01	<0.01	<0.01
Sr ppm	893.	730.	710.	810.
Te ppb	185. [10]	10.	9.0	4.0
W ppm	1.0	17. [2]	2.0	15. [2]
Zn ppm	88.	70.	66.	47.
Zr ppm	195.	90.	75.	25.

Appendix 4. Average chemical compositions for porphyry dikes from the Hattu schist belt. Medians of the least altered samples. Number of samples is shown in parentheses. High concentrations that are likely due to alteration were replaced by values based on published data or abundances in other subgroups, shown in parentheses after the actual concentrations. (): value based on literature (For Au: Tilling et al., 1973; Anhaeusser et al, 1975; Kwong and Crocket, 1978; Saager and Meyer, 1984; Kontas et al., 1986, 1990; Nurmi et al., 1991. For the other elements: Govett, 1983, and references therein), []: value based on other subgroups, <: value below detection limit, -: not analyzed. Detection limit/2 was substituted for values below the detection limit when performing mass transfer calculations.

	Subgroup 1 (4)	Subgroup 2 (4)	Subgroup 3 (11)
SiO ₂ %	59.85	63.00	66.00
TiO ₂ %	0.60	0.59	0.39
Al ₂ O ₃ %	15.55	16.45	15.80
Fe ₂ O ₃ %	6.24	5.03	3.72
MnO %	0.12	0.08	0.06
MgO %	3.81	2.25	1.85
CaO %	5.22	4.16	3.40
Na ₂ O %	3.26	4.27	4.88
K ₂ O %	2.33	1.67	2.21
P ₂ O ₅ %	0.17	0.17	0.15
LOI %	1.27	1.24	1.00
Ag ppm	0.14 (0.1)	0.14 (0.1)	0.12 (0.1)
As ppm	7.0 (2)	5.5 (2)	4.6 (2)
Au ppb	5.0 (2)	3.0 (2)	5.0 (2)
B ppm	28. (20)	5.0	30. (20)
Ba ppm	872.	641.	922.
Bi ppm	0.1 (0.05)	<0.1	0.1 (0.05)
Co ppm	30.	15.	14.
CO ₂ %	1.10 [0.02]	0.02	0.55 [0.02]
Cr ppm	149.	70.	59.
Cu ppm	36.	26.	22.
Li ppm	70.	49.	40.
Mo ppm	4.0 (2)	5.0 (2)	3.0 (2)
Ni ppm	54.	20.	30.
Pb ppm	2.0	7.0	16.
Rb ppm	84.	67.	84.
S %	0.23 [0.16]	0.59 [0.16]	0.16
Sr ppm	731.	741.	830.
Te ppb	120. (10)	136. (10)	60. (10)
W ppm	<1.0	3.0 [2]	2.0
Zn ppm	66.	93.	63.
Zr ppm	113.	103.	91.


Appendix 5. References for the Australian and Canadian lode gold deposit data used in the comparisons with the Hattu occurrences.

Deposit	Host rocks	Reference
Braminco	felsic	Studemeister and Kiliias, 1987
Lady Bountiful	felsic	Cassidy and Bennett, 1993
Lamaque	felsic	Kerrich, 1983
Lawlers	felsic	Perring et al., 1990
Renabie	felsic	Studemeister and Kiliias, 1987
Poprhyry	felsic	Allen, 1987
Rundle	felsic	Love and Roberts, 1991
Westonia	felsic	Perring et al., 1990
Corinthian	mafic	Perring et al., 1990
East Malartic	mafic	Kerrich, 1983
Edward's Find	mafic	Perring et al., 1990
Golden Crown	mafic	Perring et al., 1990
Golden Pond	mafic	Pattison et al., 1986
Griffin's Find	mafic	Perring et al., 1990
Hoyle Pond	mafic	Downes et al., 1984
Hunt	mafic	Phillips and Groves, 1984
Kalgoorlie	mafic	Phillips, 1986
Mt Charlotte	mafic	Perring et al., 1990
Mt Pleasant	mafic	Perring et al., 1990
North Kalgurli	mafic	Perring et al., 1990
Ora Banda	mafic	Perring et al., 1990
Paddington	mafic	Perring et al., 1990
Rundle	mafic	Love and Roberts, 1991
San Antonio	mafic	Ames et al., 1991
Sons of Gwalia	mafic	Perring et al., 1990
Victory	mafic	Clark et al., 1989
Wiluna	mafic	Perring et al., 1990
Carolin	sedimentary	Ray et al., 1986
Clunes	sedimentary	Binns and Eames, 1989
Hemlo	sedimentary	Harris, 1989
Hemlo	sedimentary	Kuhns, 1986
Hemlo	sedimentary	Pan et al., 1991



Tätä julkaisua myy


GEOLOGIAN
TUTKIMUSKESKUS (GTK)
Julkaisumyynti
02150 Espoo

 0205 5020
Telexi: 123185 geolo fi
Telekopio: 0205 5013

GTK, Väli-Suomen
aluetuomisto


Kirjasto
PL 1237
70211 Kuopio
 0205 5030
Telekopio: 0205 5013

GTK, Pohjois-Suomen
aluetuomisto

Kirjasto
PL 77
96101 Rovaniemi
 0205 5040
Telexi: 37295 geolo fi
Telekopio: 0205 5014

Denna publikation säljes av


GEOLOGISKA
FORSKNINGSCENTRALEN (GFC)
Publikationsförsäljning
02150 Esbo

 0205 5020
Telex: 123185 geolo fi
Telefax: 0205 5012

GFC, Distriktsbyrån för
Mellersta Finland


Biblioteket
PB 1237
70211 Kuopio
 0205 5030
Telefax: 0205 5013

GFC, Distriktsbyrån för
Norra Finland


Biblioteket
PB 77
96101 Rovaniemi
 0205 5040
Telex: 37295 geolo fi
Telefax: 0205 5014

This publication can be obtained
from


GEOLOGICAL SURVEY
OF FINLAND (GSF)
Publication sales
FIN-02150 Espoo, Finland

 +358 205 5020
Telex: 123185 geolo fi
Telefax: +358 205 5012

GSF, Regional office for
Mid-Finland

Library
P.O. Box 1237
FIN-70211 Kuopio, Finland
 +358 205 5030
Telefax: +358 205 5013

GSF, Regional office for
Northern Finland

Library
P.O. Box 77
FIN-96101 Rovaniemi
 +358 205 5040
Telex: 37295 geolo fi
Telefax: +358 205 5014